Theoretical Descriptions of Electron Transport Through Single Molecules: Developing Design Tools for Molecular Electronic Devices

A Thesis

submitted to the Faculty

of

Drexel University

by

Natalie R. Carroll

in partial fulfillment of the

requirements for the degree

of

Doctor of Philosophy

August 2004

Dedication

To the one who reminded me of
where I was going

To the one who taught me the
meaning of truth

You have been my rock
The example of what I strive to be

To the one who never let me forget who I was

To my life, my partner, my friend
To Bryan

Acknowledgments

I don't believe that one's accomplishments are one's own. This is why I must thank the people that made this happen and believed in me when I did not.

Kelly "From Russia With Love" Lobanov - Even from the other side of the world I felt your warm support. You have been such a force.

My girls Cassie Skinner, Jenna Simone, Kirah "Buttercup" Swain, Caroline "Bubbles" Wurster – Your friendship has helped me more than I could ever express. I love you guys.

Miriam Giguere – Thank you for giving me the opportunity to explore my artistic voice. You have completed my experience at Drexel.

Tony "Little Munchkin" Carroll – You are my favorite brother. I am so proud of you, and thank you for always being so very proud of me.

Terry Page – Thank you for all of your generous support throughout the years.

Alba Page – Every girl should have a mom like you. Since I do not have one thousand pages, I will stop at saying that you have been my greatest supporter, and the guiding light. You are the most selfless person I know, a wonderful friend and a great ally. None of this would have been possible without you…it all started with you.

To my Ph. D. defense committee for all of your time, patience and encouragement from the beginning to the end: Dr. Sally Solomon, Dr. Robert Hutchins, Dr. Reinhard Schweitzer-Stenner, Dr. Leonard Finegold, Dr. Spiridoula Matsika, and Dr. Peter Wade.

To other influential professors: Dr. Carey Rosenthal, Dr. Anthony Addison, Dr. Kevin Owens for so many insightful discussions, Dr. Alan Smith, Dr. Yen Wei, Dr. Alan Bandy, Dr. Peter Wade, Dr. Joe Foley, Dr. Amar Nath, Dr. Yian-Ming Yuan.

A very special thank you to Dr. Nikita Matsunaga. You have been so supportive of my journey through graduate school and you always took time to help me when I needed guidance.

To my awesome advisor Dr. Karl Sohlberg. I have learned so much from you. Thank you for your patience, commitment to my education, and to the education of every person in your lab. You have set an example that I will always attempt to live up to.

To all the students I ever had. You have made my experience at Drexel so unique. I had a great time with all of you.

To my beautiful family in Ecuador, South America. You have been unconditional and always so supportive of everything I have done. You are greatly responsible for who I am today.

To my “new” beautiful family in Florida. You immediately accepted me into your family and I became a daughter, sister, aunt, and friend with no questions asked. You have no idea how much you mean to me and how your love has supported me.

A special thank you to Holly Burnside for all of the helpful comments on this manuscript.

I would also like to thank my fellow graduate students, laboratory mates and friends at Drexel University, William Erb, Melissa Mertzman, Sister Dr. Rose Mulligan, Jun Tian, Jim Tu, Rob Pascoe, Patrick Ndungu, Susan Rutkowsky, Stephanie Schuster, Hamid Shirazi, James Iiani, Nucleus Xu, Virginia Nesmith, Edith Smith, Wolfgang Nadler, Maryanne Fitzpatrick, Ari Silver, Jill Allenbaugh, Shuping Zhuo, Xiang-E Zheng, and Shuhui Cai.

Table of Contents

List of Figures

List of Tables

Abstract

Theoretical Descriptions of Electron Transport Through Single Molecules: Developing Design Tools for Molecular Electronic Devices

Natalie R. Carroll

Karl W. Sohlberg, Ph. D.

There are vast numbers of organic compounds that could be considered for use in molecular electronics. Hence there is a need for efficient and economical screening tools. Here we develop theoretical methods to describe electron transport through individual molecules, the ultimate goal of which is to establish design tools for molecular electronic devices. To successfully screen a compound for its use as a device component requires a proper representation of the quantum mechanics of electron transmission. In this work we report the development of tools for the description of electron transmission that are: Charge self-consistent, valid in the presence of a finite applied potential field and (in some cases) explicitly time-dependent. In addition, the tools can be extended to any molecular system, including biosystems, because they are free of restrictive parameterizations. Two approaches are explored: (1) correlation of substituent parameter values (σ), (commonly found in organic chemistry textbooks) to properties associated with electron transport, (2) explicit tracking of the time evolution of the wave function of a nonstationary electron. In (1) we demonstrate that the σ correlate strongly with features of the charge migration process, establishing them as useful indicators of electronic properties. In (2) we employ a time-dependent description of electron transport through molecular junctions. To date, the great majority of theoretical treatments of electron transport in

molecular junctions have been of the time-independent variety. Time dependence, however, is critical to such properties as switching speeds in binary computer components and alternating current conductance, so we explored methods based on time-dependent quantum mechanics. A molecular junction is modeled as a single molecule sandwiched between two clusters of close-packed metal atoms or other donor and acceptor groups. The time dependence of electron transport is investigated by initially localizing an electron on the donor and following the time development of the corresponding non-stationary wavefunction of the time-independent Hamiltonian. We demonstrate that the time-dependent treatment of electron transport predicts physically intuitive results, while providing insights not available from time-independent methods.

Chapter 1. Background

1.1 Electron Transport Applications

Electron transport through individual molecules is a central aspect in nanotechnology, a field that deals with dimensions from inter-atomic distances to the size of current silicon transistor devices (~90 nm) [1]. As a result, nanotechnology has become relevant in a wide spectrum of disciplines ranging from biology to computer science. In biological systems, electron transport is central to the biochemical pathways that govern the redox state of complexes, the reactivity of substrate intermediates and the optical properties of biomolecules [2-4]. Accurate control over electron transport is a task that has been perfected by enzymes and their supporting molecules throughout evolution. For us to use the electron transport properties of molecules as efficiently as do biosystems, however, we must understand fundamental aspects through experimentation and theory.

Electron transport is the key to functional electronic device components, and is responsible for imparting interesting current/voltage (IV) characteristics to molecules integrated into circuits [1, 4-8]. One obvious application of molecular devices is in the computer industry, where the well-known and empirically observed “Moore’s Law” states that the typical feature size in electronic devices has decreased geometrically with time over the past four decades. The first computers ever built took up entire rooms and had vacuum tubes that collectively

weighed 30 tons. Nowadays the devices in our computers are small enough to carry, with transistor sizes of approximately 70 nm in length. This dramatic progression has given rise to the steady improvements in computer performance that have come to be an expectation of the computer hardware industry [1, 9]. An extrapolation based on Moore's Law, however, projects that in order to maintain this progression, in the near future it will be necessary to fabricate devices with feature sizes on the scale of individual molecules.

1.2 Molecular Electronic Devices

1.2.1 Fabrication of Devices

In order to perform electrical measurements on molecular devices, it is necessary to integrate them into circuits. What follows is a brief review of the common ways molecular devices are fabricated.

I. Self-assembled monolayers (SAMs) can be composed of thio-terminated organic molecules. A clean metal surface is immersed in a solution containing the species of interest for the monolayer assembly to take place. The molecules of the monolayer bond to the metal surface through the thio end. The other end of the molecule may be sulfur terminated or not, and remains exposed for the electrical measurements. Many types of dithiolated molecules have been incorporated into SAM devices ranging from saturated systems like alkanes to

polyaniline oligomers. Once the SAMs are formed, they are densely packed with intermolecular distances as low as 0.5 nm [4].

In order to measure the electrical properties of SAM molecules, a Scanning Tunneling Microscope (STM) is often used [10]. A STM uses a tip composed of platinum or tungsten, which when close enough to the surface of a conducting sample, will tunnel electrons [11]. These types of measurements have revealed interesting non-linear I/V characteristics in SAM molecules, which will be discussed shortly [12, 13]. Figure 1.1 shows a schematic for a SAM device with sulfur-terminated 1,4-(ethynylphenyl)phenylene as the molecular component. The figure also shows the STM tip. This would be the setup in order to perform electrical measurements on the device.

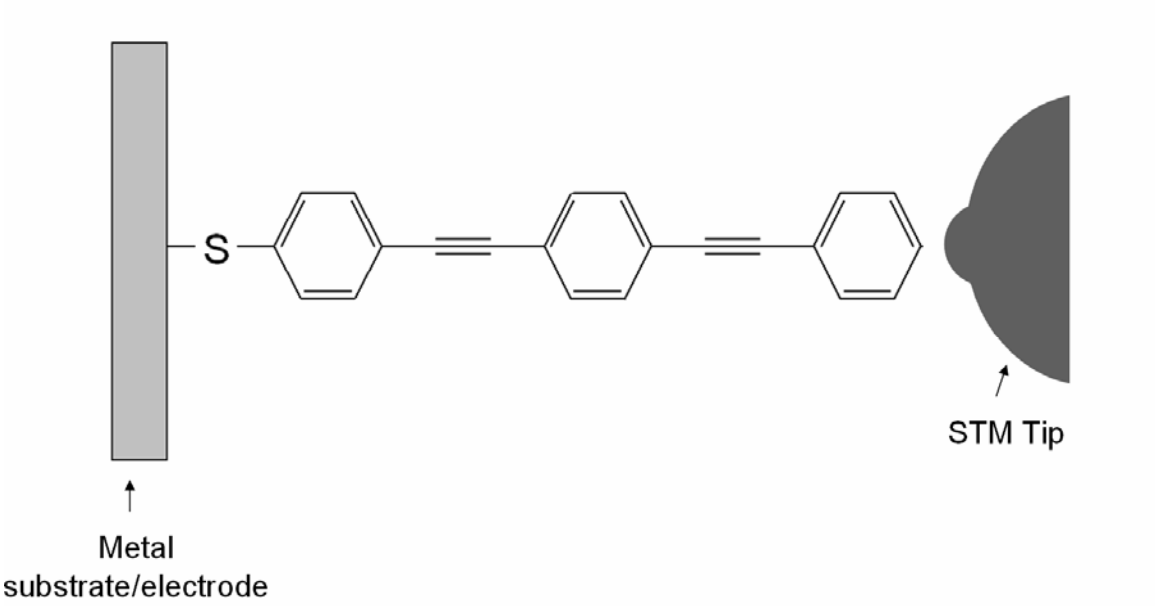

Figure 1. 1 A schematic of a Self-Assembled Monolayer (SAM) device with thio-terminated 1,4-(ethynylphenyl)phenylene as the molecular component.

II. Nanopores are conceptually similar to SAMs in the sense that the molecules assemble onto a metal surface, but the contact between the metal surface and molecule is controlled in attempts to limit one molecule (or a few) to a nanoscale window of metal. (Figure 1.2) As the name implies, a pore is etched into some type of material. Typically, a Si_3N_4 membrane (supported by a silicon wafer) is etched so that the bottom of the pore just breaks the surface of the membrane on the side where the molecules will be assembled. The pore is filled with metal through vapor deposition. The electrode, composed of the membrane with metal-filled pores and the supporting silicon wafer, is immersed in a solution

containing the molecule of interest. The thiolate ends of the molecule self-assemble on the exposed window of gold metal, and the other ends may or may not be coated with metal (through vapor deposition) [12]. Figure 1.2 is an idealized schematic for a nanopore device with the same molecular component as in figure 1.1.

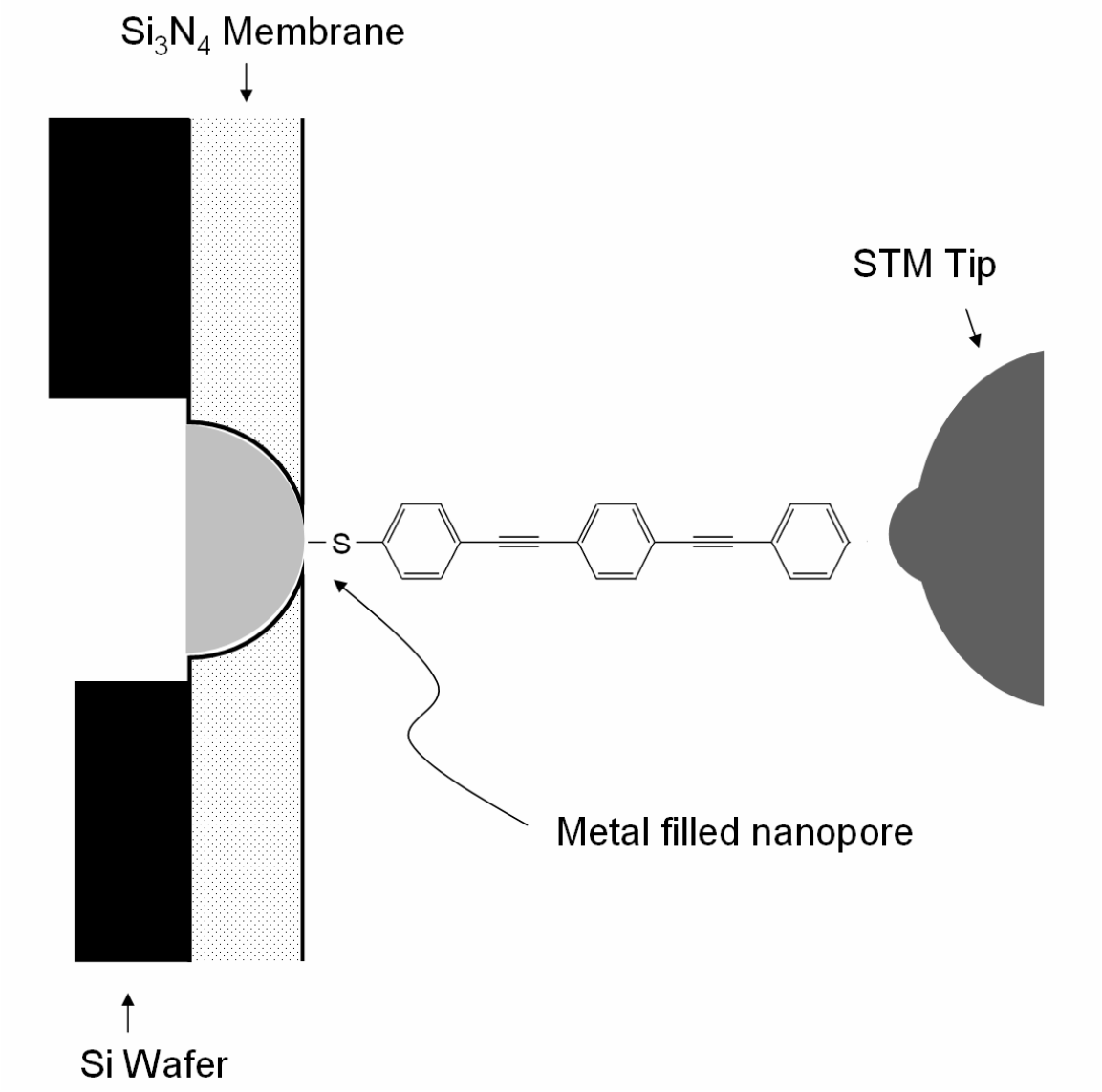

Figure 1. 2. Idealized schematic of a nanopore device.

In order to show all of the device components in figure 1.2, the size scale is not accurate. Figure 1.3 shows a more realistic picture of a nanopore device flanked by two gold electrodes [12].

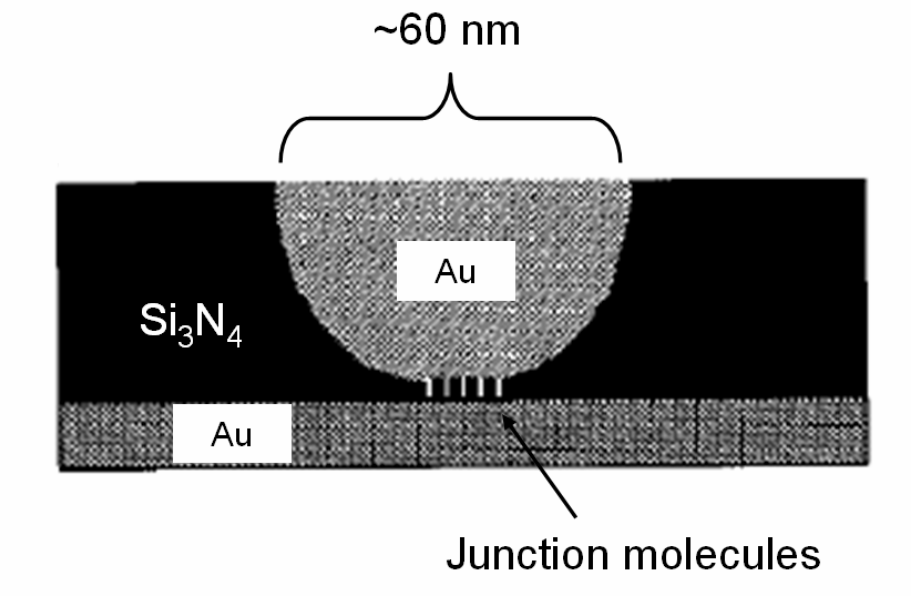

Figure 1. 3. A nanopore device flanked by two gold electrodes [12].

III. Break junctions are constructed by pulling a thin metal wire until it "breaks", while immersed in a solution containing the molecule of interest. Figure 1.4 shows a scanning electron microscope image of metal wire before failure [14]. The molecules then self-assemble on the metal surface similarly to how they assemble in SAM devices. The whole device is then removed from the solution. There will generally be a number of molecules between the ends of the

broken wire, but ideally only one is captured between the tips due to the curvature of the electrodes [9, 15]. Figure 1.5 is an outline of how break junctions are constructed [15].

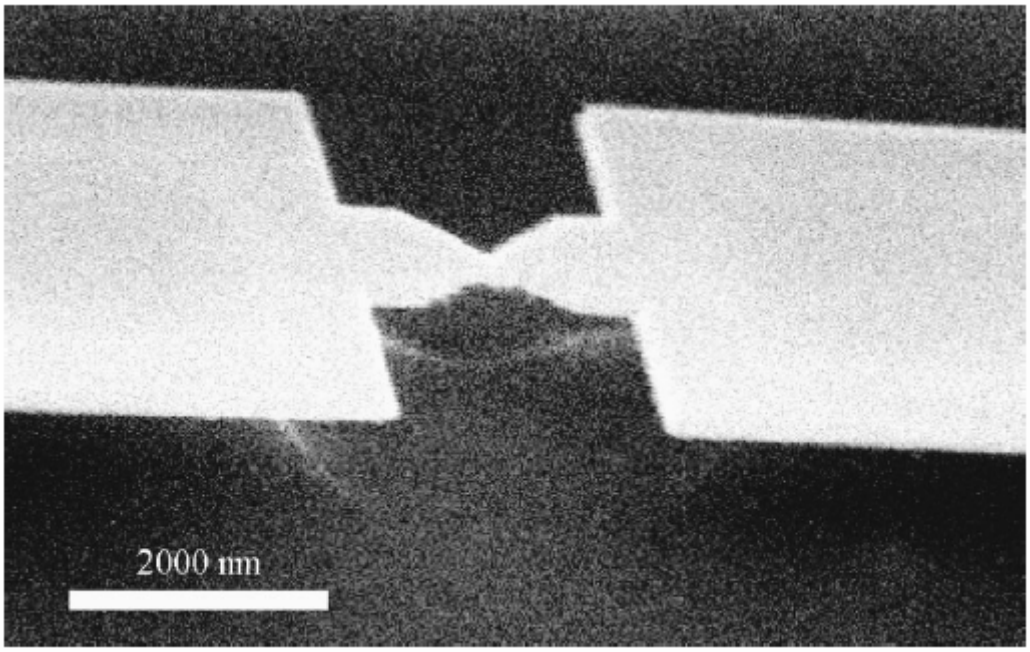

Figure 1. 4. Scanning electron microscope image of a break junction before failure [14].

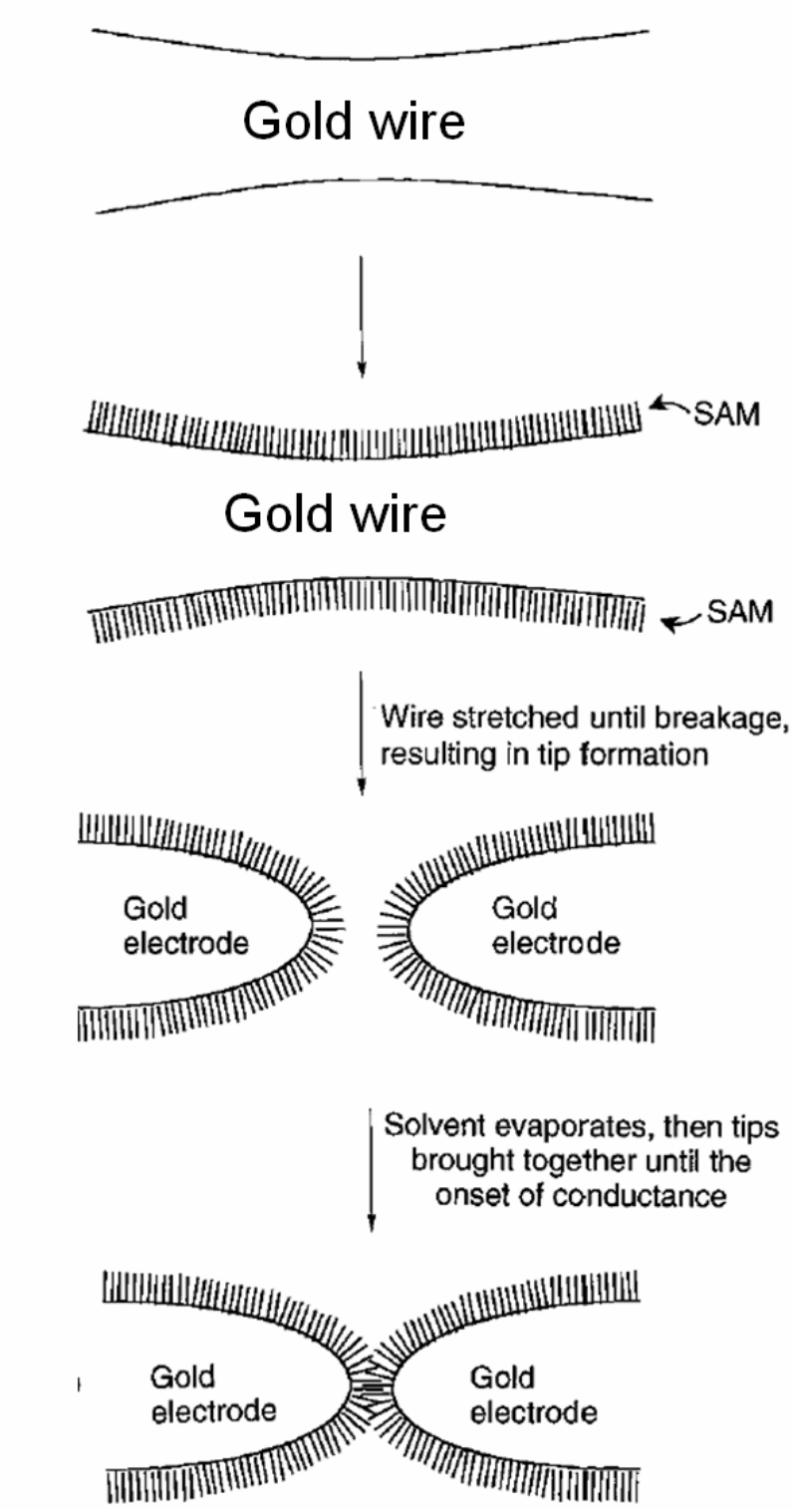

Figure 1. 5. Overview of the fabrication of a break junction [15].

1.2.2 Properties of Devices and Chemical Substituent Effects

Much empirical information about electron transport through individual molecules has come from the emerging field of molecular electronics. Indeed numerous compounds have exhibited behavior that promises utility in molecular electronic devices [1, 4-8]. In this field, the prospect of "tuning" electronic properties has motivated investigations into the substituent effect on transport properties. For example, Reynolds *et al.* suggest that methyl (~CH_3) substituted thienylene-vinylene oligomers demonstrate enhanced carrier hopping transport due to the electron-donating nature of the ~CH_3 group [16]. Substituents have also been found to alter the band gap structure in the conducting polymer poly(difluoroacetylene) [17], and alter the transport behavior in metal-molecule-metal systems containing functionalized conjugated organic compounds [18, 19].

Perhaps the most dramatic substituent effect comes from the work of Chen *et al.*. They reported the fabrication and characterization of molecular electronic devices based on self-assembled monolayers (SAMs) of conjugated organic molecules sandwiched between two gold electrodes [4, 8, 12, 13, 20, 21]. They found that the current/voltage (*I/V*) characteristics of such molecular electronic junctions (based on phenylene-ethynylene derivatives) exhibit a very strong substituent dependence. In particular, the introduction of a nitro (~NO_2) substituent produces a nonlinear current/voltage characteristic, termed negative differential resistance (NDR). Because NDR may be used to effect binary switching and memory storage, both fundamental to digital computation,

molecular devices that exhibit NDR have stimulated considerable interest. They hint that it may be possible to create digital computer device elements at the molecular scale [6, 10, 12, 13, 15, 22].

1.3 Theoretical Studies

1.3.1 Time-independent studies

Today, theoretical descriptions of electron transport in molecular junctions almost invariably involve the application of time-independent (electron) scattering theory. A review of the fundamentals of time-independent scattering theory in application to molecular electronic junctions may be found in a 2003 review article by Sohlberg and Matsunaga [9]. The work is closely related to the theory of scanning tunneling microscopy [23] in the sense that there is potential barrier to electron flow through which electrons tunnel, but in the case of molecular junctions the barrier is the molecule itself [9, 24]. A recent special issue of *Chemical Physics* [25] contains articles from many experts on the subject of molecular electronics, with strong representation from theorists. Additionally, the scientific literature has numerous reports of theoretical studies that shed light into electrical conduction in nano-sized devices [17, 19, 26-34].

Similarly to the experimental work discussed in section 1.2, theoretical studies have examined aspects that affect electron transport. For example, the influence on electron tunneling due to molecular orbital alignment [10], contact

geometry effects [35], and charge injection barriers [36] have been the focus of theoretical investigations. Despite the considerable body of theoretical work, questions still remain about the influence of an applied potential, about the importance of the interface between the metal electrode and the molecule, and about the role of the junction molecule itself, etc. [33, 37, 38].

1.3.2 Time-dependent studies

There have been virtually no theoretical investigations of the time-dependence of electron transport, which is an aspect of electron transport that affects the switching speeds of binary computer components, and alternating current (AC) conductance. Of the very few time-dependent treatments, most notable is the work of Baer and coworkers [36]. They have recently studied AC impedance in molecular junctions using time-dependent density functional theory [39]. The time dependence is incorporated into their calculations as a perturbation

$$\hat{H}(t) = \hat{H}_e + \hat{W}(t), \tag{1.1}$$

where $\hat{H}_e$ is the unperturbed Hamiltonian, and $\hat{W}(t)$ contains an external and time dependent electric field pulse

$$f(t) = e^{-(t-T_0)^2/2T^2}, \tag{1.2}$$

with a duration of time T [24, 40]. From this, they derive information on the AC conductance and impedance in molecules, and non-adiabatic state couplings

[39, 41]. Their approach, however, makes it difficult to extract atomistic details about the movement of charge across molecular devices.

Additionally, they have employed a numerical equivalent to time-dependent correlation functions (not explicit time dependence) to examine gate-response in three-terminal devices [42].

1.4 Electron transport models

The collection of work on molecular junctions has lead to different models used to explain the process of electron transport. What follows is a brief description of the foremost models.

Hopping transport – This transport occurs between regions of localized charge within the molecule, which may be a result of chemical composition or imperfections in a device [43]. The electron effectively "hops" from site to site through thermal excitations.

Quantum mechanical tunneling – This transport occurs when an incident electron is able to tunnel through a barrier which is presumably posed by the molecule. The electron transport rate (K_{ET}) is dependent on the tunneling distance (molecular length) through

$$K_{ET} = A(T)e^{(-\beta \cdot R)}, \tag{1.3}$$

where A(T) is a pre-factor depending on temperature, β which is an exponential factor dependent on the chemical nature of the junction molecule, and R is the distance between the donor and acceptor regions [9, 44].

Resonant tunneling – This transport occurs when there is double barrier to in the electron transport, resulting in a “well” where eigenstates can exist. If an incident electron attains the energy of an eigenstate within the “well” upon tunneling through the first barrier, the electron will have a finite probability of tunneling through the second barrier. The existence of a double barrier to electron transport is greatly determined by molecular structure and the nature of chemical substituents [45-47].

1.5 Outline of Thesis

The bulk of this work is devoted to developing methods for the theoretical description of electron transport through single molecules. The ultimate objective of this area of research is to develop design tools that could aid in the fabrication of molecular electronic devices. Although the main focus is in the field of molecular electronics, the methods developed here are based on a completely general electronic structure description, which makes the methods easily extendable to any system.

This thesis is divided into two general sections: the time independent and time dependent studies of electron transport. Chapter 2 will expand on the computational and theoretical techniques used to correlate electron transport properties to pre-existing data, i.e. substituent parameter values. This chapter suggests that the substituent parameter values may be employed as a design tool for the fabrication of electronic devices. Chapter 3 is divided into two

sections. The first part of this chapter will discuss the theoretical methods employed to study the effect a potential field has on a molecular device. The second part of chapter 3 and all of chapter 4 will discuss two ways to specify a time-dependent wavefunction, and (as opposed to the methodology developed by Baer and coworkers) will allow us to time-evolve the wavefunction so that we can track charge through the molecule over time. This approach gives us (a) an atomistic view of time-dependent electron flow and (b) insights into the chemical aspects that govern the electron transport event.

The thesis concludes with a conclusion, then four appendices containing general information on the theoretical methods used, and the codes that perform the calculations necessary for each study in Chapters 2, 3 and 4.

Chapter 2. Correlation of Substituent Parameter Values to Electron Transport Properties.

2.1 Introduction

The influence of a functional group on the chemical and physical properties of a molecule, better known as the substituent effect, is central to chemistry. In the 1930's, in one of the early attempts to quantify this effect, Hammet noted that substituents systematically change the free energy of proton dissociation of benzoic acids and the free energy of hydrolysis of ethyl benzoates [48]. By plotting the substituent induced changes in these chemical processes on orthogonal axes, a linear trend, termed a linear free energy relationship (LFER), was revealed. From the correlation Hammet developed a set of substituent parameter values (σ), which may be used as a tool to predict the reactivity properties of other substituted aromatic compounds [48]. Upon examination of a table of σ values it is evident that they correlate with qualitative ideas about the electron withdrawing and donating effects of their corresponding substituents, i.e. they implicitly contain electronic structure information. For electron withdrawing groups, $\sigma > 0$ (for ~NO_2, $\sigma = 0.81$), as opposed to electron donating groups where $\sigma < 0$ (for ~CH_3, $\sigma = -0.14$) [48]. The magnitude of the parameter quantifies the strength of the effect.

Seven decades later, Hammet's work continues to motivate the search for other properties correlated to substituent parameters. While much of the research in chemistry considers chemical changes resulting from variation of the

functional groups present in a system, recent results that explicitly correlate physical observables to substituent parameter values include experimental measurements of NMR chemical shifts [49], electrochemical parameters [49], dipole moments [50], hydrogen bond distances [51], electron affinities [52] and aromatic radical stabilities [53]. Theoretical calculations have been reported on the effect of substituents on thermodynamic values [54], barriers to proton transfer [55], bond dissociation energies [56] and molecular orbital energies [49].

In the emerging field of molecular electronics, the promise of "tuning" the electronic properties of materials with the substituent effect has motivated investigations into the dependence of electronic structure on the functional groups present. For example, Reynolds *et al.* suggest that methyl (~CH_3) substituted thienylene-vinylene oligomers demonstrate enhanced carrier hopping transport due to the electron donating nature of the ~CH_3 group [16]. Substituents have also been found to alter the band gap structure in the conducting polymer poly(difluoroacetylene) [17], and the transport behavior in metal-molecule-metal systems containing functionalized conjugated organic compounds [18, 19].

Recently, a substituent effect with potentially far-reaching ramifications has been observed. Chen *et al.* have reported the fabrication and characterization of molecular electronic devices based on self-assembled monolayers (SAMs) of conjugated organic molecules sandwiched between two gold electrodes [4, 8, 12, 13, 20, 21]. They found that the current/voltage (*I/V*) characteristics of such molecular electronic junctions based on phenylene-

ethynylene derivatives exhibit a very strong substituent dependence. In particular, the introduction of a nitro (~NO_2) substituent produces a nonlinear current/voltage characteristic termed negative differential resistance (NDR). NDR describes the situation where the current *I* passing through a device decreases as the potential difference *V* applied across the device is increased. Since *I(V)* typically has a positive slope overall, NDR gives rise to peaks in the *I(V)* curve of such devices. Because NDR may be used to effect binary switching and memory storage, both fundamental to digital computation, molecular devices that exhibit NDR have stimulated considerable interest. They hint at the to creation of digital computer device elements at the molecular scale [6, 10, 12, 13, 15, 22].

Motivated by the experimental and theoretical evidence outlined above, and the observation that σ values implicitly contain electronic structure information, we report a novel application of σ values. We correlate σ values with two aspects of electron transport: electron transport energies and explicit calculations of charge transfer in polyenic wires containing substituted phenyl groups.

The goal of the present study is to test the capability of σ values for predicting molecular electronic device properties. The development of such devices is a challenging goal, one that if realized could revolutionize computation, and hence remote sensing, medicine etc. If σ values have sufficient predictive power, they would serve as an efficient and economical

screening tool for selecting appropriate chemical species from which to fabricate devices and therefore accelerate the development of molecular electronics.

2.2 Theoretical Models

2.2.1 Electron transport model

A simple description of electron transport across a molecular is as follows (Figure 2.1): Starting with a neutral species, an electron from the donating electrode is placed into the Lowest Unoccupied Molecular Orbital (LUMO) of the neutral junction molecule. The energy cost associated with attaching an electron to a neutral molecule is the vertical attachment energy denoted E_v. The anionic species then relaxes, allowing the molecular geometry to respond to the additional negative charge into the radical anion. The energy difference between the radical anion, (now fully relaxed) and the relaxed neutral species is the adiabatic attachment energy denoted E_a. The adiabatic attachment energy is the negative of the electron affinity (EA), i.e. E_a = -EA [46]. As the electron moves from the junction to the accepting electrode, renuetralization occurs from the relaxed radical anion geometry. The energy cost of this process is the vertical detachment energy denoted E_n. Figure 2.1 shows a potential energy profile for a ~NO_2 substituted (2'-amino-4-ethynylphenyl-4'- ethynylphenyl-5'-nitro-1-benzenethiolate) molecular junction, and the energies associated with the electron transfer process, which are collectively termed electron transport

energies. According to experimental and theoretical evidence, the chemical nature of a substituent can alter the potential energy profile along the electron transport coordinate and therefore alter the electron transport properties of the molecular junction [45, 46]. Specific implications of changing the electron transport energies for the transport properties of molecular junctions are discussed in Ref. [46].

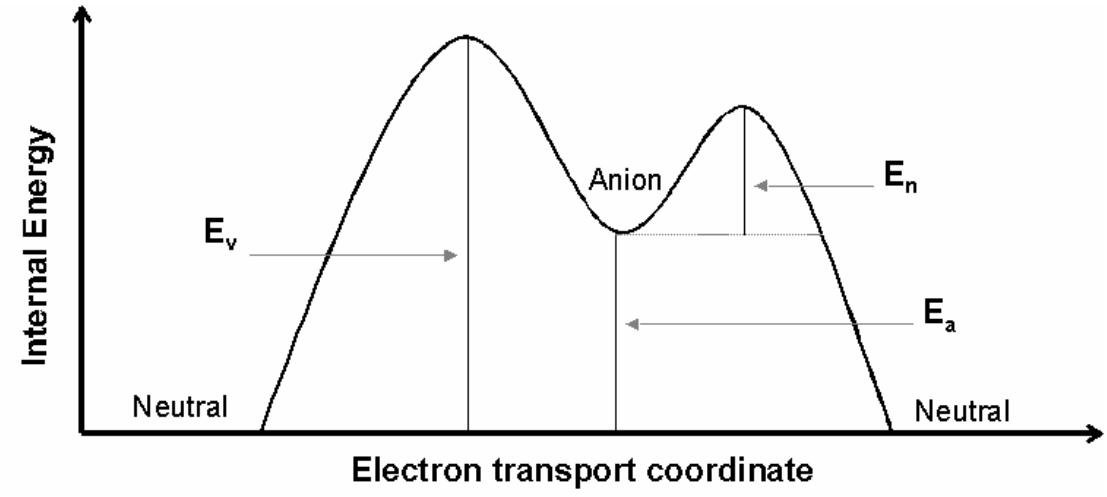

Figure 2. 1. The potential energy surface of Negative Differential Resistance (NDR) exhibiting molecules. The axes are in arbitrary units.

To examine the substituent effect on electron transport energies, we have carried out *ab initio* computations of E_a, E_v, and E_n at the HF/6-31++G [57-61] level of theory for 16 different substituted benzene molecules. As a consistency check, a subset of these calculations was repeated with density functional theory

methods (DFT/B3LYP/6-311+G**) [60-63]. All computations were performed with the GAMESS code [64].

2.2.2 Charge transfer and molecular resistance model

To calculate charge transfer and estimate molecular resistance, we employ a method similar to one developed by Gonzales and Morales [65], where information about the electron transport properties of a molecule is extracted from semi-empirical ZINDO/S-CI calculations of its ground electronic state and charge transfer state (CTS). Gonzales and Morales considered donor-bridge-acceptor (D-B_n-A) systems, i.e. D = ~CH_3, A = ~CHO, and B_n = $(CH=CH)_n$, where n=1 to 10 specifies the length of the acetylenic bridge [65]. In these systems, the electron donor and acceptor groups on opposite sides of the molecule mimic an applied potential.

After identifying the CTS, they obtained the charge transfer (Q_a) from orbital analysis of the carbonyl group (CO) in the acceptor portion of the molecule. Charge transfer Q_a^n is calculated by monitoring the change in the CO charge between the ground and charge transfer states for the molecules (n=1 to 10) in the series. The normalized charge transfer (Q_r^n) is found by dividing all Q_a^n by the charge transfer Q_a^0 of a hypothetical base molecule (CH_3-$(CH=CH)_n$-CHO where n=0) derived by extrapolation. Finally, molecular resistance is estimated by using the formula

$$R_m = 12.91\left[\frac{1}{Q_r^n} - 1\right] \quad , \qquad (2.1)$$

where the factor of 12.91 ($kJ \cdot s \cdot C^{-2}$) relates the inverse of a quantum of conductance ($2e^2/h$, where *e* is the elementary charge expresses in atomic and *h* is Planck's constant), to the molecular resistance in $k\Omega$ and Q_r^n is used as an estimate of molecular transmissivity [65, 66].

We have developed an *ab initio* implementation of the Gonzales and Morales semiempirical method [60] to calculate the Q_a to CO from the ground state to the charge transfer state during excitation. This straight-forward extension into an *ab initio* methodology allows application of the method to molecular systems containing elements not included in the subset of available semiempirical parameterizations, and should facilitate future extension to more sophisticated electronic structure techniques. We now detail the implementation.

Initially, Hartree-Fock (HF) electronic structure calculations including full geometry optimization are carried out for the system of interest. Next, single-point configuration interaction (CI) calculations are performed, including all possible single excitation configuration state functions (CSF) from valence to virtual orbitals.

The CTS is the one with a dominant CSF describing a $\pi \rightarrow \pi*$ type transition, which can be identified by examining the CI expansion coefficients. For example, if a CSF has the occupancy vector $\bar{v}$ = (2,2,2,2,2,0,0,0,0,0), it indicates that a ground electronic state is the Hartree-Fock configuration with 10 molecular orbitals of which 5 lowest energy orbitals are doubly occupied. On the other hand, if a dominant CSF for an electronic state has the occupancy vector $\bar{v}_{CTS}$ = (2,2,2,2,1,1,0,0,0,0), a HOMO electron has been excited to the LUMO.

This CSF characterizes an excited electronic state, but not necessarily a CTS. Charge transfers are not always HOMO→LUMO transitions, especially in molecules that are not as highly conjugated. To ensure charge transfer with $\pi \rightarrow \pi^*$ character, the orbital eigenvectors are inspected to identify those with the largest contributions from p (π type) orbitals orthogonal to the plane of the molecule.

To calculate Q_r, the density matrix (P) is calculated for the ground state and CTS from molecular orbital expansion coefficients ($\bar{C}$) and overlap matrix (S) from standard quantum chemical code output and an occupancy vector ($\bar{v}$) for the state(s) in question [16, 46]. The general density matrix expression can be written in terms of the occupancy vector as

$$P_{\mu\nu} = \sum_{i=1}^{M} v_i C_{\mu i} C_{\nu i}^{*} , \qquad (2.2)$$

where M is the number of molecular orbitals, v_i guarantees that only the nonzero occupancy orbitals are integrated into P, and **C** is the matrix of molecular orbital eigenvectors, which are themselves linear combinations of atomic orbitals, and $C_{\mu i}$ is the contribution of atomic orbital "i" to molecular orbital "μ". Multiplying the ground or excited state $P_{\mu\nu}$ elements by the $S_{\mu\nu}$ elements, one arrives at a Mulliken population (ρ) for all atoms. For atom A this is

$$\rho_A = \sum_{\mu \in A}^{L} \sum_{\nu}^{L} P_{\mu\nu} S_{\mu\nu}, \qquad (2.3)$$

where L is the number of expansion coefficients (atomic orbitals) and the μ index includes only those L centered on atom A. The charge transfer (Q_a) can be determined by taking the difference in electronic population on the carbonyl group acceptor atoms (CO) between the ground state and CTS

$$Q_a = \rho_{CO,CTS} - \rho_{CO,ground} . \quad (2.4)$$

In order to calculate the molecular resistance, the Q_r is needed. We extrapolated Q_a for the molecule CH_3-$(CH{=}CH)_n$-CHO where n = 0, and divided the Q_a^n by the Q_a^0. The molecular resistance is obtained by using equation (2.1) as suggested by Gonzales and Morales [65].

We adopt the Mulliken population analysis in our charge distribution calculations. This choice demands the use of a small atom-centered basis set. Of course one can variationally approach the true energy of a molecule by adding more basis functions, but determination of the electron population is basis set dependent. In fact it has been reported that Mulliken derived populations are unpredictable, erratic and do not converge as larger and more sophisticated basis sets are used. [67, 68]. Larger basis sets result in mathematical overlaps that lack a physical interpretation. Hence for a more realistic picture of the electron assignment to atoms in molecules, we require functions akin to the chemically intuitive atomic orbitals, i.e. a small basis, which can reveal consistent trends in charge distribution [67, 69-72]. The geometry optimizations, configuration interactions (CI) and charge transfer calculations were therefore carried out with an STO-6G [73-75] basis. Since INDO based semiempirical methods were designed to reproduce small basis HF results, our adopted population analysis scheme allows direct comparison to literature results [65, 76].

2.2.3 Statistical and Data Analysis

We seek the correlation of two independent variables. Therefore, an analysis was employed that equally weighs the σ values and the calculated electron transport quantities, (i.e. electron transport energies or charge transfer) and separates the error in the correlated independent variables to obtain the 95.5% confidence interval.

To weigh both independent variables equally, we identify the "best fit" line that minimizes the sum of the squares of the perpendicular distances from the line to the data points (x_i, y_i). Instead of minimizing the sum of the squares of the residuals as in a traditional least-squares fit [77], we minimized $\varepsilon(m, b)$ with respect to m and b,

$$\varepsilon = \sum_i \left(\frac{1}{m^2+1}\right)^2 \left[(m^2 x_i - m y_i + bm)^2 + (y_i - m x_i - b)^2\right], \qquad (2.5)$$

where m is the slope, b is the y-intercept and (x_i, y_i) are the coordinates of the i^{th} data point.

Next, we define the 95.5% confidence interval as an ellipse (figure 2.3), in which the major axis is the "best fit" line defined by optimized m and b values from equation 2.5. To obtain separable deviations for x and y, (x_i, y_i) is transformed into (x_i", y_i") so that the "best fit" line and the centroid of (x_i", y_i") coincide with the x-axis and the origin respectively. The deviations s_x and s_y are substituted into the standard equation of an ellipse yielding a 95.5% confidence interval (y_{ellip}) defined over the x_{ellip} domain

$$y_{ellip} = \pm\sqrt{4s_y^2\left(1 - \frac{(x_{ellip})^2}{4s_x^2}\right)} \quad . \qquad (2.6)$$

2.3 Results and Discussion

2.3.1 Correlation of substituent parameter values to electron transport energies

To explore the substituent effect on electron transport we performed a series of calculations on 16 substituted benzenes with substituents for which parameter values were available. In order to simulate the electron transport events, each molecule in the study underwent four total energy calculations. E_I -an initial geometry optimization of the neutral species, E_{II} - a single point energy calculation of the one-electron reduced molecule at the optimized neutral geometry, E_{III} - a geometry optimization of the one-electron reduced species, and E_{IV} a single point energy calculation for the neutral species at the optimized radical anion geometry. The three electron transport energies were obtained as follows: $E_v = E_{II} - E_I$, $E_a = E_{III} - E_I$, and $E_n = E_{IV} - E_{III}$, and they are vertical attachment energy, adiabatic attachment energy, and vertical renuetralization energy, respectively. Figure 2.2 shows the points in the electron transport coordinate at which the E_I through E_{IV} are calculated in order to get the electron transport energies. Of the three electron transport energies, the one that correlated best to σ values is the vertical attachment energy E_v with an R^2 value of 0.595. Table 2.1 provides the electron transport energies for each substituent

used in the study and the R^2 value for each series. Figure 2.3 shows the E_v vs. σ data and the 95.5% confidence interval.

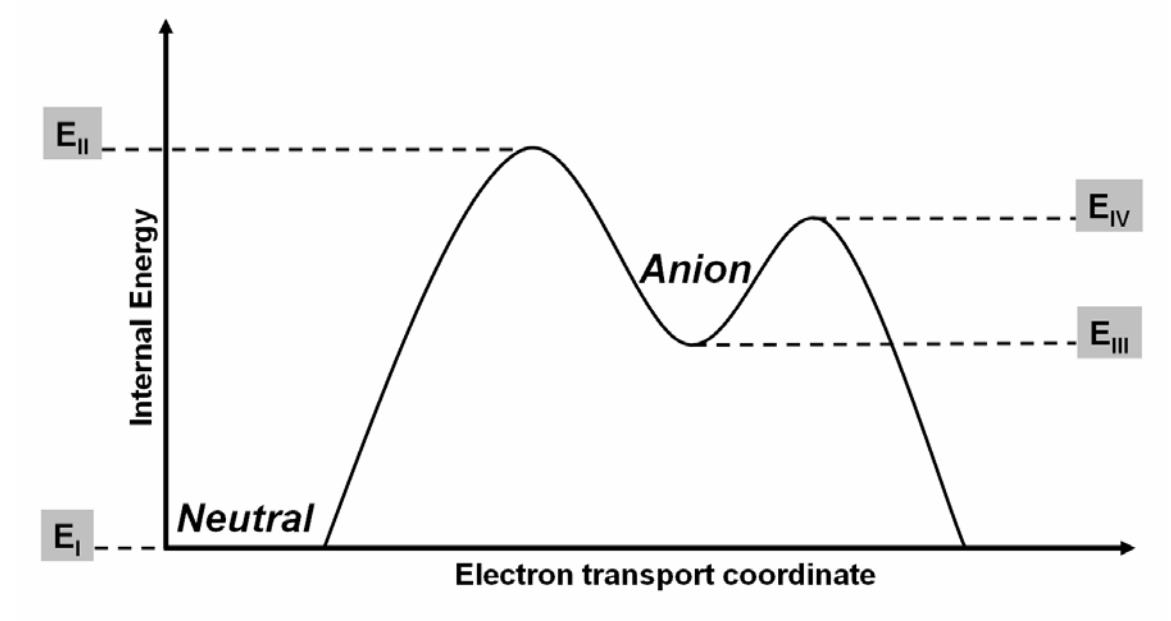

Figure 2. 2. Points along the electron transport coordinate at which the energies are calculated in order to obtain the electron transport energies (E_v – vertical attachment energy, E_a – adiabatic attachment energy, and E_n – reneutralization energy).

Table 2. 1. Calculated electron transport energies in atomic units for the series of16 different substituted benzenes.

Substituent	**Substituent Parameter Value** σ	E_v	E_a	E_n
hydroxy	-0.38	0.084	0.075	-0.066
amino	-0.30	0.094	0.037	-0.037
methyl	-0.14	0.041	0.084	-0.083
methoxy	-0.12	0.088	0.080	-0.070
hydrogen	0.00	0.092	0.093	-0.085
fluoro	0.15	0.074	0.065	-0.056
chloro	0.24	0.072	0.063	-0.053
acetoxy	0.31	0.033	0.015	-0.001
dichloromethyl	0.32	0.046	0.033	-0.032
difluoromethyl	0.35	0.075	0.035	-0.035
carboxy	0.44	0.032	0.013	0.006
trichloromethyl	0.46	0.034	-0.016	0.073
acetyl	0.47	0.030	0.014	0.001
trifluoromethyl	0.53	0.045	0.026	-0.032
cyano	0.70	0.039	0.029	-0.018
nitro	0.81	-0.034	-0.057	0.080
	R^2	**0.595**	**0.560**	**0.519**

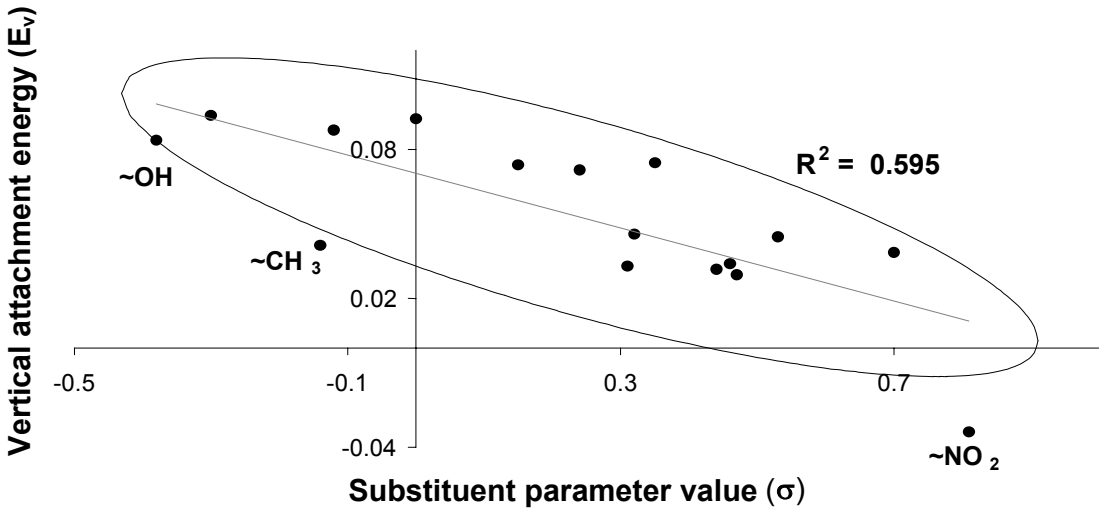

Figure 2. 3. Correlation of vertical attachment energy (Ev) in atomic units to substituent values (σ). The ellipse represents the 95.5% confidence interval.

As a check, calculations of E_v were repeated for 10 of the molecules (benzene molecules with the substituents: ~CH_3, ~NH_2, ~OH, ~H, ~F, ~Cl, ~$CHCl_2$, ~CHF_2, ~CF_3, and ~NO_2) using density functional theory (BL3LYP/6-311++G*) [60-63]. While the DFT calculations resulted in smaller values for E_v, they produced the same trend in the correlation of substituent parameters to electron attachment energies. Figure 2.4 shows the correlations of electron attachment energies (E_v) to σ, as calculated with DFT and HF theory, and their respective correlation coefficients squared.

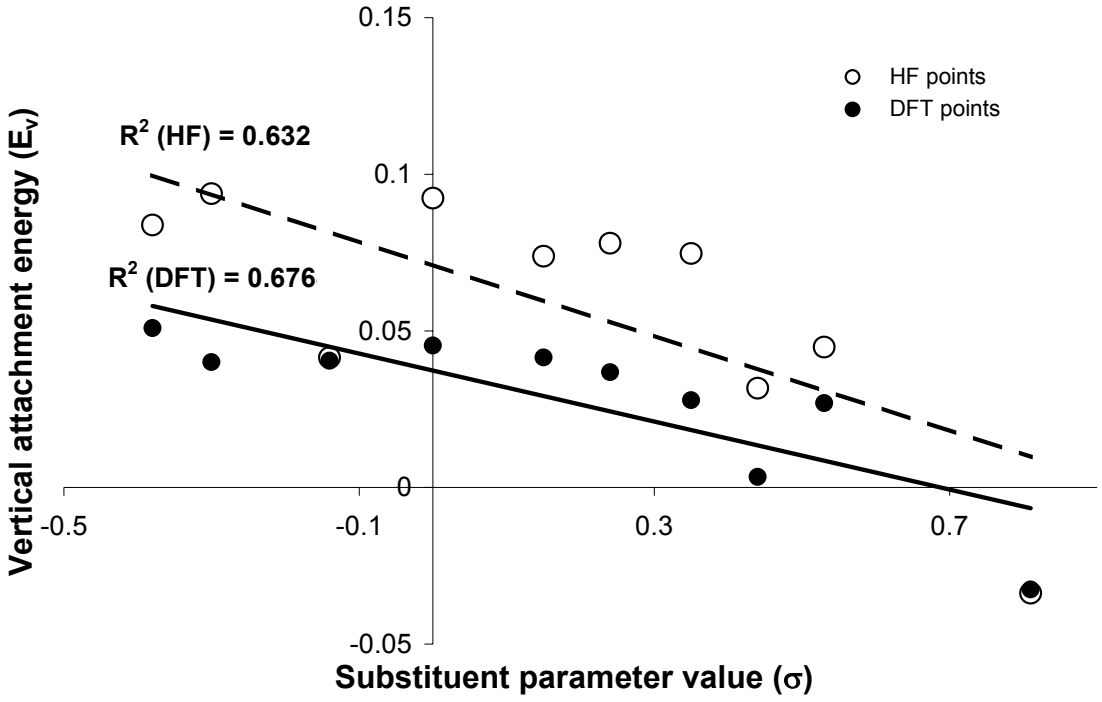

Figure 2. 4. Electron attachment energies (E_v) calculated by Density Functional Theory (DFT) and Hartree-Fock Theory (HF), correlated to the sigma parameter values (σ).

The observed trend is consistent with chemical intuition. In the presence of an electron-withdrawing substituent, the core of the molecule should be more positive and therefore be more favorable for electron attachment. Conversely, in the presence of an electron-donating substituent, the core of the molecule should be more negatively charged and less favorable for electron attachment. Figure 2.3 shows that attachment energies are indeed generally lower for systems with substituents of more positive σ.

The calculated E_v were also correlated to a different substituent parameter value; the resonance parameter (σ^-). This parameter accounts for the resonance interaction between a substituent and a negative (electron rich) site on a molecule [48, 78]. Since our working model of electron transport involves a one electron reduction, one might expect a better correlation using the σ^- values and in fact that is the case. As illustrated in Figure 2.5, for a subset of 12 substituents for which both parameter value types were available, (σ and σ^-) the correlation of E_v to σ^- has an $R^2 = 0.721$ and the correlation of E_v to σ has an $R^2 = 0.635$. The result demonstrates that the σ^- have a slightly improved correlation to the electron attachment energy, but a significance F-test revealed that the difference between the correlations was not statistically meaningful [77, 79].

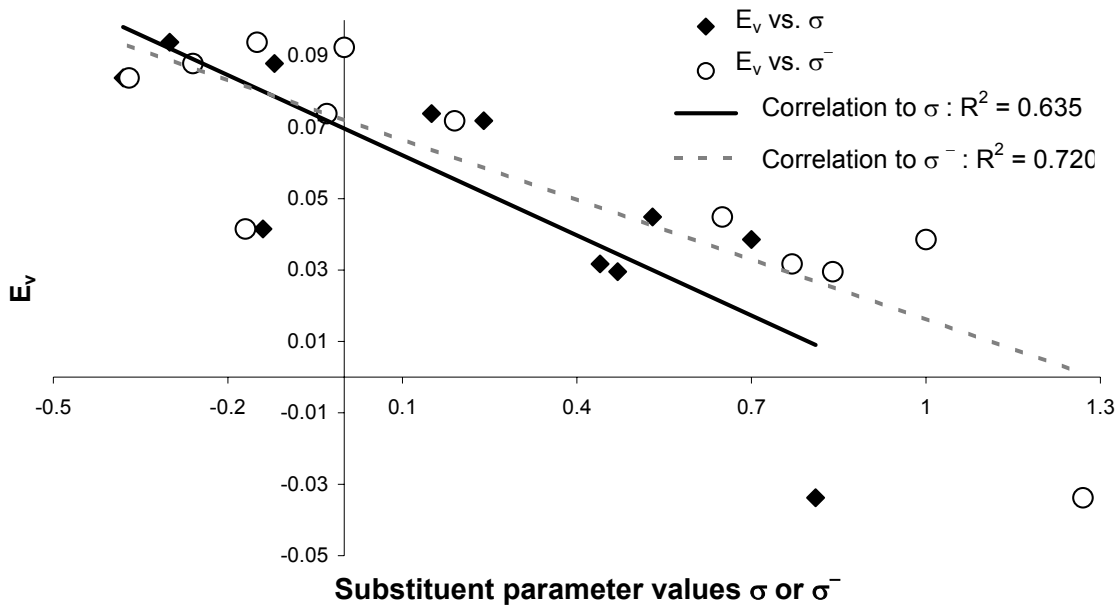

Figure 2. 5. Correlations of electron attachment energies (E_v) to σ and σ^- for 12 substituted benzene rings.

Ref. [46] suggests that NDR in a molecular junction is more probable for junction molecules with larger E_n. The above correlations suggest that to favor NDR one should consider substituents with high σ or σ^-. The electron withdrawing nature tends to stabilize the radical anion formed during electron transport giving rise to higher E_n.

2.3.2 Correlation of substituent parameter values to normalized charge transfer and molecular resistance

The electron transfer energies describe the energy profile experienced by an electron being transmitted across a molecule; therefore they implicitly contain information on the electron transport properties of a compound. Since we seek to determine the ability of sigma parameters to predict electron transport properties, a more desirable approach is to correlate the σ values explicitly to electronic transfer.

To validate our *ab initio* approach to the Gonzales and Morales semiempirical method of estimating electron transport, we performed calculations for their series of molecules, CH_3-$(HC{=}CH)_n$-COH with n = 1 to 10 and reproduced their normalized charge transfer (Q_r^n) results. Figure 2.6 shows a graphical comparison of normalized charge transfer, calculated by Gonzales and Morales and our *ab initio* implementation. The agreement is excellent.

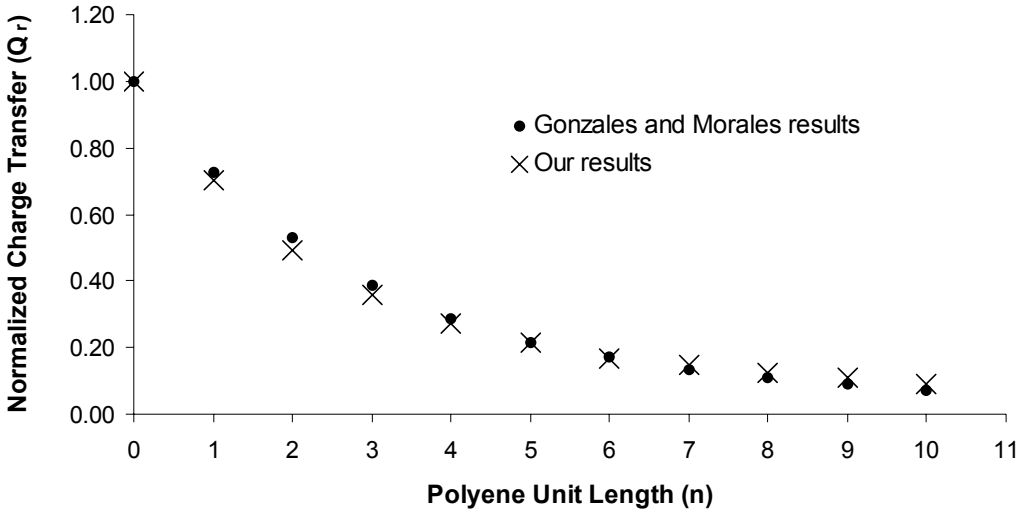

Figure 2. 6. Graphical comparison of normalized charge transfer (Q_r) calculations between the Gonzales and Morales result and our *ab initio* implementation.

The substituent effect on charge transfer and molecular resistance was next examined in a polyenic wire with a functionalized benzene ring embedded in it (see Figure 2.7). The charge transfer procedure was applied to the base molecule 5-(4-Penta-1,3-dienyl-phenyl)-penta-2,4-dienal, and to all the molecules resulting from the placement of 16 different substituents on the x site. Figure 2.7 shows the base molecule and the x site. The Q_r calculations on the 16 substituents resulted in the best correlation to the σ values with an R^2=0.863, which is illustrated in Figure 2.8. This correlation excludes the ~NO_2 substituent because it is an outlier at 95.5% confidence. Evidently the electron transport properties introduced by the ~NO_2 substituent are not wholly captured in its σ

value. The striking effect of the ~NO_2 group is further illustrated by looking at the molecular resistance (R_m) data. Figure 2.9 shows the plot of R_m vs. σ values. The substituent data points are the same as the ones on Figure 2.7. The high resistance result reflects the electron-withdrawing group's ability to accumulate charge before destabilizing the species; in essence behaving as an electronic charge sink.

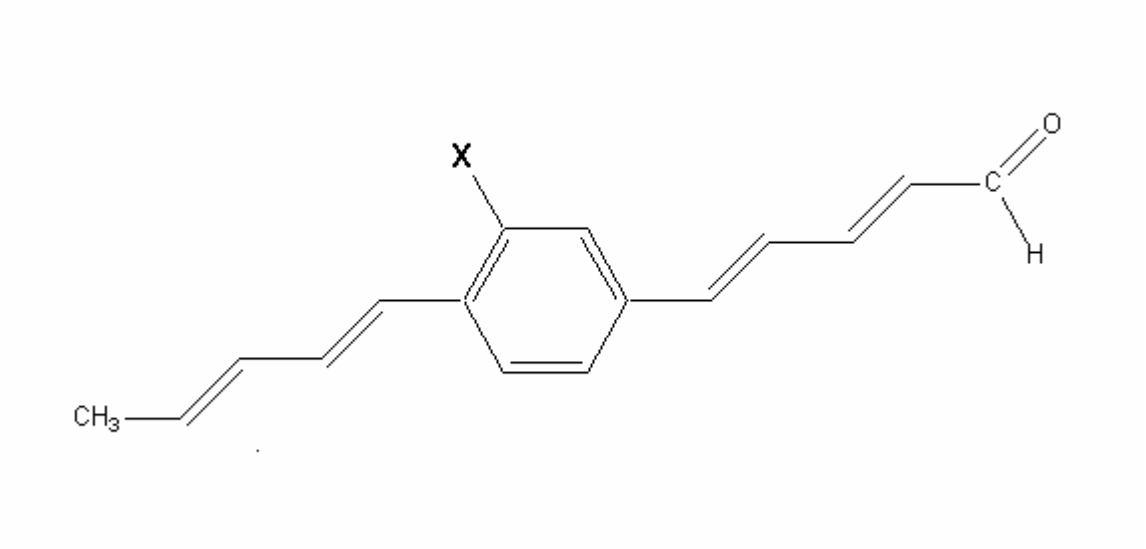

Figure 2. 7. The base molecule used in the normalized charge transfer (Q_r). The x site was replaced with the substituents ~OH, ~NH_2, ~CH_3, ~OCH_3, ~H, ~F, ~Cl, ~O_2CCH_3, ~$CHCl_2$, ~CHF_2, ~CO_2H, ~CCl_3, ~$OCCH_3$, ~CF_3, ~CN, and ~NO_2.

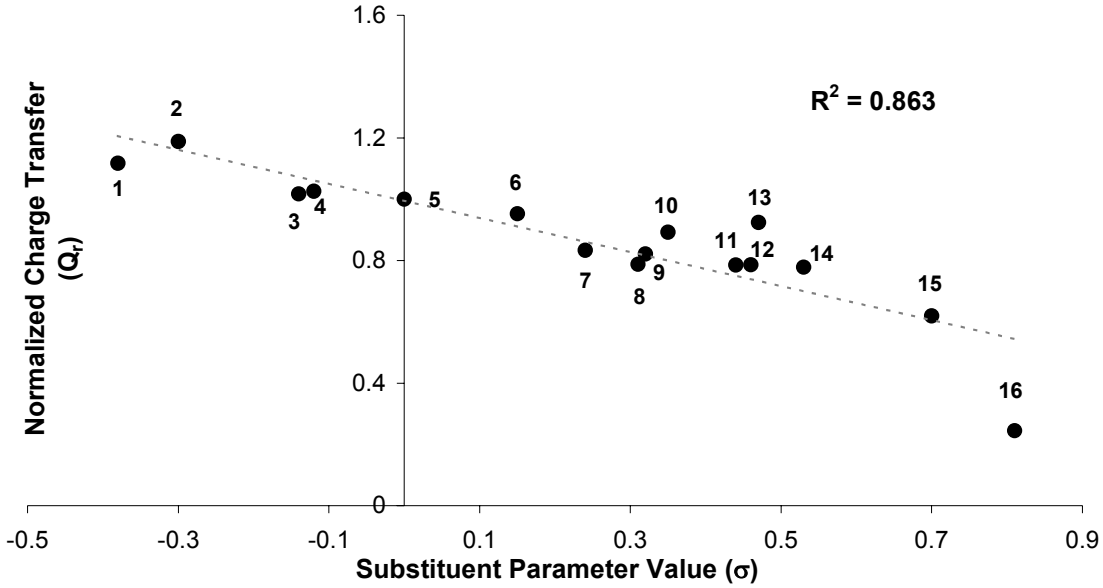

Figure 2. 8. Correlation of Normalized Charge Transferred (Q_r) to substituent parameter values (σ). The substituents are: 1= ~OH, 2= ~NH_2, 3= ~CH_3, 4= ~OCH_3, 5= ~H, 6= ~F, 7= ~Cl, 8= ~O_2CCH_3, 9= ~$CHCl_2$, 10= ~CHF_2, 11= ~CO_2H, 12= ~CCl_3, 13= ~$OCCH_3$, 14= ~CF_3, 15= ~CN, 16= ~NO_2.

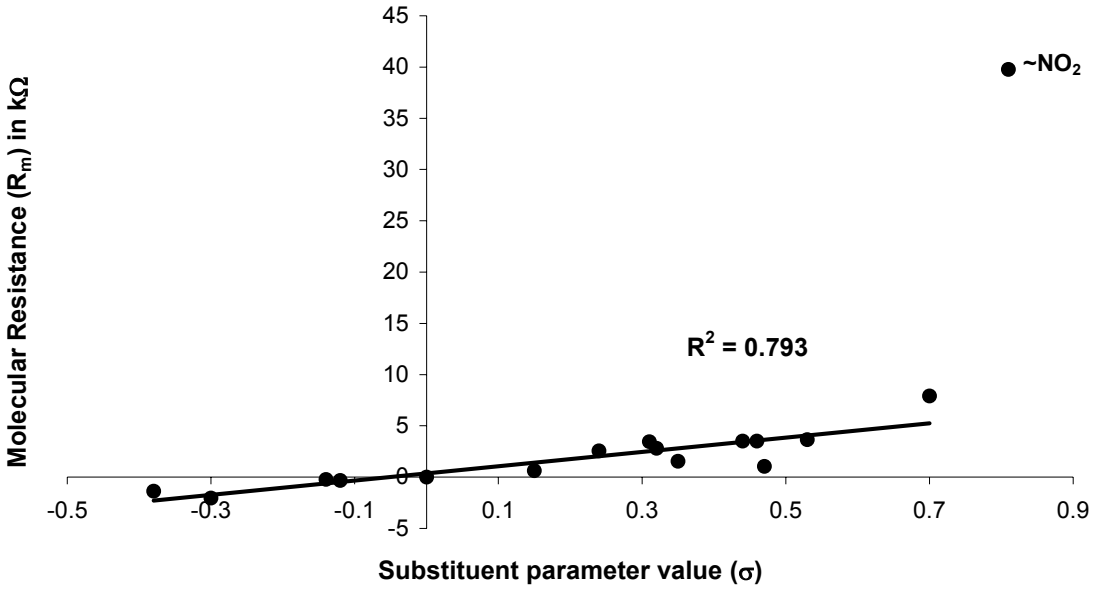

Figure 2. 9. Correlation of Molecular Resistance (R_m) to substituent parameter values (σ). The substituents appear in the order: ~OH, ~NH_2, ~CH_3, ~OCH_3, ~H, ~F, ~Cl, ~O_2CCH_3, ~$CHCl_2$, ~CHF_2, ~CO_2H, ~CCl_3, ~$OCCH_3$, ~CF_3, ~CN, and ~NO_2.

In conclusion, a priori selection of a molecule for use in an electronic device will require screening tools because of the large number of organic compounds that could be chosen. We have investigated the possible use of substituent parameter values (σ) as a predictor of the electron transport properties of molecules. We show that the energies controlling electron attachment and detachment correlate weakly to σ, but normalized charge transfer correlates strongly to σ. This work suggests that substituent parameter values may be of some value as an economical semi-quantitative predictor of electron transport properties.

Chapter 3. Time dependence of electron transport I: a molecular orbital basis.

3.1 Introduction

As outlined in the Introduction, to date there have been very few applications of time-dependent analysis to the study of electron transport properties in molecular electronic junctions. In this chapter, the application of time-dependent quantum mechanics to the study of electron transport across a molecular junction is reported.

Electron transport is investigated by following the time development of a localized electron wavefunction, which is expanded in a basis of eigenfunctions of the time-independent Hamiltonian for the entire device complex, (here referred to as the “supermolecule”). The electronic structure of the supermolecule is described with extended Hückel molecular orbital methodology, but two enhancements are required: First, high state density due to the presence of metallic clusters demands that orbital occupancy be set by Fermi-Dirac statistics. Second, the presence of an applied potential field requires that the Hamiltonian matrix be constructed in a charge-self-consistent manner. Variations in the junction molecule, contact geometry and applied potential are investigated. The results reveal: (i) no appreciable buildup of charge on the junction molecule in the presence of an applied potential and (ii) significant sensitivity of electron transport to the junction molecule/electrode contact geometry. The method (as well as its software implementation) is essentially completely general. There is no

requirement that the source of sink electrons be metallic, or even that the system to be studied bear any resemblance to nano-electronics at all, although that is the focus of this study.

3.2 Theoretical Methods

3.2.1 The model

We employ a cluster model of a molecular junction. In the cluster model, the metal electrodes on either side of the junction molecule are modeled as finite clusters of metal atoms. An example is shown in Figure 3.1. Collectively, we will refer to the metal electrodes *and* the junction molecule as the "supermolecule" or "device complex". To construct the model, the isolated dithiolated junction molecule (a single hydrogen atom replaces each metal cluster), is first optimized at the DFT-B3LYP/6-31G* level of theory [57-59]. The clusters are then constructed with the metal atoms fixed in a packing arrangement consistent with that of the pure metal. The cluster sizes must be chosen so that they are sufficiently large to exhibit bulk-like behavior. Our clusters include all atoms up to and including second-nearest neighbors to the junction molecule's binding site. This yields a cluster of 18 atoms exposing a (111) surface onto which the junction molecule is bonded. This choice of cluster size is supported by the work of Cheng and Wang, who report the onset of bulk-like behavior in the

photoelectron spectrum of finite metal clusters comparable to or smaller in size than those employed in the present thesis work [80].

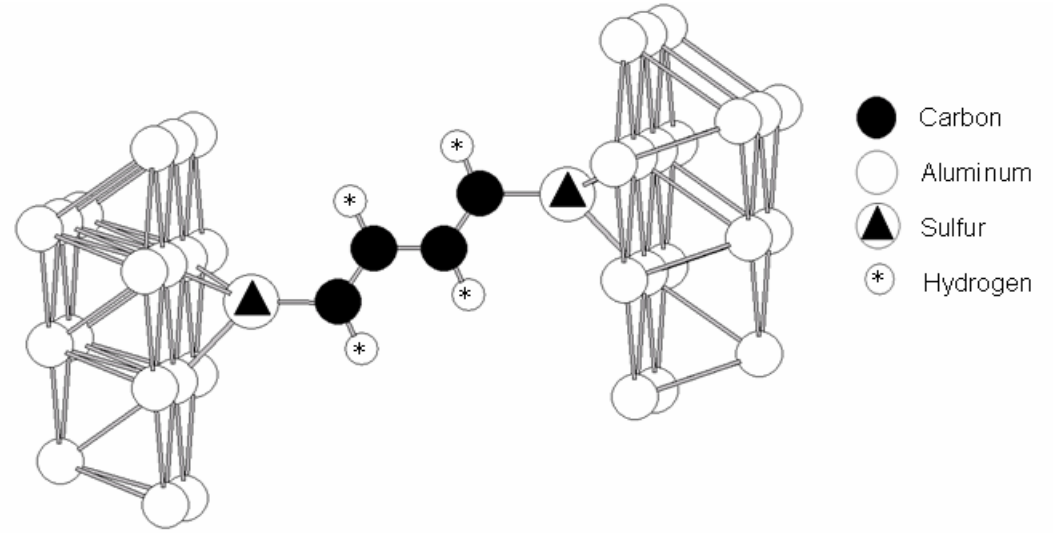

Figure 3. 1. Example of a molecular junction considered in this study. The metal electrodes are modeled as finite clusters of metal atoms and the molecule is geometry optimized.

As an additional check, a density of states (DOS) calculation was performed on the Al_{18}-(111) surface cluster. First, a single point energy calculation is carried out on the Al_{18}-(111) cluster with extended Hückel theory. Since there are 4 atomic orbitals assigned to every metal atom, the calculation generates 72 molecular orbitals and 72 state energies. The DOS is generated by adding up all the states that exist within a particular window of energy. Overlaps

between the energy windows (1 eV) are not used to calculate the Al_{18}-(111) DOS, therefore there is no smoothing, however, these conditions of energy window and overlap yield desirable features, as will be discussed [81]. Figure 3.2 shows the DOS for the Al_{18} cluster (solid line) and the bulk (111) surface (dashed line). The x-axis is the number of molecular orbitals present, and the y-axis is the average value for the corresponding energy interval. This was compared with a DOS calculation by Hammer *et al.* for an infinitely periodic model of the aluminum (111) surface [81, 82]. Comparing the two plots reveals the same qualitative features. The bulk calculation by Hammer *et al.* is performed on an effectively infinite surface. This yields a denser continuum of states so that peaks that are less well resolved than in the Al_{18} DOS. The Al_{18} cluster, however, shows relative peak and valley alignment to the DOS for the infinitely periodic surface, demonstrating that our metal cluster captures bulk-like electronic properties. Our electronic structure calculations for the supermolecules also give indications that the minimum cluster size to reasonably approximate a bulk metal electrode has been surpassed, (vide infra).

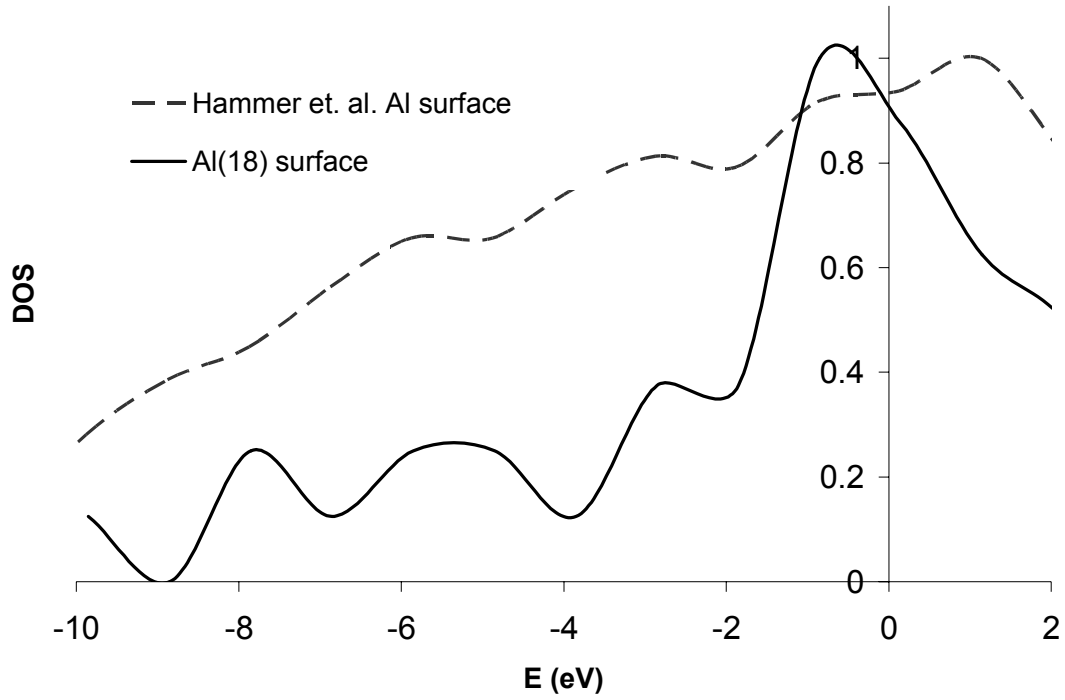

Figure 3. 2. Density of States (DOS) calculations for the Al_{18} cluster and an infinitely periodic Al (111) surface [81].

3.2.2 Time dependence

The time dependent description of electron transport through a molecular junction ultimately reduces to performing dynamical calculations that track the evolution (delocalization) of a localized electron's wavefunction by solving the time dependent Schrödinger equation (TDSE)

$$-i\hbar d\Psi(\mathbf{r},t)/dt = H\Psi(\mathbf{r},t). \quad (3.1)$$

Here “H” is the total energy operator and $\Psi(r,t)$ is the wavefunction, which depends on the spatial coordinates “**r**” and time “t”. In the case of a time-independent Hamiltonian, the wavefunction $\Psi(\mathbf{r},t)$ is separable into spatial ($\Phi(\mathbf{r})$) and time-dependent ($T(t)$) parts and may be written

$$\Psi(\mathbf{r},t) = T(t)\Phi(\mathbf{r}). \tag{3.2}$$

If we denote the eigen-solutions of the time-independent Schrödinger equation (TISE) as $\phi_k(\mathbf{r})$ so that

$$H\phi(\mathbf{r}) = E\phi(\mathbf{r}), \tag{3.3}$$

we may write the spatial part of the time-dependent wavefunction in the form of an expansion in a basis of eigenfunctions $\phi_k(\mathbf{r})$ of the time-independent Schrödinger equation

$$\Phi(\mathbf{r}) = \Sigma_k\, b_k\phi_k(\mathbf{r}). \tag{3.4}$$

Here the b_k are the expansion coefficients of the localized electron at time t=0. In essence they are the contributions from each molecular orbital to the wavefunction of the spatially restricted electron. Substitution of this expansion into the TDSE and separation of variables yields,

$$\Psi(\mathbf{r},t) = \Sigma_k\, b_k\, [\exp(-iE_kt/\hbar)]\phi_k(\mathbf{r}). \tag{3.5}$$

Equation 3.5 is completely general and in the limit of an infinite expansion gives an exact solution of the TDSE.

We employ a one-electron (extended Hückel) treatment, so in our case the $\phi_k(r)$ are molecular orbitals of the device complex and the E_k are their

corresponding orbital energies. Perhaps the most intuitive description of the spatial distribution of the electron wavefunction is in terms of atomic orbitals. To facilitate this description, the ϕ_k may in turn be written as a linear combination of "n" atomic orbitals (χ_n)

$$\phi_k = \Sigma_i \, c_{ki}\chi_i \tag{3.6}$$

The first step is therefore to carry out an electronic structure calculation on the device complex to find its molecular orbitals ϕ_k in a basis of atomic orbitals χ_i. The time dependence of the localized electron wavefunction in terms of the atomic orbital basis, is found by substitution of equation 3.6 into equation 3.5 and is given by,

$$\Psi(\mathbf{r},t) = \Sigma_i \; [\Sigma_k \, b_k c_{ki} \, (\exp(-iE_k t/\hbar))]\chi_i(\mathbf{r}) \tag{3.7}$$

In more compact notation, we may write

$$\Psi(\mathbf{r},t) = \Sigma_i \, d_i(t)\chi_i(\mathbf{r}), \tag{3.8}$$

where

$$d_i(t) = \Sigma_k \, b_k c_{ki} \, (\exp(-iE_k t/\hbar)). \tag{3.9}$$

This representation is useful because it allows us to partition the wavefunction for the non-stationary electron into contributions from each atomic orbital, and to do so at any time. In chemical terms, it allows us to speak of the electron moving across the molecular space through the atomic orbitals.

3.2.3 Specifying the initial localization of the electron

Representation of the wavefunction in an atomic orbital (AO) basis also facilitates setting the initial conditions, i.e. localizing the electron. We may localize the electron by selecting coefficients a_i such that the localized electron wavefunction f is given by

$$f = \Sigma_i \, a_i \chi_i \tag{3.10}$$

For example, we may "place" the electron initially into a specific atomic orbital "i" by setting $a_i = 1$ and the remaining $a_j = 0$. To time propagate this localized wavefunction by the method described above, we must express *f* in the molecular orbital (MO) basis,

$$f = \Sigma_k \, b_k \phi_k. \tag{3.11}$$

This is done with the usual transformation of basis. We integrate over the localized electron wavefunction f with an arbitrary molecular orbital ϕ_n and equate to the case where f is expanded in an MO basis by

$$\int \phi_n f d\tau = \int \phi_n \Sigma_k \, b_k \phi_k d\tau = \Sigma_k \, b_k \int \phi_n \phi_k d\tau. \tag{3.12}$$

Here the integral with volume element $d\tau$ is over all electronic coordinates. Since the MOs form an orthonormal basis, $\int \phi_n \phi_k d\tau = \delta_{nk}$ and it follows that,

$$b_n = \int \phi_n f d\tau \tag{3.13}$$

or in expanded form,

$$b_n = \int (\Sigma_k \, c_{nk} \chi_k)(\Sigma_i \, a_i \chi_i) d\tau. \tag{3.14}$$

Exchanging the order of integration and summation yields,

$$b_n = \Sigma_k \, \Sigma_i \, c_{nk} \, a_i \int \chi_k \chi_i \, d\tau = \Sigma_k \, \Sigma_i \, c_{nk} \, a_i \, S_{ki}. \tag{3.15}$$

where S_{ki} is an overlap integral over AO basis functions. This is the result we seek. The coefficients of the expansion of the localized wavefunction in the MO basis are given in terms of a simple summation over overlap integrals. The c_{nk} and overlap integrals are “free” since they are products of the electronic structure calculation for the supermolecule. We may place the electron in any linear combination of AOs by specifying the a_i and easily transform this expansion into the MO basis with equation 3.15. The time propagation of the initially localized wavefunction is then given exactly by equation 3.11.

3.2.4 Determining time-integrated atomic-orbital occupancy probability

From the time development of the electron wavefunction, we seek answers to questions such as, “Given an electron initially localized on the donor electrode, what is the probability that it has reached the acceptor electrode after time Δt?”

It is a trivial matter to calculate the probability $\rho_i(t)$ for the occupancy of a given AO (index i) at time t. The probability is simply the norm of the expansion coefficient of that particular AO in the time dependent wavefunction at the specified value of t, in other words,

$$\rho_i(t) = [d_i^*(t)d_i(t)]. \qquad (3.16)$$

Here “*” denotes complex conjugation. We note that if a set of independent samplings of a system yield probabilities ρ_i that a particular state of

the system is sampled, the time integrated probability that the state has never been occupied P_i^{not} after N samplings is

$$P_i^{not} = \Pi_{t=1..N} [1-\rho_i(t)]. \quad (3.17)$$

In the case of our expansion in an atomic orbital basis, the probability that orbital χ_i is not occupied at time t is given by

$$\rho_i^{not}(t) = 1- d_i^*(t)\, d_i(t). \quad (3.18)$$

If we assume that the occupancy of χ_i at time t is independent of the probability of its occupancy at t-δt, the probability that χ_i has never been occupied over a set of times t is given by

$$P_i^{not} = \Pi_t(1- d_i^*(t)\, d_i(t)). \quad (3.19)$$

This probability will go asymptotically to zero as the number of sampling times increases.

Obviously, the assumption that the occupancy of χ_i at time t is independent of the probability of its occupancy at t-δt is not generally valid. Consider a stationary state. If the contribution of orbital i is d_i at time t, it will be d_i at all future times t+δt as well. In this case, the occupancy of χ_i at time t is perfectly correlated to the probability of its occupancy at t-δt and P_i^{not} = (1- $d_i^*(t)$ $d_i(t)$), with no time product.

The above two cases represent two extremes. We require a technique for computing the time integrated probabilities that accounts for the possibility that the occupancy of an orbital at time t is, to some degree, *correlated* to the probability of its occupancy at t-δt. One approach is to sample the time dependent wavefunction at very widely spaced times (δt very large) so that the

approximation of independence is more likely to be valid, but a more rigorous and efficient approach is to account for the correlation. To do so we define the correlation factor $\kappa(t)$ where

$$\kappa(t) = \{ [d(t)\cdot d(t-\delta t)]^{*} \; [d(t)\cdot d(t-\delta t)]\}^{1/2} \qquad (3.20)$$

We note that $\kappa(t) = 1$ for a stationary state and $\kappa(t) = 0$ if the wavefunction at time t is orthogonal to (completely uncorrelated with) that at $t - \delta t$. The norm is used since $d(t)\cdot d(t-\delta t)$ is, in general, complex. We employ the correlation factor to attenuate adjacent factors in the time product by the degree to which they are correlated, $(1.-\kappa(t))$. The time integrated probability that state "i" has never been occupied in a set of discrete samplings in time, is given by

$$P_i^{not} = \Pi_t\{1- \; [d_i^{*}(t)\; d_i(t)] \; [1.-\kappa(t)]\}. \qquad (3.21)$$

3.2.5 Determining the time-independent MOs of the supermolecule

We employ a charge-self-consistent implementation of the semi-empirical Mulliken Wolfsberg Helmholtz (a.k.a. "MWH" or "Extended Hückel") electronic structure method to construct the molecular orbitals of the supermolecule [83]. In this method, experimental data is used to simplify the construction of the energy matrix (H). The elements of H are given by

$$H_{ij} = \left\langle \chi_i \left| \hat{H} \right| \chi_j \right\rangle . \qquad (3.22)$$

The diagonal elements (H_{ii}) are approximated by the negative of the valence orbital ionization energy (VOIE) for the corresponding atomic orbital $\chi_{i\,[83]}$. The

off-diagonal elements are taken to be overlap-weighted averages of the corresponding VOIE values according to the standard MWH formula with the Wolfsberg-Helmholtz constant set to the usual 1.75 [83].

One implication of using VOIEs is that all atoms of an element will be assigned the same orbital ionization energy regardless of their location in a molecule, resulting in a method that is insensitive to an atom's chemical environment, an assumption that is not generally valid. For example, in regions of low charge density we may expect the effective ionization energy to increase, since removing an electron from a positively charged center requires more energy than removing an electron from a neutral center. Conversely, in regions of increased electron density, we may expect the effective ionization energy to decrease, since removal of an electron from a negatively charged center requires less energy than from the corresponding center when neutral. To account for this effect, a self-consistent charge (SCC) procedure was employed in the construction of the energy matrix. In the SCC procedure, the diagonal elements of the energy matrix are assumed to have quadratic dependence on the atomic charge (q)

$$H_{ii,n}(q_n) = -(A_{i,n}q_n^2 + B_{i,n}q_n + C_{i,n}). \qquad (3.23)$$

Here "n" is the atom index and "i" denotes the specific atomic orbital. The constants $A_{i,n}$ and $B_{i,n}$ are derived from electronic structure calculations for the cation, neutral and anionic forms of an isolated atom of the same type as atom "n" and are taken from published tables [83]. $C_{i,n}$ is the regular VOIE for an orbital of type i on an neutral atom of type n. As a practical matter, the electronic

structure code initially assumes uncharged atoms (q_n=0). From equation 3.23, when orbital "i" is centered on an uncharged atom n, $H_{ii,n} = -C_{i,n}$. The program computes the molecular orbitals, and based upon a subsequent population analysis, the resulting atomic charges (q_n). The $H_{ii,n}$ are reset based on these charges by using equation 3.23, H is reconstructed, and the molecular orbitals are recomputed, resulting in new atomic charges. The process is iterated to self-consistency. By considering atomic charge, a property that depends on the atomic arrangement, equation 3.23 accounts for the influence a chemical environment has on the energy of an atom's electron. As described in the Results and Discussion section (3.3.1), the self-consistent charge (SCC) procedure makes a significant improvement in the electronic structure description over what is achieved with a traditional MWH calculation. It is also critical in cases of a finite applied potential, as will now be discussed.

3.2.6 Applying a Potential

The driving force for electron transport across a molecular junction arises from establishing a difference in potential between the two electrodes. In order to mimic this experimental condition the metal clusters are placed at different potentials. As an initial guess, the potential drop is distributed linearly across the intervening junction molecule. To do so, the device complex is aligned so that the electrodes are parallel to the y-z plane and the molecule's longest dimension is aligned with the x-axis. In cases where the junction molecule is not perfectly

planar, the molecule's average plane is calculated along the longest dimension, and aligned to the x-z plane. Figure 3.3 shows the alignment and reference coordinate system for the benzene-1, 4-dithiol (BDT) complex. The potential drop therefore occurs along the x-axis, which is perpendicular to the electrodes.

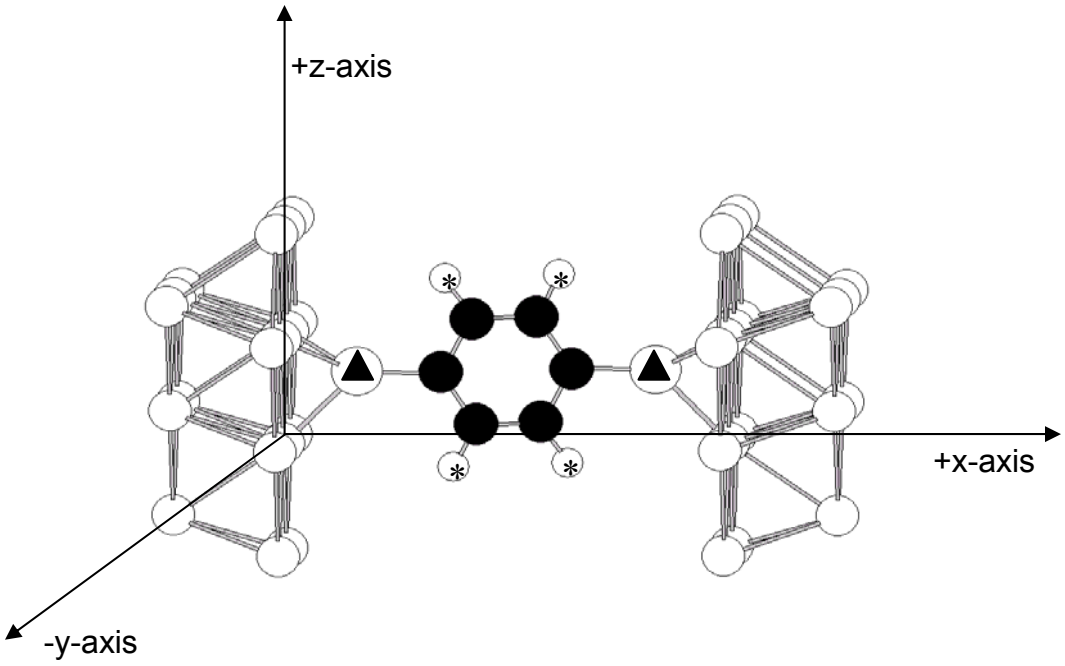

Figure 3. 3. Reference coordinate system for the benzene-1, 4-dithiol (BDT) complex. Black spheres are carbon, white spheres are aluminum, triangles are sulfurs and asterisks are hydrogens.

The voltage is applied (V_{ap}) across the molecule by choosing one reference atom at each electrode. In this study, the reference atoms are the

aluminums ligated to the sulfurs at the terminal ends of the junction molecule. $V_{ap}/2$ is subtracted from the low potential electrode and added to the high potential electrode, which results in a potential difference equal to V_{ap} across the junction. The initial variation in potential is a linear between the electrodes, i.e. the potential depends linearly on the x-coordinate. This relationship is used to determine V_{ap} for every atom in the junction molecule.

We next rewrite equation 3.23 to account for V_{ap}. Under a finite applied potential, the H_{ii} are dependent on charge and position and have the form

$$H_{ii,n}(x_n, q_n) = A_{i,n}q_n^2 + B_{i,n}q_n + C_{i,n} + V_{ap}(x_n) \qquad (3.24)$$

where "i" is the atomic orbital index with atomic position x_n. The energy matrix is iterated to charge self consistency as discussed in the previous section.

The use of a self-consistent charge procedure requires a second modification of the standard MWH method. The atomic charges are approximated by an atomic orbital population analysis, which depends on the molecular orbital occupancies. In the canonical SCC procedure, the MO populations are set by assuming a ground state occupancy vector, that is, the lowest N/2 MOs (N is the total number of electrons) are full and form the occupied space. The remaining MOs are empty and form the virtual space. The energetic region between the occupied and virtual space is the HOMO-LUMO gap (analogous to the band gap in a solid). During the self-consistent charge procedure, if the ordering of the MO energies changes so that orbitals become degenerate or close to degenerate within the gap, the ground state configuration (as defined by the occupancy vector with the lowest corresponding energy) may

change from one iteration to the next. This gives rise to a discontinuous change in the charge distribution as a function of orbital energy. The self-consistent charge procedure may therefore jump back and forth among two or more configurations and never achieve convergence. In our representation of a molecular junction, the problem is particularly acute because the presence of two large clusters of metal atoms (the donor and acceptor electrodes) means that there is very high state density at the Fermi level, the threshold between the occupied and virtual spaces. In fact, if the state density is not high it is a clear indication that the donor and acceptor clusters are not sufficiently large to adequately approximate metallic electrodes. A valid cluster model therefore essentially guarantees this orbital crossing problem. The problem is further exacerbated by an applied potential.

The root of the convergence problem is the discontinuous change in the charge distribution with orbital energy. To resolve the problem, we employ an occupancy vector whereby the MO occupancies are allowed to be fractional, and because electrons are fermions, the occupancies are set by Fermi-Dirac statistics. In this way the orbital occupancies vary continuously (between 0 and 2) with orbital energy. Setting the orbital occupancies requires setting the Fermi level (an insightful discussion may be found in Ref. [28]) and this has been a matter of considerable debate in the molecular electronics community. *Within our description of the molecular junction, we employ a method of setting the Fermi level that is rigorous and parameter-free*. The Fermi level is initially set by assuming a ground state occupancy vector and placing the Fermi Level in the

middle of the HOMO-LUMO gap. The occupancies of the MOs of the supermolecule are set by Fermi-Dirac statistics and the total occupancy is then computed. If the total occupancy exceeds the number of electrons in the device complex, the Fermi level is lowered. If the total occupancy is less than the total number of electrons in the supermolecule, the Fermi level is raised. The procedure is iterated until the total occupancy is equal to the total number of electrons in the device complex to within a specified convergence criterion (typically 1×10^{-5} elementary charge units). We have found that the SCC procedure typically converges in 20-30 iterations when employing the Fermi-Dirac occupancy vector. In its absence, even with complicated momentum-weighted optimization schemes, the convergence often required 1000 or more iterations, if it could be achieved at all.

3.3 Results and Discussion

3.3.1 Code validation

We first note that with the SCC and Fermi-Dirac occupancy vector procedures turned off, the electronic structure code is a generic extended Hückel molecular orbital program and gives results in essentially exact agreement with commercial codes [84]. This code has been used successfully over many years for MO calculations [46, 85-87]. Next we observe that performing the SCC procedure results in molecular orbital energies that are closer to those obtained

by more accurate first-principles electronic structure calculations. Figure 3.4 shows the HOMO through HOMO(-4) molecular orbital energies for an isolated water molecule as calculated by Extended Hückel Theory (EHT), our code with the SCC implementation, and density functional theory (DFT) at the B3LYP/6-31G* level of theory [57-59, 62]. Note that the SCC procedure offers a more accurate representation of the electronic structure than can be obtained by EHT alone.

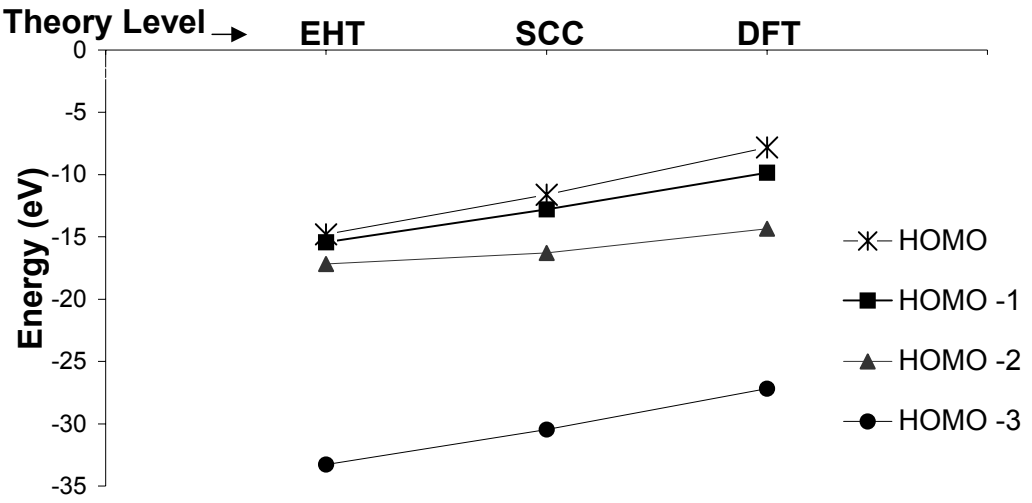

Figure 3. 4. Molecular orbital (MO) energies for the water molecule at three levels of theory. Note that the use of self-consistent-charge leads to a significant improvement in the accuracy of the MO energies, where first-principles density functional theory (DFT) calculations are used as a benchmark. The MOs shown are the 4 highest occupied molecular orbitals (HOMO to HOMO-3)

3.3.2 Influence of an applied potential on the electronic structure and charge distribution

Before investigating the time dependence of electron transport, we performed calculations to examine how an applied potential (V_{ap}) affects the steady-state distribution of charge across a molecular junction. The molecular junction was modeled as a single molecule sandwiched between two clusters of aluminum atoms and bonded to each cluster through a thiol linkage (Figure 3.5). Each cluster is made up of 18 aluminum atoms arranged in the native face-centered cubic close packing arrangement with the (1,1,1) Miller surface exposed. Each cluster contains all second-nearest-neighbors to the terminal sulfur atoms in the molecule, which form the contacts between the junction molecule and the electrodes. Benzene (as benzene-1, 4-dithiol or BDT) and butane (as butane-1, 4-dithiol or BuDT) were employed as junction molecules. The applied potential V_{ap} was varied from 0.0 to 3.0 (V). Figure 3.5 (two panels) shows a surface plot representing the change in charge from the zero-applied–potential case as a function of V_{ap} and the x-position across the junction. The inserts show the dithiol-molecular complexes used in the calculations. The results demonstrate that in both cases, the molecule behaves remarkably like a conducting wire, transferring charge from donor to acceptor electrode while exhibiting no marked charge buildup. This result is consistent with the widely discussed hypothesis that resistance in a molecular junction is predominantly due to the contacts, provided there is a conduction channel available through which charge can flow [31]. It also agrees with earlier theoretical calculations

showing that a benzene-1,4-dithiol in contact with two gold electrodes exhibits little charge buildup in the conjugated ring due to charge transfer from the Au [33].

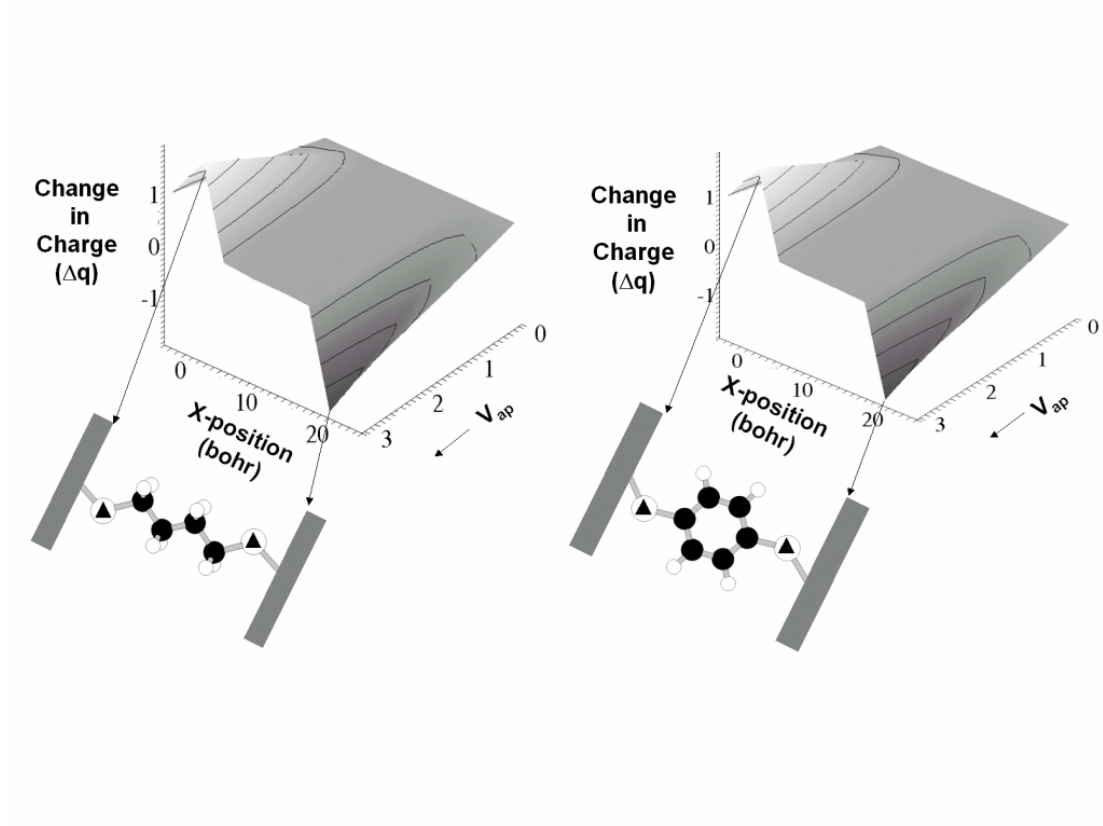

Figure 3. 5. Left panel – Butane-1,4-dithiol (BuDT) molecular junction and the spatial redistribution of charge under various applied potentials. Right panel - same for benzene-1,4-dithiol (BDT) molecular junction. Black spheres are carbon, white spheres are hydrogen, and triangles are sulfurs. 1 bohr = 0.5292 Å.

Based upon calculations with the SCC procedure on smaller systems, we analyzed the molecular orbital energies for a BDT junction as a function of the applied potential. Figure 3.6 shows the molecular orbital fluctuations in the Fermi region of the device. Figure 3.7 shows how the HOMO-LUMO gap changes with applied potential for BDT. The insert is the junction used in the calculation. There are significant fluctuations in the molecular orbital energies and even orbital crossings. This reveals why Fermi-Dirac statistics are necessary when assigning electron occupancy; there is a high density of states around the Fermi level. In fact, before the Fermi-Dirac implementation, convergence was impossible around Vap = 2.0 V (i.e. where the HOMO-LUMO gap $\approx$ 0.0).

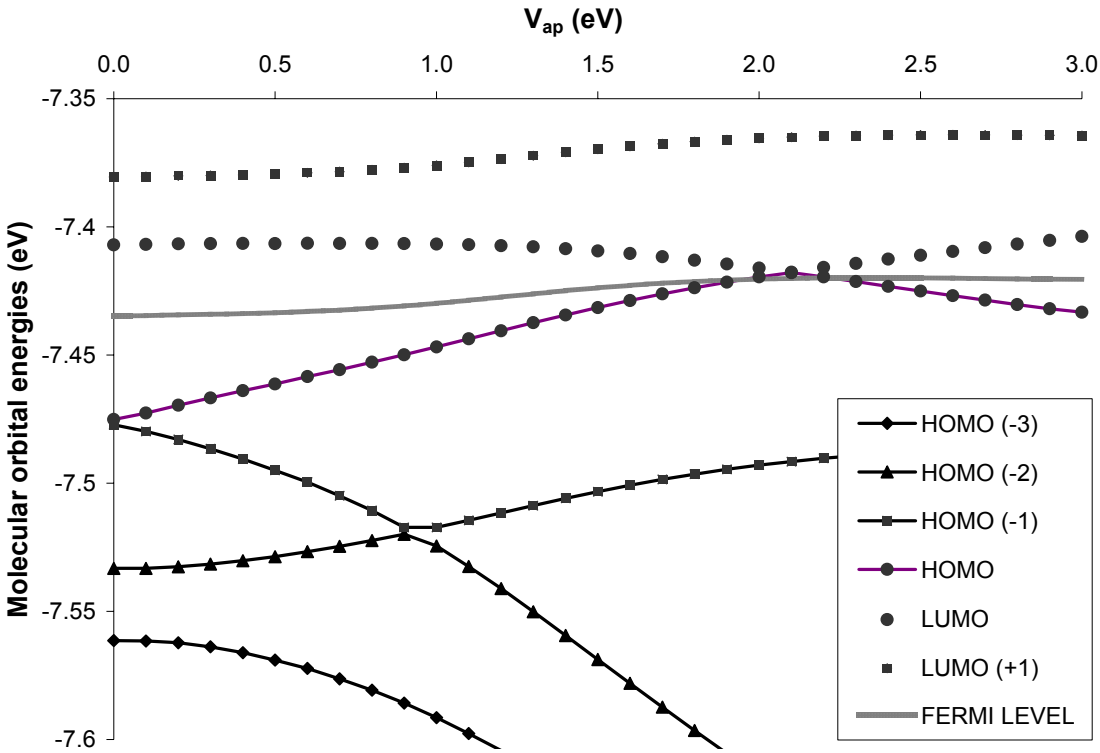

Figure 3. 6. Molecular orbital fluctuations in the Fermi region of the benzene-1,4-dithiol (BDT) molecular junction.

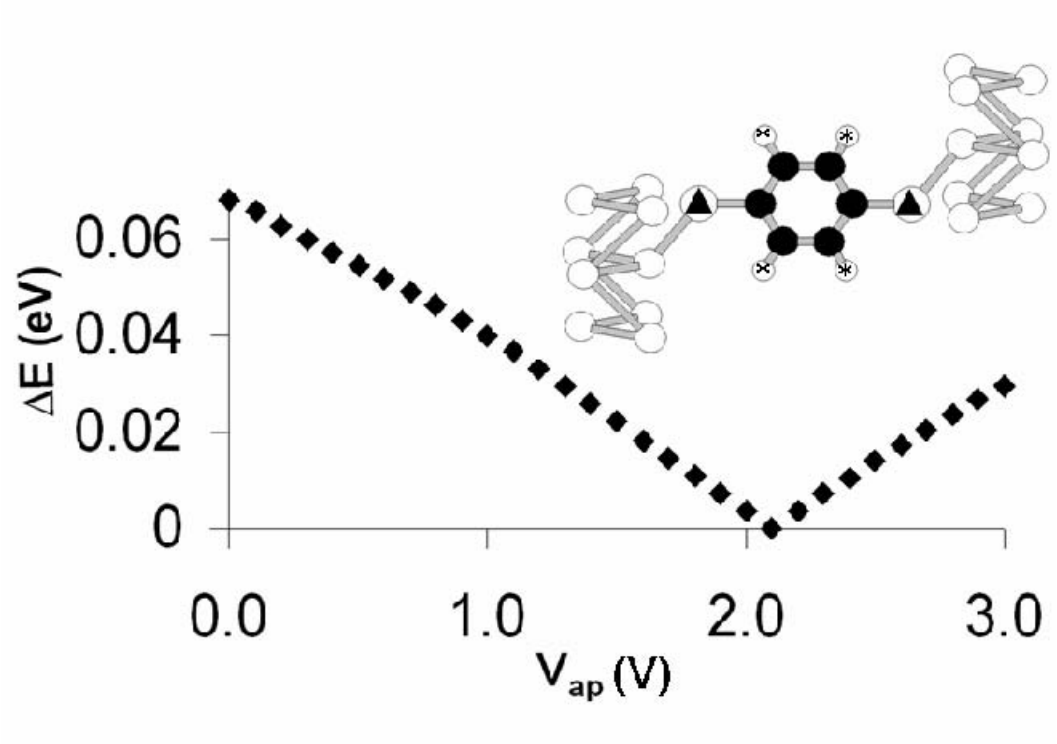

Figure 3. 7. Difference between LUMO and HOMO (band gap or ΔE) as a function of V_{ap} in the BDT device complex. Atom identities are indicated in Fig. 3. 1.

Next we consider the effect of V_{ap} on the time dependence of electron transfer. An electron is initially localized onto the donor electrode and the TDSE solved to reveal its time evolution. Figure 3.8 shows the integrated probability that the transported electron has reached the acceptor electrode as a function of time. For BDT it takes 150 atomic time units (2.4189×10^{-17} s = 0.024189 fs) to reach the acceptor, (time when probability exceeds 90%) at V_{ap} = 1.0. The process is approximately 33% longer in BuDT at the same V_{ap}. These processes are on the order of a few femtoseconds, in excellent agreement with known

transit times in molecular junctions [88, 89]. It is worth noting that such transit times are orders of magnitude shorter than most molecular vibrational periods, i.e. the molecule is essentially rigid for the duration of the electron transport event. We also note that the transport time in BDT is unaffected by V_{ap}.

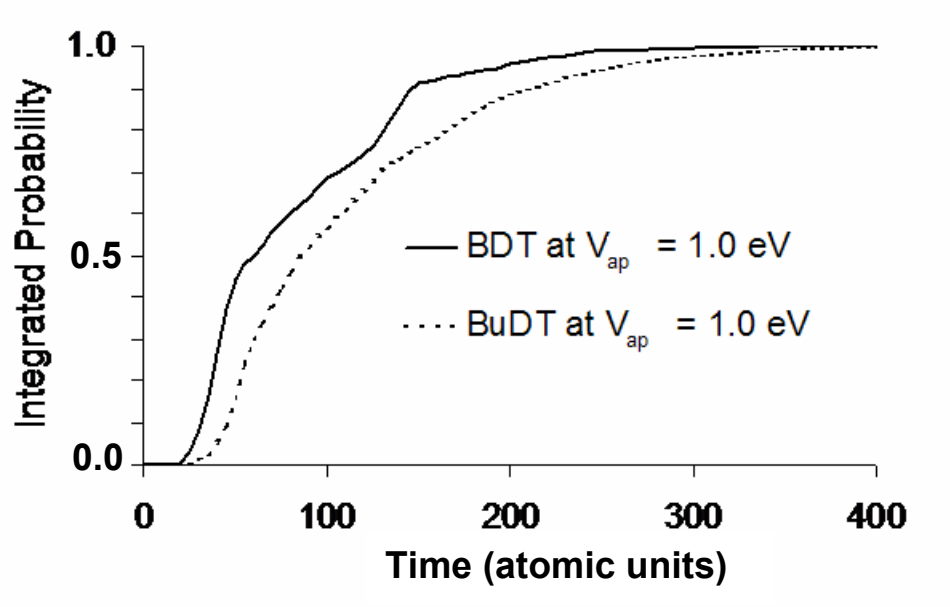

Figure 3. 8. Integrated probability on acceptor orbitals as a function of time (in atomic units) for the benzene-1,4-dithiol (BDT) and butane-1,4-dithiol (BuDT) supermolecules.

3.3.3 Influence of contact geometry and junction molecule length

To investigate the effects of contact geometry effect and junction molecule length on the time dependence of electron transport, we used the polyacetylenic

series MC-S-$(CH=CH)_n$-S-MC (where n=1 to 10) as the junction molecules and MC are the metal clusters. For the electrodes, we employed 18-atom-aluminum (Al) clusters exposing the (1,1,1) Miller face. Again, these clusters include all the second-nearest-neighbors to the Al atoms involved in bonding to sulfur. We considered two contact geometries: type I - sulfur (S) complexed to a triad of aluminum atoms (a nominal *hcp* site), and type II - sulfur bonded straight onto an aluminum atom (referred to as an "*atop*" site). Two sets of devices were then assembled by placing the n=1 to10 polyacetylenic series between electrodes in both types (I and II) of contact geometries. Figure 3.9 (2 panels) shows the two device types for the n=2 junction molecule. The bond length between S and Al (2.284 Å) was obtained from the average Al-S distance in the Al_2S_3 crystal structure obtained by Krebs et al. [90].

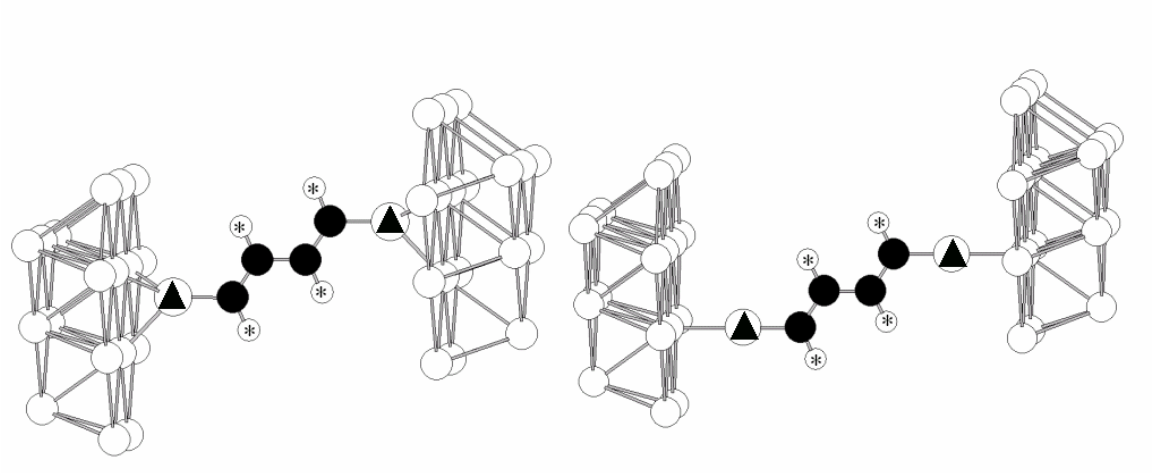

Figure 3. 9. MC-S-$(CH=CH)_n$-S-MC where n=2 device in the different contact geometries. Left panel – S bonded at *hcp* site, which is over the aluminum triad center. Right panel – S bonded on *atop* site. Atom identities are indicated in Figure 3.1.

We calculated the time dependence of electron transport for the polyacetylenic series MC-S-$(CH=CH)_n$-S-MC for two different contact geometries as shown in Figure 3.9. We performed all calculations at V_{ap}=0.0 because of the result in the previous section suggesting that transport times of conjugated molecules do not depend appreciably on V_{ap}.

Figure 3.10 shows the time required to reach 95% probability as a function of acetylene unit n for both contact geometry types. The result is consistent with the expectation that as the molecule increases in length, the transport time increases in an approximately linear fashion. Note that there is an appreciable difference in transport time between the *hcp* and *atop* bonded junction molecules, and that transport time is shorter when the contact geometry is *atop*.

This is theoretical confirmation of the widely discussed hypothesis that contact geometry strongly influences the electron transport in molecular junctions.

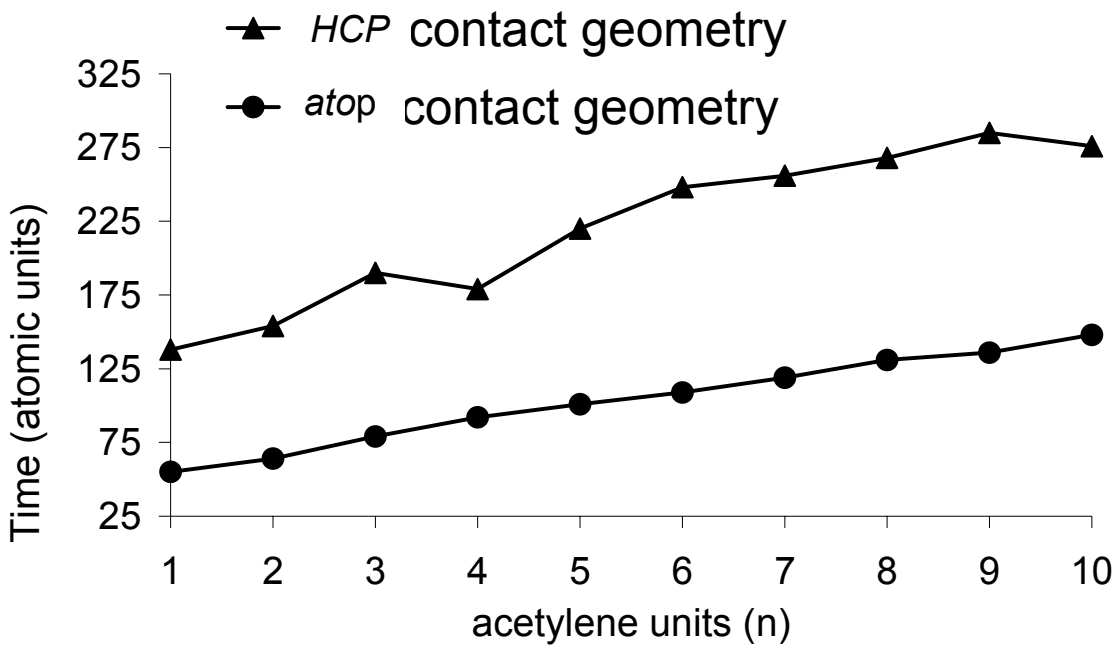

Figure 3. 10. The time required to attain 95% probability as a function of acetylene unit "n" for the *hcp* and *atop* contact geometries.

3.3.4 The substituent effect

We also considered the effect of chemical substituents on the junction molecule on time-dependence of electron transport. It was reported in chapter 2

that tabulated substituent parameters correlate well with charge transfer for a donor group to an acceptor group in donor-bridge-acceptor systems, where the bridge contains a substituted aromatic ring [47]. For the present study, the 2- [4-(2-mercapto-vinyl)-phenyl]-ethenethiol species was used as the base molecule and placed between two 18-atom Al clusters with the sulfurs bonded at the *hcp* site. Figure 3.11 shows the base device complex. The x represents the position at which 10 chemical groups were placed in order to examine the substituent effect on the time-dependence of electron transport. The substituent groups (~x) considered were: ~OH, ~CH_3, ~OCH_3, ~H, ~F, ~Cl, ~COOH, ~CF_3, ~CN, and ~NO_2. The time dependence of electron transport for the substituted aromatic wires was calculated, and the results were correlated with tabulated substituent parameters. No statistically significant correlation was found between substituent parameter value and the time required (time when probability exceeds 90%) for the transported electron to reach the acceptor electrode. The average value was calculated to be 286 atomic time units for the electron transport event to take place, relatively independent of (data not shown) the chemical substituent.

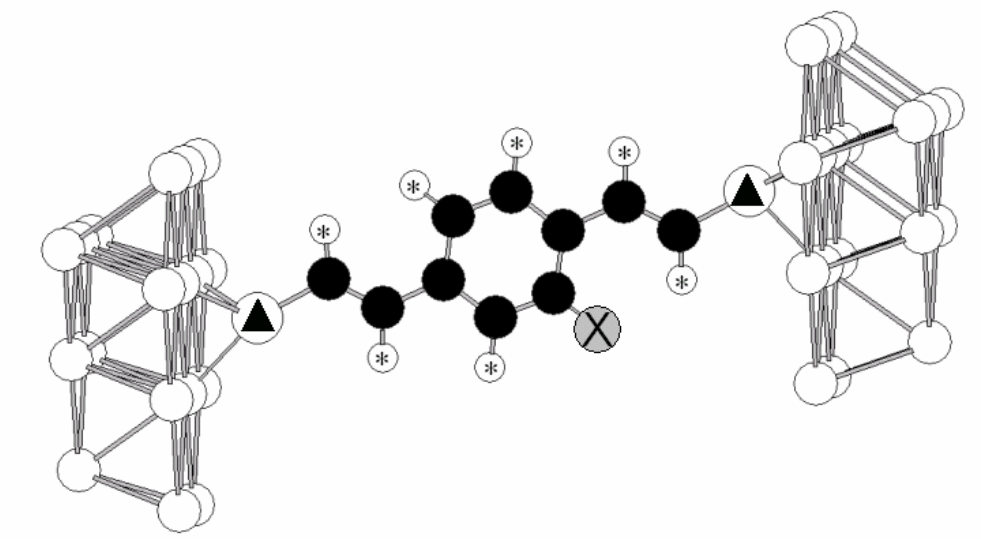

Figure 3. 11. The base device complex for the substituent effect study. The x position was replaced with the substituents ~OH, ~CH_3, ~OCH_3, ~H, ~F, ~Cl, ~CO_2H, ~CF_3, ~CN, and ~NO_2. Atom identities are indicated in Figure 3.1.

Overall, our results demonstrate that transport time depends on molecular length to a greater degree than on chemical substituents. This is supported by experimental evidence provided by Page *et al.*, which suggests that electron tunneling occurs efficiently in polypeptide chains of 14 Å or less, regardless of the chemical nature of the chain molecule [91]. All molecules in the substituent effect study reported here are close to this 14 Å threshold. Therefore both the work of Page and ourselves suggest that there is no appreciable enhancement in tunneling electron transfer due to chemical substituents unless the molecular species is considerably longer than 14 Å. An investigation of the substituent effect upon much longer junction molecules would be computationally demanding

(junctions as large as the one shown in figure 3.10 take several days on a UNIX box with a Pentium III processor) and is beyond the scope of the present work.

3.4 Conclusions

In section 3.2, the junction is modeled as a single molecule sandwiched between two clusters of aluminum atoms. The time development of a localized electron wavefunction is followed by solving the time-dependent Schrödinger equation in a basis of eigenfunctions of the time independent Schrödinger equation for the entire device complex. It is shown that due to high density of states in the vicinity of the Fermi level resulting from the presence of metallic clusters, the occupancy vector in the solution of the time independent Schrödinger equation must be set with Fermi-Dirac statistics. Furthermore, to properly handle finite applied potentials, the Hamiltonian matrix must be constructed in a charge-self-consistent manner.

The calculations suggest that for two simple junction molecules (butane-dithiol and benzene-dithiol) the molecule behaves remarkably like a conducting wire, transferring charge from donor to acceptor electrode while exhibiting no marked charge buildup. This result is consistent with the widely discussed hypothesis that resistance in a molecular junction is predominantly due to the contacts (metal-molecule interfaces). Computed transit times are in excellent agreement with known transit times in molecular junctions.

It is shown that the time for electron transport across the junction increases monotonically with molecular length over a polyacetylenic series MC-S-$(CH=CH)_n$-S-MC, where n=1 to 10. This transport time, however, shows considerably sensitivity to contact geometry.

An investigation of transport time, for a set of functionally substituted junction molecules, showed no statistically significant correlation of the transit time to substituent parameter. It is suggested, based on other literature reports, that the efficiency of transport is relatively insensitive to the junction molecule species for junctions shorter than some critical threshold, which the junctions considered here presumably do not exceed.

Chapter 4. Time-dependence of electron transport II: a Configuration Interaction basis

4.1 Introduction

In Chapter 3 we studied the time dependence of electron transport through molecular junctions by following the time evolution of an initially localized electron by integration of the time dependent Schördinger equation (TDSE). We constructed the time dependent wave function based on a semiempirical (extended Hückel) electronic structure description of the system. The use of a semiempirical electronic structure description introduces two important approximations: i) empirical parameterization of certain fundamental integrals that occur in the solution of the time independent Schrödinger equation, ii) neglect of electron correlation effects. For a more robust description of the time dependence of electron transport, we seek to remove these two approximations. The use of *ab initio* electronic structure theory will serve to remove the restrictive parameterizations, but not all *ab initio* methods include electron correlation. Non-correlated *ab initio* methods, (i.e. Hartree-Fock theory) generate solutions to the Schrödinger equation that account for the electron–electron interactions in an average way. (Refer to Appendix B for more information on Hartree-Fock theory and an example calculation.) Numerous methods exist that attempt to recover some of the energy lost by treating electron-electron interactions this way. Collectively, these are referred to as post-Hartree-Fock methods, and the recovered energy is called the correlation energy (E_{corr}) defined as

$$E_{corr} = \varepsilon_0 - E_0 , \quad (4.1)$$

where ε_0 is the exact non-relativistic energy of the system, and E_0 is the Hartree-Fock energy [69]. The correlation energy physically corresponds to the fact that an electron's motion is "correlated" to that of all of the other electrons in the system. In this chapter we describe the time dependence of electron transport in a donor-bridge-acceptor (D-B-A) molecular system by tracking the time evolution of a correlated and *ab initio* description of the electronic structure of a nonstationary state.

4.2 Theoretical Methods

4.2.1 Background on Configuration Interaction

At the very beginning of a standard quantum chemical calculation, a set of atomic orbitals is assigned to each atom in the molecule. The molecular orbitals are then built as linear combinations of atomic orbitals (LCAO-MO) and the molecular orbital energies are obtained. With an appropriate method and basis set, the ground state of a molecule is appropriately described and the calculation could stop here. There are cases, however, where the molecule is better described as a "mixture" of electronic configurations. The configuration interaction method (CI) performs this task by describing the overall wavefunction (Ψ) as a linear combination of ground and excited electron configurations or determinants

$$\Psi = a_o \psi_{HF} + \sum_{i=1} a_i \psi_i \,, \tag{4.2}$$

where a_i are the expansion coefficients, ψ_i are the excited determinants, a_0 is the coefficient of the Hartree-Fock (HF) ground state, and ψ_{HF} is the ground state determinant.

Slater determinants are necessitated by the Pauli exclusion principle, which states that a many-electron wavefunction must be antisymmetric with respect to the exchange of two electrons [69]. Consider a two-electron system in a basis of atomic orbitals (χ_i), with molecular orbitals (ϕ) of the form

$$\phi_n = \sum_{i=1}^{2} C_{in} \chi_i \,, \tag{4.3}$$

where C_{in} is the expansion coefficient for atomic orbital i in molecular orbital n. The two-electron ground state wavefunction can be written as a Hartree product (refer to Appendix B for more information), or the product of one-electron wavefunctions (molecular orbitals)

$$\psi' = \psi_{1\alpha}(1)\psi_{1\beta}(2), \tag{4.4}$$

where electron 1 is assigned to molecular orbital ψ_1 in a spin up (α) state, and electron 2 is also assigned ψ_1 but in a spin down (β) state. In order for ψ' to satisfy the antisymmetry condition, it must be an eigenfunction of the permutation operator ($\hat{P}_{ij}$), which exchanges the coordinates of two electrons as specified by

$$\hat{P}_{ij}\psi' = -\psi' . \tag{4.5}$$

Substituting (4.4) into (4.5) yields

$$\hat{P}_{12}\psi' = \hat{P}_{12}\psi_{1\alpha}(1)\psi_{1\beta}(2) = \psi_{1\alpha}(2)\psi_{1\beta}(1). \tag{4.6}$$

$$\psi_{1\alpha}(1)\psi_{1\beta}(2) \neq -\psi_{1\alpha}(2)\psi_{1\beta}(1), \tag{4.7}$$

therefore

$$\hat{P}_{ij}\psi' \neq -\psi', \tag{4.8}$$

and ψ' is not an eigenfunction. If the wavefunction (ψ'') is written as a linear combination of ψ' as

$$\psi'' = \psi' - \hat{P}_{12}\psi' = \psi_{1\alpha}(1)\psi_{1\beta}(2) - \psi_{1\alpha}(2)\psi_{1\beta}(1), \tag{4.9}$$

and Ψ'' is substituted for Ψ into the left hand side of (4.5), it yields

$$\hat{P}_{12}\psi'' = \psi_{1\alpha}(2)\psi_{1\beta}(1) - \psi_{1\alpha}(1)\psi_{1\beta}(2). \tag{4.10}$$

$$\psi_{1\alpha}(1)\psi_{1\beta}(2) - \psi_{1\alpha}(2)\psi_{1\beta}(1) = -(\psi_{1\alpha}(2)\psi_{1\beta}(1) - \psi_{1\alpha}(1)\psi_{1\beta}(2)), \tag{4.11}$$

and the antisymmetry condition is satisfied because

$$\hat{P}_{ij}\psi'' = -\psi''. \tag{4.12}$$

Another way of expressing Ψ'' is in determinant form

$$\psi'' = N\begin{vmatrix} \psi_{1\alpha}(1) & \psi_{1\beta}(1) \\ \psi_{1\alpha}(2) & \psi_{1\beta}(2) \end{vmatrix}, \tag{4.13}$$

where N is a normalization constant, and Ψ'' is called a Slater determinant, equivalently written as

$$\psi'' = \left| \psi_{1\alpha}(1)\psi_{1\beta}(2) \right\rangle. \tag{4.14}$$

The Slater determinant in equation 4.14 describes the ground state configuration, but other states can be described as well, i.e. an excited state in which an electron in molecular orbital 1 is placed in molecular orbital 2. Such a Slater determinant may be described as

$$\psi'' = \left| \psi_{1\alpha}(1)\psi_{2\beta}(2) \right\rangle. \tag{4.15}$$

In a CI calculation, a number of Slater determinants are generated by exciting the ground state configuration, and once spin is factored out (spin adapted Slater determinants) these are refer to as configuration state functions (CSFs). CSF1 derived from (4.14) and CSF2 derived from (4.15) would be written as vectors containing only the elements 0, 1 and 2 as CSF1 = (2,0), and CSF2 = (1,1).

In practical calculations, the basis of CSFs is truncated in some way, such as by limiting it to certain excitation types, i.e. only CSFs describing single excitations from valence to virtual orbitals are generated. The CI matrix becomes an NxN square matrix of N CSFs. Solving the eigenvalue problem for the CI matrix yields CI states (eigenvectors) defined as linear combinations of CSFs, and their corresponding state energies (eigenvalues). Comparatively, CSFs (Slater determinants) are to the CI states, what atomic orbitals are to molecular orbitals.

4.2.2 Solution of the Time-Dependent Schrödinger Equation

As in chapter 3, we seek to solve the time dependent Schrödinger equation (TDSE)

$$i\frac{\partial\Psi(\mathbf{r},t)}{\partial t} = \hat{H}\Psi(\mathbf{r},t). \tag{4.16}$$

Here “H” is the total energy operator and $\Psi(\mathbf{r},t)$ is the wavefunction, which depends on the spatial coordinates “**r**” and time “t”. In the case of a time-

independent Hamiltonian, the wavefunction $\Psi(\mathbf{r},t)$ is separable into spatial ($\psi(\mathbf{r})$) and time-dependent ($T(t)$) parts and may be written

$$\Psi(\mathbf{r},t) = T(t)\psi(\mathbf{r}). \tag{4.17}$$

If we denote the eigen-solutions of the time-independent Schrödinger equation (TISE) as $\Phi_k(\mathbf{r})$ so that

$$H\psi(\mathbf{r}) = E\psi(\mathbf{r}), \tag{4.18}$$

we may write the spatial part of the time-dependent wavefunction in the form of an expansion in a basis of eigenfunctions $\Phi_k(\mathbf{r})$ of the time-independent Schrödinger equation

$$\psi_n(\mathbf{r}) = \sum_n b_n\phi_n. \tag{4.19}$$

Here the b_n are the expansion coefficients of the nonstationary state at time t=0. This is where the present method departs from that present in chapter 3. Here the $\Phi_n(\mathbf{r})$ are taken to be CI eigenstates of the TISE, rather than extended Hückel molecular orbitals. As before, the time evolution of the nonstationary state $\Psi(\mathbf{r},t)$ is given by,

$$\Psi(\mathbf{r},t) = \Sigma_n\, b_n\, [\exp(-iE_nt)]\phi_n(\mathbf{r}). \tag{4.20}$$

It is instructive to consider the case where the overall wavefunction $\Psi_n(\mathbf{r},t)$ is written as a linear combination of two CI states (n=1 and 2)

$$\Psi(\mathbf{r},t) = b_1\phi_1 e^{-iE_1t} + b_2\phi_2 e^{-iE_2t}, \tag{4.21}$$

one can prove that it as a solution to the TDSE by substituting (4.21) into (4.16)

$$\frac{\partial\left(b_1\phi_1 e^{-iE_1t} + b_2\phi_2 e^{-iE_2t}\right)}{\partial t} = \hat{H}\left(b_1\phi_1 e^{-iE_1t} + b_2\phi_2 e^{-iE_2t}\right). \tag{4.22}$$

Upon operation, the left hand side of (4.22) becomes

$$E_1 b_1 \phi_1 e^{-iE_1 t} + E_2 b_2 \phi_2 e^{-iE_2 t}, \tag{4.23}$$

and the right hand side of (4.22) becomes

$$E_1 b_1 \phi_1 e^{-iE_1 t} + E_2 b_2 \phi_2 e^{-iE_2 t}. \tag{4.24}$$

(4.23) and (4.24) yield equivalent expressions, and therefore (3.50) is a solution of the TDSE.

The probability density of this wavefunction is

$$\Psi^* \Psi = \left(b_1 \phi_1 e^{iE_1 t} + b_2 \phi_2 e^{iE_2 t}\right)\left(b_1 \phi_1 e^{-iE_1 t} + b_2 \phi_2 e^{-iE_2 t}\right). \tag{4.25}$$

Expanding (3.54) yields

$$\Psi^* \Psi = b_1^2 \phi_1^2 + b_2^2 \phi_2^2 + b_1 b_2 \phi_1 \phi_2 e^{-i\omega t} + b_1 b_2 \phi_1 \phi_2 e^{i\omega t} \tag{4.26}$$

where $\omega = (E_2 - E_1)$. Using the trigonometric identity

$$Ae^{-i\alpha} + Ae^{i\alpha} = 2A\cos(\alpha), \tag{4.27}$$

and substituting $b_1 b_2 \phi_1 \phi_2$ for A, and ωt for α in (4.27), equation (4.26) can be written as

$$\Psi^* \Psi = b_1^2 \phi_1^2 + b_2^2 \phi_2^2 + 2 b_1 b_2 \phi_1 \phi_2 \cos(\omega t). \tag{4.28}$$

Eq. 4.28 shows that when the nonstationary state is a mixture of just two stationary states, the probability varies sinusoidally as a function of the energy difference between the two states.

4.2.3 Extending the population analysis

Tracking electron flow means tracking changes in electron density over time. An approximate but intuitive procedure for the description of electron density is population analysis, as described in Appendix A1. Performing a population analysis on a single determinant wavefunction, i.e. one state or electronic configuration, is a relatively straightforward process. For a molecular system described in terms of CI states, population analysis is more complex. This is because each CI state is a linear combination of Slater determinants or CSFs, which are products of one electron functions or molecular orbitals, which are linear combinations of atomic orbitals.

The mathematical procedure to perform a population analysis on a CI state is as follows.

I. Generate the density matrix for every CSF.

The population analysis for a single determinant or CSF is obtained by writing the density matrix **D** in terms of an occupancy vector ($\vec{v}$)

$$D_{mn} = \sum_{k=1}^{N} v_k C_{km} C_{kn}^{*} . \qquad (4.29)$$

In a system of N molecular orbitals and M CSFs, M density matrices can be calculated because every CSF has its own occupancy vector defined by the excitation if describes. For example, in a two electron system with 3 molecular orbitals (N=3), three CSFs (M=3) could be written as CSF1=(2,0,0), CSF2=(1,1,0) and CSF3=(0,2,0). Each one precisely defines the occupancy of a configuration. CSF1, CSF2, and CSF3 describe a ground state, a singly excited

state, and a doubly excited respectively. The density matrix for each configuration is defined as

$$D_{mn}^{L} = \sum_{k=1}^{N} v_k^L C_{km} C_{kn}^* \tag{4.30}$$

where L is the CSF index, v_k^L is the occupancy specified by CSF L. It is useful to point out that the molecular orbitals from which the CSFs are constructed, are calculated from a SCF-HF calculation before the CI calculation, therefore the atomic orbital coefficients (C) never change.

II. Generate the population matrix for every CSF.

The overlap matrix **S** is also calculated before the CI calculation for the SCF-HF portion, and will not change with CSF or CI states. Like the density matrix, the population matrix or **DS** can be constructed for every CSF

$$\underline{DS}_{mn}^{L} = (\sum_{k=1}^{N} v_k^L C_{km} C_{kn}^*) S_{mn} \tag{4.31}$$

III. Generate the atomic orbital populations (population vector) for every CSF.

To acquire the populations of every atomic orbital (ρ), all the contributions to a particular atomic orbital must be added

$$\rho_A^L = \sum_{m \in A}^{N} \sum_{n}^{N} DS_{mn}^{L} = \sum_{m}^{N} \sum_{n}^{N} (\sum_{k=1}^{N} v_k^L C_{km} C_{kn}^*) S_{mn} . \tag{4.32}$$

According to (4.32), an atom will have a different population depending on the CSF being described, so there will be a “set” of populations for every CSF. These sets never change from one CI state to another. As will be seen below,

what changes is the contribution from a given ρ_A^L to a CI state because the CSFs have different expansion coefficients in every CI state.

IV. Calculate the population for every CI state

To calculate the population of every atomic orbital for the J^{th} CI state (ρ_A^{JL}), the populations (ρ_A^L) from above are multiplied by the square of the CSF expansion coefficients for CI state J as described by

$$\rho_A^{JL} = \sum_L^M \sum_J^N f_{JL} f_{JL} \rho_A^L , \tag{4.33}$$

where f_{JL} is the contribution of CSF L to CI state J. The atomic charges Q_A for every CI state are found by subtracting the ρ_A^{JL} from the nuclear charge Z_A

$$Q_A^J = Z_A - \rho_A^{JL}. \tag{4.34}$$

4.2.4 Specifying the initial localization of the electron

In section 3.2.3, the electron localization was performed by placing an electron in a single atomic orbital and expanding the AO in a basis of molecular orbitals. In a system of N molecular orbitals, and N_D donor atomic orbitals, the expansion coefficients (b_n) for the N molecular orbitals are given by

$$b_n = \sum_k^N \sum_i^{N_D} C_{nk} a_i S_{ki} , \tag{4.35}$$

where a_i is the weight assigned to donor atom i. (See chapter 2 section 2.2.2.) The resultant wavefunction is not a stationary state. It is a linear combination of eigenfunctions or stationary states and will propagate over time. This procedure

is mathematically simple because the molecular orbitals themselves are linear combinations of atomic orbitals. Qualitatively, equation 4.35 is essentially gathering molecular orbitals with large contributions to the donor atomic orbital and assigning them large values of b_n.

In a CI wavefunction, the CSFs are the basis functions, and the stationary states (eigenvectors) are the CI states. The goal is to describe a localized electron as a linear combination of CI states, however, solving for (4.35) is computationally and mathematically impractical. The problem is complicated by the fact that CSFs are *products* of molecular orbitals. This added level of complexity requires a different approach to localization.

As described in section 4.2.4, the expansion coefficients (b_J) for the CI states that result in the desired electronic structure, must be found. The first step, however, is to decide on what the desired electronic structure is. As is described in section 4.2.3, the population for every atom in a CI state (ρ_A^{JL}) can be calculated. One could choose a linear combination of CI states that minimizes the charge on a donor atom. The result is a linear combination of CI states with a coefficient numerically equal to one for the largest contributing CI state, and coefficients numerically equal to zero for all others. This essentially describes only one CI state, which is a stationary state (eigenvector) of the CI matrix and it will not time propagate. Just optimizing the charge on one atom is not sufficient. The solution taken here is to optimize a charge *difference* between the donor and acceptor atoms in the molecule, and to find the linear combination of CI states

that describes a zwitterionic condition. A description of how the expansion coefficients (b_J) for the CI sates is given in Appendix A3, section 3.

4.3 Results and Discussion

4.3.1 Donor-Bridge-Acceptor System

We examine the donor-bridge-acceptor (D-B_n-A) systems, i.e. D = ~CH_3, A = ~CHO, and B_n = $(CH=CH)_n$, where n=1 to 10 specifies the length of the acetylenic bridge [65]. In these systems, the electron donor and acceptor groups on opposite sides of the molecule mimic an applied potential. The geometry optimizations, and configuration interaction (CI) calculations were carried out with an STO-6G [73-75] basis using the GAMESS quantum chemical code [64].

Consider the test molecule CH_3-$(CH=CH)_n$-CHO where n =10. The donor atom is chosen as the methyl carbon and the acceptor atom is the carbonyl oxygen. Once the (b_J) that maximize the donor-acceptor charge separation are found, the CI wavefunction can be time-propagated, and the donor and acceptor charges can be tracked over time. Figure 4.1 shows the charge fluctuations on the donor atom. Note that the charge fluctuations are approximately sinusoidal in nature and have a characteristic peak-to-peak distance. This suggests that the time dependent wavefunction may be roughly approximated by a two-state oscillation. Upon analysis of the expansion coefficients of the nonstationary state, which is optimized to maximize charge separation between the donor and

acceptor moieties, it may be seen that the problem indeed essentially breaks down into a two state description in which the states represent the extremes of electron transport; the electron localized on the donor atom and the electron localized on the acceptor atom. Furthermore the transport time is proportional to the energy difference between the two states, a simple consequence of the two-state picture. The periodicity is the oscillating frequency between contributing states to the donor-acceptor charge separation. This fluctuation arises from a transition common to all the molecules in the series. The transition is from a zwitterionic state to an adjacent zwitterionic state, but with an inverse charge separation. The transition time is defined as the peak-to-peak length divided by two and is shown in figure 4.2 as a function of molecular length (Å). As expected, the time increases as the molecular length increases, and it is noted that there is a periodic step behavior every 3-4 acetylene units.

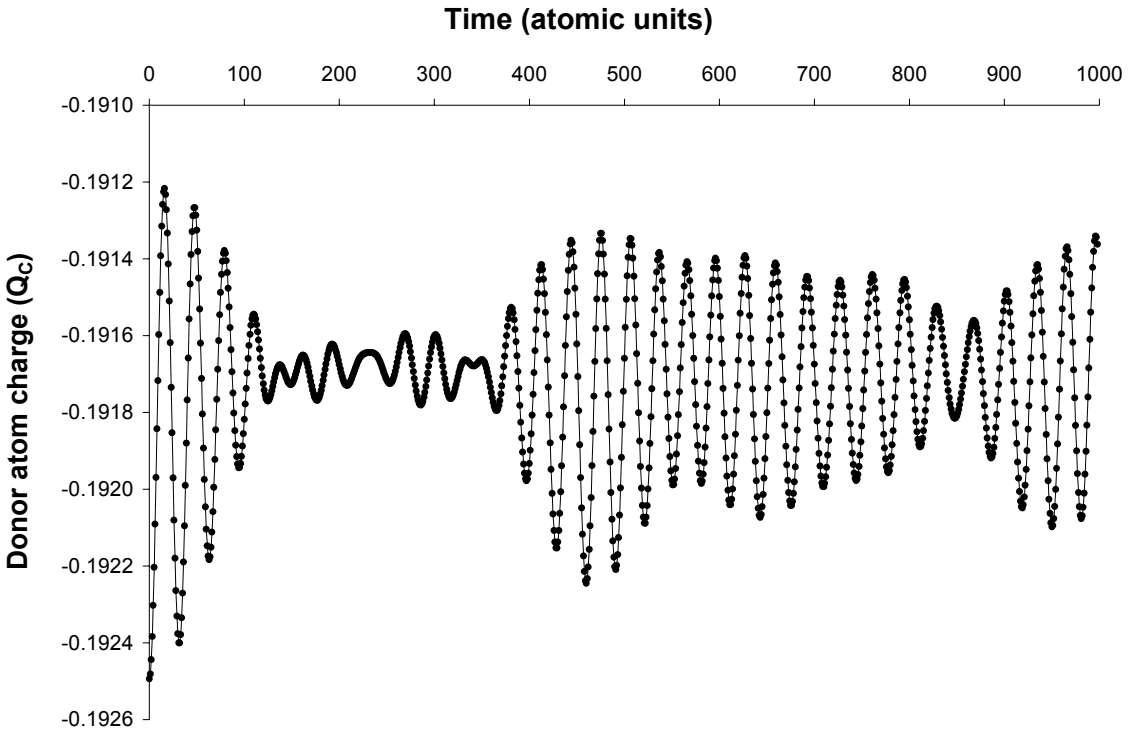

Figure 4. 1. Electronic charge fluctuations on the donor atom (methyl carbon) in the molecule CH_3-$(CH{=}CH)_n$-CHO where n =10. Adjacent points in the time domain are connected as a visual aid.

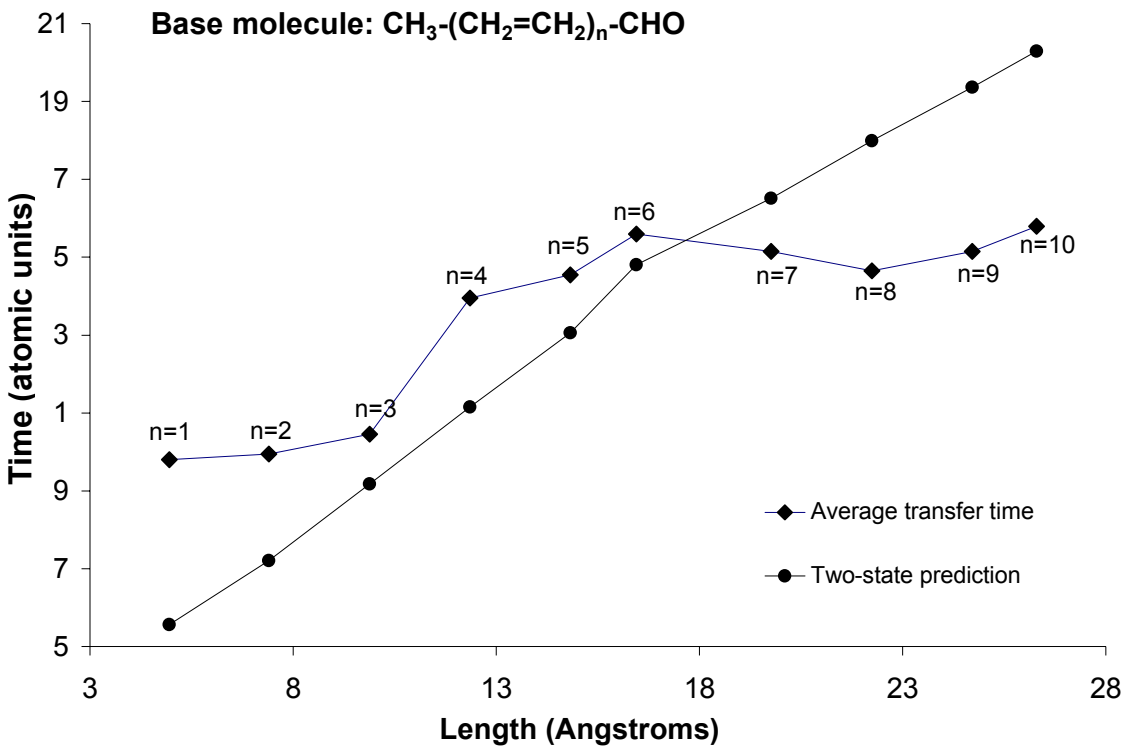

Figure 4. 2. The transition times for the molecular series CH_3-$(CH{=}CH)_n$-CHO where n =1 to 10, as calculated by propagating the configuration interaction (CI) wavefunction and as predicted by the two-state approach.

Also shown in figure 4.2 is the transition time as predicted by the two-state approach. The time, (inverse of ω), is related to the difference in energy between the two dominant contributing states to the initial charge difference optimization. The reason why there are differences between the predicted (two-state) and observed (time development of the CI wavefunction) charge transfer times is that there are other CI states that contribute to the transition besides the states used in the two-state approach, but on average they both have the same slope and

have time values in the same orders of magnitude. In reality there is a non-zero contribution from every CI state, giving rise to the modulation in the charge fluctuation graph shown in figure 4.1. In other words, the wave is not perfectly periodic. Nevertheless, the two-state model provides a qualitative understanding of the time dependence of electron transport. Within the CI state contributions, one can find transitions to other zwitterionic states (secondary transitions) which will have small contributions to the overall wavefunction. Figure 4.3 shows the transition time for a secondary transition along with the graphs shown in figure 4.2. Presumably this secondary transition modulates the two-state prediction. The result from the two-state prediction gives a degree of validation that our calculations yield a physically reasonable result.

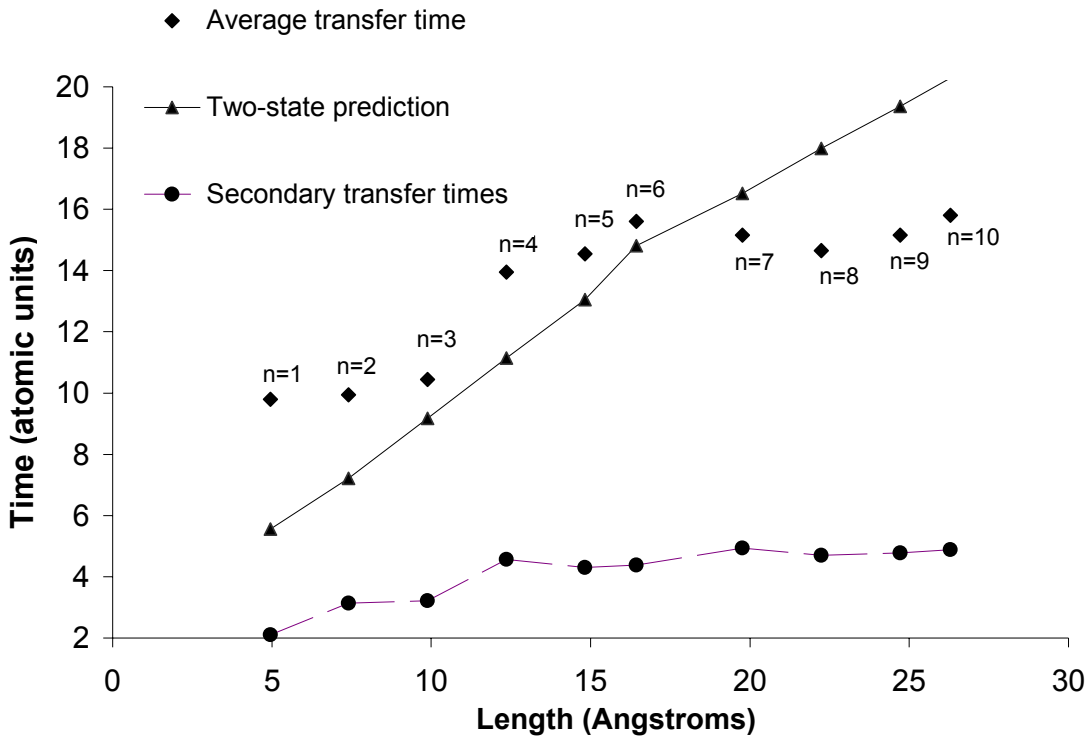

Figure 4. 3. Comparison of secondary transfer times with the two-state prediction and average transfer time as calculated by time developing the CI wavefunction times for the molecular series CH_3-$(CH{=}CH)_n$-CHO where n =1 to 10.

4.3.2 Differential resistance molecule

We examine the charge flow through a molecule which has two chemically different electron transport pathways with nearly symmetrically equivalent coordinates. The molecule is acetaldehyde-(4-ethyl-cyclohexa-1,3-dienyl) and is shown in figure 4.4. Most notably, each limb of the ring between the donor (D) and acceptor (A) represents a possible electron transport path, one being

conjugated and the other saturated. The molecule was geometry optimized at the HF/STO-6G level of theory [73-75] with the GAMESS code [64]. We initially localize the electron as described in section 4.5 on the methyl donor atom and assign the oxygen atom of the carbonyl group as the acceptor. As the wavefunction is time propagated, it is anticipated that the resistance toward electron flow will differ between the conjugated part of the molecule and the saturated part of the molecule. Figure 4.5 shows the accumulation of charge on the conjugated and saturated sections of the ring over time. Figure 4.5 indicates that the time-dependent fluctuation in charge is similar in frequency for both sections of the molecule, but the amplitude is greater on the conjugated section. This suggests that the speed of electron transfer is governed by the dimensions of the molecule, but that the charge flux depends on the chemical environment.

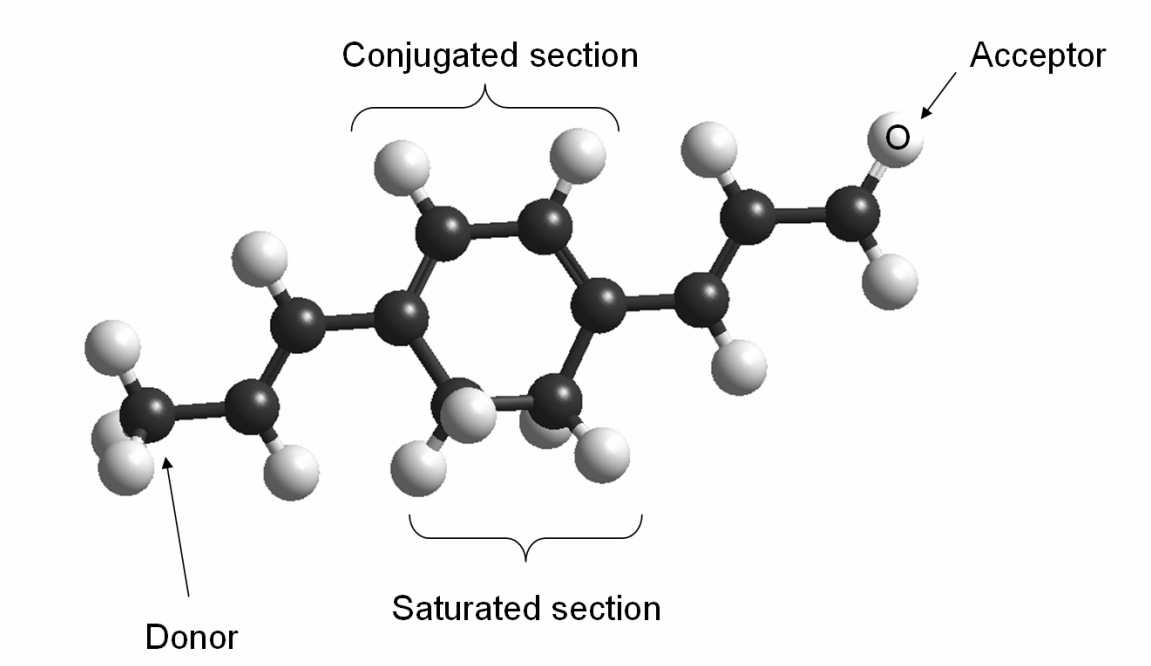

Figure 4. 4. The molecule used in the differential resistance study, acetaldehyde-(4-ethyl-cyclohexa-1,3-dienyl).

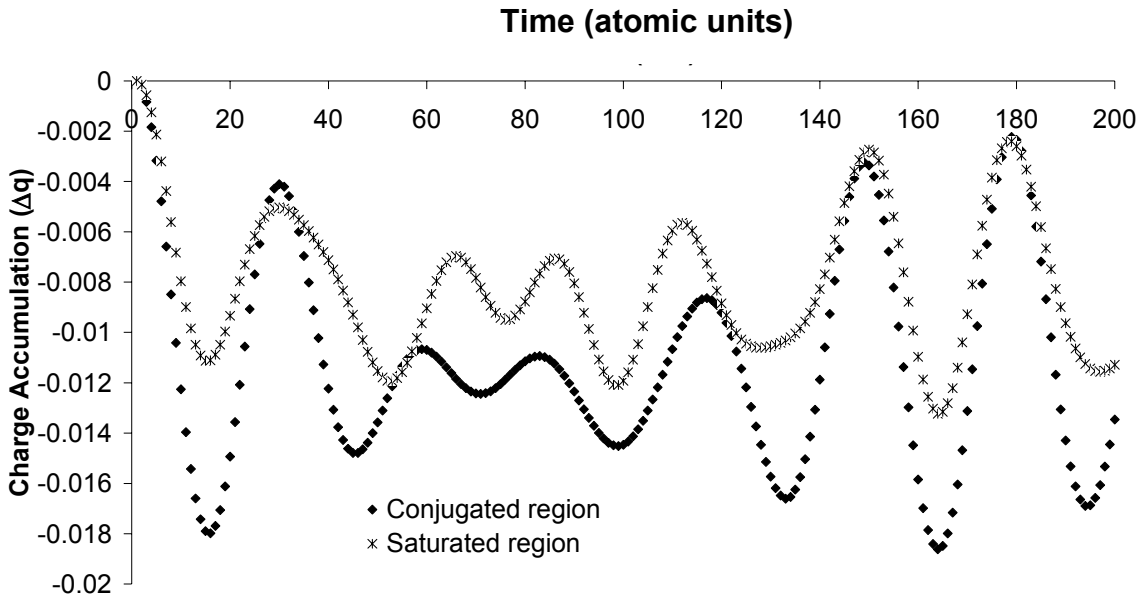

Figure 4. 5. Charge accumulation over time on the conjugated and saturated regions of acetaldehyde-(4-ethyl-cyclohexa-1,3-dienyl).

Figure 4.5 also indicates that there are different frequencies dominating conduction through the two channels (conjugated vs. saturated). We performed a Fourier analysis and generated a power spectrum for each signal in figure 4.5. The Fourier analyses were carried out at time intervals of 0.1 a.u. for 4096 data points, yielding a time range from 0.0 to 409.5 a.u.. Figure 4.6 shows the power spectra that correspond to figure 4.5. The major frequencies are the same for the conjugated and saturated portions of the molecule, but the intensities are different.

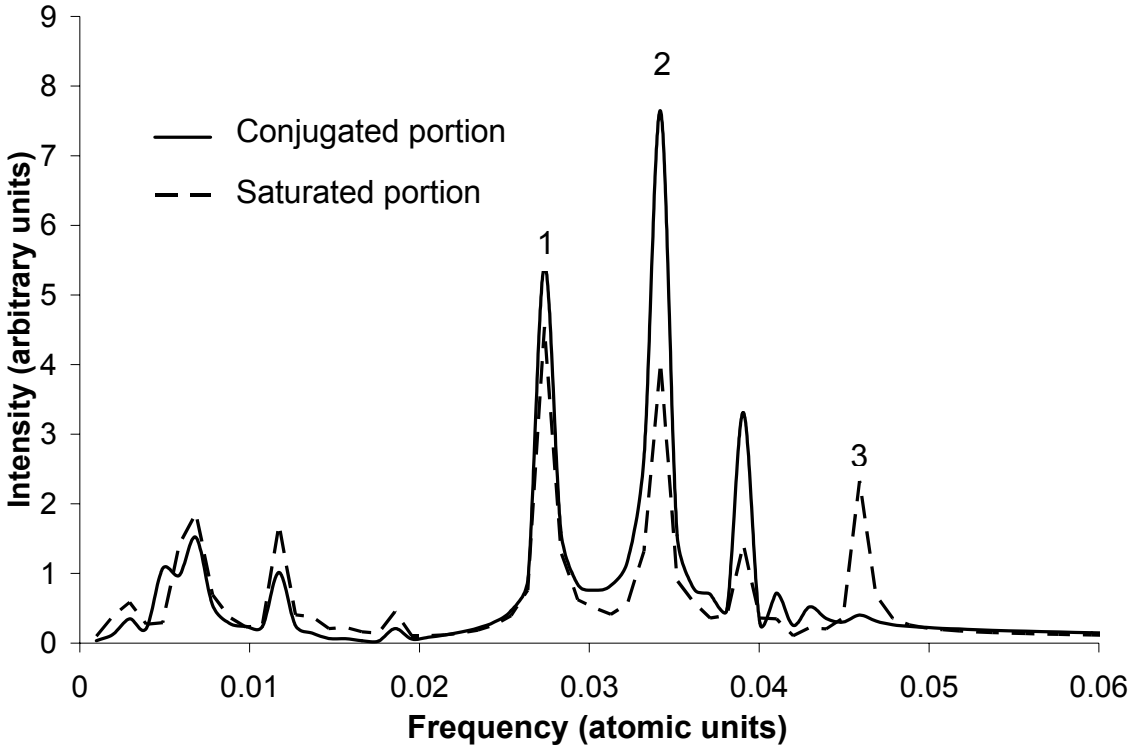

Figure 4. 6. Power spectra of charge fluctuation signals from the conjugated and saturated portions of the molecule.

For the conjugated portion, figure 4.6 shows that peaks 1 and 2 are the dominant frequencies, which correspond to transitions from CI state 4 to 7 (ν=0.0271 a.u.) and CI state 9 to 13 (ν=0.0340 a.u.) respectively. As described in section 3.2.2, the population for each state can be obtained, and we can use this information to look at the charge distribution in the molecule. This is analogous to examining atomic orbital contributions to molecular orbitals, but since CI states are combinations of Slater determinants, more than one density matrix is required to describe each state. The state populations account for all

the determinants and their contributions, yielding a compact picture of charge distribution. Peak 1 describes a transition from a state (4) with no negative charge to a state (7) with a negative charge on the conjugated portion of the molecule. The most interesting feature of this state is that it is the one with the largest charge difference between the conjugated and saturated regions (transverse polarity). Peak 2 is the largest peak for the conjugated channel, and it is a transition between states (9 and 13) that both have high and similar transverse polarities.

The conduction channel for the saturated portion of the molecule has Peak 1 as its largest contributor. This conduction channel also contains a nearly unique frequency (virtually absent from the conjugated power spectra in figure 4.6) at peak 3, a transition between states 11 and 17 (ν=0.0455 a.u.). State 11 has a high transverse polarity, but state 17 has an even charge distribution in the ring. The uniqueness of peak 3 and a possible reason for it being a very important peak in this conduction channel, is that state 17 places more negative charge on the saturated portion than any other state.

Overall, both conduction channels appear to use states that place negative charge on the conjugated portion more than any other state. In the case of the saturated portion, there is a unique frequency that modulates the signal, allowing some charge to flow through this section of the molecule.

4.4 Conclusions

In section 3.2, a molecular junction is modeled as a single molecule sandwiched between two clusters of aluminum atoms. The time development of a localized electron wavefunction is followed by solving the time dependent Schrödinger equation in a basis of eigenfunctions of the time independent Schrödinger equation for the entire device complex. It is shown that the time for electron transport across the junction increases monotonically with molecular length over a polyacetylenic series MC-S-$(CH=CH)_n$-S-MC, where n=1 to 10. Computed transit times are in excellent agreement with known transit times in molecular junctions.

In the present chapter the nonstationary wavefunction is expanded in a linear combination of CI states. We find that transition times are mainly governed by two states, and that the difference in energy between the two states is related to the electron transfer times. We also note that while there are differences between the predicted (two-state) and observed (time development of the CI wavefunction) transfer times, the two-state approach reveals qualitative information about the electron transfer process like the nature of the states that are intimately involved, i.e. zwitterionic states. Furthermore, the comparison of the predicted and observed approach serves as verification that our calculations yield physically reasonable results. Again, electron transit times are found to be in excellent agreement with known transit times in molecular junctions. The advantage of time evolving a CI wavefunction is that it provides a better

electronic structure description because CI captures some of the correlation energy, and avoids restrictive parameterizations.

The disadvantage of the CI methodology is that the treatment of full devices, including metal electrodes, is computationally impractical at this point in time. The methods discussed in Chapter 3 are not as robust because they treat the wavefunction as an uncorrelated one-electron product, but they are computationally more practical if one desires to perform these calculations on a supermolecule.

A calculation was also performed on a molecule that contains regions of differing resistance along parallel electron transport coordinates. The result shows that there is a lower resistance to electron transfer through the conjugated portion of the ring, and that electron transfer is affected by molecular length and resistance due to chemical groups. It was shown that conduction through both portions of the ring is governed by the same frequencies, and that most of the frequencies are transitions that place electronic charge on the conjugated part of the molecule. The exception is the frequency that contributes almost exclusively to the saturated channel, which is a transition to the state that places more negative charge on the saturated portion than any other state.

Overall, the methodology is not restricted to electron transport in molecular electronic junctions and may potentially be applied in any environment where electron transport occurs from one molecular component to a second through a third. The current practical limit is determined by computational hardware resources.

Bibliography

1. Chau R, Boyanov B, Doyle B, Doczy M, Datta S, Hareland S, Jin B, Kavalieros J and Metz M. Silicon nano-transistors for logic applications. Physica E 2003; 19: 1-5.

2. Mathews CK and Van Holde KE. Biochemistry. The Benjamin/Cummings Publishing Comp., Menlo Park, CA, 1996.

3. Stryer L. Biochemistry. W. H. Freeman and Company, New York, NY, 1995.

4. Leatherman G, Durantini EN, Gust D, Moore TA, Moore AL, Stone S, Zhou Z, Rez P, Liu YZ and Lindsay SM. Carotene as a Molecular Wire: Conducting Atomic Force Microscopy. J. Phys. Chem. B 1999; 103: 4006.

5. Niemeyer CM. Tools for the Biomolecular Engineer. Science 2002; 297: 62.

6. Bandyopadhyay A and Pal AJ. Key to designing functional organic molecules for binary operation with large conductance switching. Chem. Phys. Lett. 2003; 371: 86-90.

7. Horowitz G. Field-effect transistors based on short organic molecules. J. Mater. Chem. 1999; 9: 2021-26.

8. Davis WB, Svec WA, Ratner MA and Wasielewski MR. Molecular-Wire Behavior in p-phenylenevinylene Oligomers. Nature 1998; 396: 60-63.

9. Sohlberg K and Matsunaga N. Nanoelectronics with Single Molecules. American Scientific Publishers, Stevenson Ranch, California, 2003.

10. Fan FF, Yang J, Cai L, Price DWJ, Dirk SM, Kosynkin DV, Yao Y, Rawlett AM, Tour JM and Bard AJ. Charge Transport through Self-Assembled Monolayers of Compounds of Interest in Molecular Electronics. J. Am. Chem. Soc. 2002; 124: 5550-60.

11. Atkins P. Physical Chemistry. W.H. Freeman and Company, New York, 1998.

12. Chen J, Reed MA, Rawlett AM and Tour JM. Large On-Off Ratios and Negative Differential Resistance in a Molecular Electronic Device. Science 1999; 286: 1550-52.

13. Chen J, Wang W, Reed MA, Rawlett AM, Price DW and Tour JM. Room-temperature Negative Differential Resistance in Nanoscale Molecular Junctions. App. Phys. Lett. 2000; 77: 1224-26.

14. Kergueris C, Bourgoin J-P, Palacin S, Esteve D, Urbina C, Magoga M and Joachim C. Electron transport through a metal-molecule-metal junction. Phys. Rev. B 1999; 59: 12505.

15. Reed MA, Zhou C, Muller CJ, Burgin TP and Tour JM. Conductance of a Molecular Junction. Science 1997; 278: 252-54.

16. Reynolds S, Sheperd JT, Main C, Marshall JM and Maud JM. A comparative study of photoconductivity and carrier transport in oligomeric films. J. Non-Cryst. Sol. 2000; 266-269: 994-98.

17. Salzner U. Theoretical Analysis of Poly(difluoroacetylene) PDFA. Synth. Met. 2003; 135-136: 311-12.

18. Chen H, Lu JQ, Wu J, Note R, Mizuseki H and Kawazoe Y. Control of substituent ligand over current through molecular devices. An ab initio molecular orbital theory. Phys. Rev. B 2003; 67: 113408.

19. Bredas JL and Heeger AJ. Influence of donor and acceptor substituents on the electronic characteristics of poly(paraphenylene vinylene) and poly(paraphenylene). Chem. Phys. Lett. 1994; 217: 507.

20. Joachim C. Bonding more atoms together for a single molecule computer. Nanotechnology 2002; 13: R1.

21. Rawlett AM, Mickelson ET, Reinerth WA, Jones LI, Kozaki M, Burgin TP, Tour JM, Chen J, Zhou CW, Muller CJ, Deshpande MR, Reed MA, Bumm LA, Cygan MT, Dunbar TD, Weiss PS and Allara DL. Molecular Scale Electronics. Materials Research Society 2001; 582: H9.2.1.

22. Reed MA and Tour JM. Computing with Molecules. Scientific American 2000; 282: 86.

23. Doyen G, Koetter E, Vigneron JP and Scheffler M. Theory of scanning tunneling microscopy. App. Phys. A 1990; 51: 281-88.

24. Kroemer H. Quantum Mechanics for Engineering, Materials Science, and Applied Physics. Prentice-Hall, Englewood Cliffs, NJ, 1994.

25. Special issue: Molecular Electronics, Chem. Phys. 2002; 281:

26. Emberly EG and Kirczenow G. Models of electron transport through organic molecular monolayers self-assembled on nanoscale metallic contacts. Phys. Rev. B 2001; 64: 235412.

27. Lang ND and Avouris P. Electrical conductance of individual molecules. Phys. Rev. B 2001; 64: 125323.

28. Datta S, Tian W, Hong S, Reifenberger R, Henderson JI and Kubiak CP. Current-Voltage Characteristics of Self-Assembled Monolayers by Scanning Tunneling Microscopy. Phys. Rev. Lett. 1997; 79: 2530-33.

29. Tian W, Datta S, Hong S, Reifenberger R, Henderson JI and Kubiak CP. Conductance spectra of molecular wires. J. Chem. Phys. 1998; 109: 2874-82.

30. Pantelides ST, DiVentra M and Lang ND. Molecular electronics by the numbers. Physica B 2001; 296: 72.

31. DiVentra M, Pantelides ST and Lang ND. First-Principles Calculation of Transport Properties of a Molecular Device. Phys. Rev. Lett. 2000; 84: 979-82.

32. Magoga M and Joachim C. Conductance of molecular wires connected or bonded in parallel. Phys. Rev. B 1999; 59: 16011-21.

33. Xue Y, Datta S and Ratner MA. Charge transfer and "band lineup" in molecular electronic devices: A chemical and numerical interpretation. J. Chem. Phys. 2001; 115: 4292-99.

34. Bredas JL, Calbert JP, da Silva Filho DA and Cornil J. Organic semiconductors: A theoretical characterization of the basic parameters governing charge transport. PNAS 2002; 99: 5804-09.

35. Palacios JJ, Louis E, Perez-Jimenez AJ, San Fabian E and Verges JA. An ab initio approach to electrical transport in molecular devices. Nanotechnology 2002; 13: 378.

36. Yaliraki SN, Kemp M and Ratner MA. Conductance of molecular wires: Influence of molecule-electrode binding. J. Am. Chem. Soc. 1999; 121: 3428-34.

37. Emberly E and Kirczenow G. Electrical conductance of molecular wires. Nanotechnology 1999; 10: 285.

38. Seminario JM, De la Cruz CE and Derosa PA. A Theoretical Analysis of Metal-Molecule Contacts. J. Am. Chem. Soc. 2001; 123: 5616-17.

39. Baer R, Seideman T and Neuhauser D. *Ab Initio* study of the alternating current impedance of a molecular junction. J. Chem. Phys. 2004; 120: 3387-96.

40. Baer R and Neuhauser D. *Ab Initio* Electrical Conductance of a Molecular Wire. J. Quant. Chem. 2003; 91: 524-32.

41. Baer R. Non-adiabatic couplings by time-dependent density functional theory. Chem. Phys. Lett. 2002; 362: 75-79.

42. Baer R and Neuhauser D. Anti-coherence based molecular electronics: XOR-gate response. Chem. Phys. 2002; 281: 353-62.

43. Schwarz R. Dispersive transport in disordered semiconductors. J. Non-Cryst. Sol. 1998; 227-230: 148-52.

44. Davis WB, Wasielewski MR, Ratner MA, Mujica V and Nitzan A. Electron transfer rates in bridged molecular systems: A Phenomenological Approach to Relaxation. J. Phys. Chem. A 1997; 101: 6158-64.

45. Matsunaga N and Sohlberg K. The Substituent Effect on Nonlinear Current Voltage Characteristics in a Two-Terminal Molecular Electronic Device. J. Nanosci. Nanotech. 2001; 1: 275-79.

46. Matsunaga N and Sohlberg K. The Effect of Substituents on Molecular Electronic Junctions. J. Nanosci. Nanotech. 2002; 2: 659-67.

47. Vedova-Brook N, Matsunaga N and Sohlberg K. Correlating substituent parameter values to electron transport properties of moelcules. Chem. Phys. 2004; 299: 89-95.

48. Carey FA and Sundberg RJ. Advanced Organic Chemistry: Part A - Structure and Mechanisms. Plenum Press, New York, 1990.

49. Aguilar-Martinez M, Bautista-Martinez JA, Nacias-Ruvalcaba N, Gonzales I, Tovar E, Marin del Alizal T, Collera O and Cuevas G. Molecular Structure of Substituted Phenylamine alpha-OMe- and alpha-OH-p-Benzoquinone Derivatives. Synthesis and Correlation of Spectroscopic, Electrochemical and Theoretical Parameters. J. Org. Chem. 2001; 66: 8349-63.

50. El Azami M, Bitit N, Kerbal A, Lahlou S, Lyazidi SA, Desvergne J, Bouas-Laurent H and Bassani D. Hammett type correlations for intramolecular charge transfer (ICT) dipole moments of 4'-substituted 9-styrylacridines in the ground state and in the excited state. Heterocycles 2001; 55: 2325-40.

51. Bertolasi V, Nanni L, Gilli P, Ferretti V, Gilli G, Issa YM and Sherif OE. Intramolecular N-H...O=C hydrogen bonding assisted by resonance. Intercorrelation between structural and spectroscopic data for six b-diketo-arylhydrazones derived from benzoylacetone or acetylacetone. New J. Chem. 1994; 18: 251-61.

52. Dillow GW and Kebarle P. Substituent Effects on the Electron Affinities of Perfluorobenzenes C_6F_5X. J. Am. Chem. Soc. 1989; 111: 5592-96.

53. Mishima M, Huh C, Nakamura H, Fujio M and Tsuno Y. Electron Affinities of Benzaldehydes. Substituent Effects on Stabilities of Aromatic Radical Anions. Tet. Lett. 1993; 34: 4223-26.

54. Pankratov AN. Electrophilic Aromatic Substitution Regioselectivity for Benzene Derivatives In Terms of Cationic Localization Energies From Semiempirical Quantum Chemical Computations. Journal Of Molecular Structure (THEOCHEM) 2000; 507: 239-44.

55. Bernasconi CF and Wenzel PJ. Carbon-to-Carbon Identity Proton Transfers from Propyne, Acetimide, Thioacetaldehyde, and Nitrosomethane to Their Respective Conjugate Anions in the Gas Phase. An ab Initio Study. J. Org. Chem. 2001; 66: 968-79.

56. DiLabio GA, Pratt DA, LoFaro AD and Wright JS. Theoretical Study of X-H Bond Energetics (X = C, N, O, S): Application to Substituent Effects, Gas Phase Acidities, and Redox Potentials. J. Phys. Chem. 1999; 103: 1653-61.

57. Ditchfield R, Hehre WJ and Pople JA. Self-consistent molecular-orbital methods. IX. Extended Gaussian-type basis for molecular-orbital studies of organic molecules. J. Chem. Phys. 1971; 54: 724-28.

58. Hehre WJ, Ditchfield R and Pople JA. Self-consistent molecular orbital methods. XII. Further extensions of Gaussian-type basis sets for use in molecular orbital studies of organic molecules. J. Chem. Phys. 1972; 56: 2257-61.

59. Francl MM, Pietro WJ, Hehre WJ, Binkley JS, Gordon MS, DeFrees DJ and Pople JA. Self-consistent molecular orbital methods. XXIII. A polarization-type basis set for second-row elements. J. Chem. Phys. 1982; 77: 3654-65.

60. Clark T, Chandrasekhar J, Spitznagel GW and Schleyer PvR. Efficient diffuse function-augmented basis sets for anion calculations. III. The 3-21 + G basis set for first-row elements, lithium to fluorine. J. Comput. Chem. 1983; 4: 294-301.

61. Spitznagel GW. Diplomarbeit. Erlangen, 1982. (Referenced in GAMESS).

62. Hertwig RH and Koch W. On the parameterization of the local correlation functional. What is Becke-3-LYP? Chem. Phys. Lett. 1997; 268: 345-51.

63. Krishnan R, Binkley JS, Seeger R and Pople JA. Self-consistent molecular orbital methods. XX. A basis set for correlated wave functions. J. Chem. Phys. 1980; 72: 650-54.

64. Schmidt MW, Baldridge KK, Boatz JA, Elbert ST, Gordon MS, Jensen JH, Koseki S, Matsunaga N, Nguyen KA, Su S, Windus TL, Dupuis M and Montgomery JA. General Atomic and Molecular Electronic Structure System. J. Comp. Chem. 1993; 14: 1347-63.

65. Gonzales C and Morales RGE. Molecular Resistivities in Organic Polyenic Wires I. A One-dimensional Photoconduction Charge Transfer Model. Chem. Phys. 1999; 250: 279-84.

66. Hernandez CT and Morales RGE. Bridge Effect in Charge-Transfer Photoinduction Channels. I. Aromatic Carbonyl Compounds. J. Phys. Chem. 1993; 97: 11649-51.

67. Jensen F. Introduction to Computational Chemistry. John Wiley and Sons Ltd., Chichester, England, 1999.

68. Tsuzuki S, Uchimaru T, Tanabe K and Yliiniemela A. Comparison of atomic charge distributions obtained from different procedures: basis set and electron correlation effects. Journal Of Molecular Structure (THEOCHEM) 1996; 365: 81-88.

69. Szabo A and Ostlund NS. Modern Quantum Chemistry. Introduction to Advanced Electronic Structure Theory. Dover, Mineola, N.Y., 1996.

70. Segall MD, Shah R, Pickard CJ and Payne MC. Population analysis of plane-wave electronic structure calculations of bulk materials. Physical Review B 1996; 54: 16317-20.

71. Young DC. Computational Chemistry. John Wiley & Sons Inc., New York, N.Y., 2001.

72. Foresman JB and Frisch A. Exploring Chemistry with Electronic Structure Methods. Gaussian, Inc., Pittsburgh, PA, 1996.

73. Hehre WJ, Stewart RF and Pople JA. Self-consistent molecular-orbital methods. I. Use of Gaussian expansions of Slater-type atomic orbitals. J. Chem. Phys. 1969; 51: 2657-64.

74. Hehre WJ, Ditchfield R, Stewart RF and Pople JA. Self-consistent molecular orbital methods. IV. Use of Gaussian expansions of Slater-type orbitals. Extension to second-row molecules. J. Chem. Phys. 1970; 52: 2769-73.

75. Gordon MS, Bjorke MD, Marsh FJ and Korth MS. Second-row molecular orbital calculations. 5. A minimal basis INDO for sodium-chlorine. J. Am. Chem. Soc. 1978; 100: 2670-78.

76. Anderson WP, Edwards WD and Zerner MC. Calculated Spectra of Hydrated Ions of the First Transition-Metal Series. Inorg. Chem. 1986; 25: 2728-32.

77. Harris DC. Quantitative Chemical Analysis. W. H. Freeman and Company, New York, N.Y., 1995.

78. Hansch C and Leo A. Substituent Constants For Correlation Analysis in Chemistry and Biology. Wiley-Interscience, New York, N.Y., 1979.

79. Miller JC and Miller JN. Statistics for Analytical Chemistry. John Wiley and Sons, New York, N.Y., 1988.

80. Wang L-S, Wu H and Cheng H. Photoelectron spectroscopy of small chromium clusters: Observation of even-odd alternations and theoretical interpretation. Phys. Rev. B 1997; 55: 12884-87.

81. Hammer B and Norskov JK. Electronic factors determining the reactivity of metal surfaces. Surf. Sci. 1995; 343: 211-20.

82. Hammer B. Personal communication. 4/14/2004;

83. McGlynn SP, Vanquickenborne LG, Kinoshita M and Carroll DG. Introduction to Applied Quantum Chemistry. Holt, Rinehart and Winston, Inc., New York, 1972.

84. Hyperchem 6.02. Hypercube, Inc., Waterloo, Ontario, Canada, 2000.

85. Pan YH, Sohlberg K and Ridge DP. Reactions of Co_{1-4}^{+} and $Co_4(CO)_n^{+}$ with Cyclohexane: C-H Activation as a Function of Cluster Size and Ligand Substitution. J. Am. Chem. Soc. 1991; 113: 2406.

86. Sohlberg K and Chen Y. The Structure and Dynamics of the CS_2 Molecular Ion. J. Chem. Phys. 1994; 101: 3831.

87. Ekeberg D, Uggerud E, Lin H, Sohlberg K, Chen H and Ridge DP. Dehydrogenation of Ethane by CpM^{+} (M = Fe, Co, Ni) in the Gas Phase. An FT-ICR-MS Study. Organometallics 1999; 18: 40.

88. Joachim C, Gimzewski JK and Tang H. Physical principles of the single C_{60} transistor effect. Phys. Rev. B 1998; 58: 16407-17.

89. Olson M, Mao Y, Windus TL, Kemp M, Ratner MA, Leon N and Mujica V. A conformational study of the influence of vibrations on conduction in molecular wires. J. Phys. Chem. B 1998; 102: 941-47.

90. Krebs B, Schiemann A and Laege M. Synthesis and crystal structure of a novel hexagonal modification of aluminum sulfide with five-coordinated aluminum. Z. Anorg. Allg. Chem. 1993; 619: 983-88.

91. Page CC, Moser CC, Chen X and Dutton LP. Natural engineering principles of electron tunneling in biological oxidation-reduction. Nature 1999; 402: 47-52.

Appendix A. General Theory of Population Analysis and Obtaining Atomic Charges

In a quantum chemical calculation, whether it is semi-empirical or *ab initio*, the molecular orbitals and corresponding molecular orbital energies are obtained by solving an eigenvalue problem, i.e. diagonalizing a matrix representation of the Hamiltonian **H**. This matrix is constructed with valence orbital ionization energies (VOIEs) in the case of semi-empirical calculations or with the Fock operator in Hartree-Fock (*ab initio*) calculations [1].

In a basis of N atomic orbitals, the resultant molecular orbitals (ϕ) are written as linear combinations of atomic orbitals (χ)

$$\phi_i = \sum_{j=1}^{N} c_{ji}\chi_j \,, \tag{A1}$$

where c_{ji} is the expansion coefficient for atomic orbital χ_j in molecular orbital i. The density matrix **D** is constructed from the molecular orbitals. **D** contains all the information about the electron distribution and charge density, and its elements are defined as

$$D_{ij} = 2\sum_{n=1}^{N/2} c_{in}c_{jn}^{*} \,, \tag{A2}$$

where the summation index includes only the occupied molecular orbital coefficients which are then multiplied by 2 in a closed shell system between there are two electrons assigned to each occupied orbital. From equation A2, **D** is intuitively related to the wavefunction's probability density.

To partition electrons over the molecule into atomic orbital contributions, Mulliken population analysis uses the overlap matrix **S** [1, 2] to obtain a population matrix denoted **DS**. **S** is obtained from the integrals between two atomic orbitals and is often calculated at the beginning of quantum chemical calculations. The elements of **S** are defined as

$$S_{ij} = \int \chi_i \chi_j d\tau \,, \tag{A3}$$

and they may be thought of as characterizing the strength of interaction between atomic orbitals χ_i and χ_j.

The elements of the Mulliken population matrix or **DS** matrix are defined as

$$\underline{DS}_{ij} = \sum_{ij}^{N} D_{ij} S_{ij} \,. \tag{A4}$$

It is important to note that **DS** is a matrix whose elements are products of the elements of **D** and **S**, not the matrix dot product *between* **D** and **S**. The population for atom A (ρ_A) can be obtained from adding all contributions centered on atom A and is written as

$$\rho_A = \sum_{i \in A}^{N} \sum_{j}^{N} \underline{DS}_{ij} \,, \tag{A5}$$

where the "i" index includes only those **DS** elements that are centered on atom A.

In order to calculate the charge on atom A (Q_A), the population is subtracted from the nuclear charge (Z_A) as,

$$Q_A = Z_A - \rho_A \,. \tag{A6}$$

References

1. Jensen F. Introduction to Computational Chemistry. Wiley, Chichester, England, 1999.

2. Szabo A and Ostlund NS. Modern Quantum Chemistry. Introduction to Advanced Electronic Structure Theory. Dover, Mineola, N.Y., 1996

Appendix B. Modifications to DRAGON code

In chapter 3 the theoretical methods used to calculate the time-dependence of electron transport and the application of a potential field across molecular junctions are discussed. This appendix provides a description of DRAGON, the FORTRAN program that performs those calculations.

Karl Sohlberg wrote the first version of DRAGON in 1991. It was primarily used to perform molecular orbital calculations by using Extended Hückel theory. The results from DRAGON calculations have been published and the code's robustness has been validated over the years [1]. Later versions of the code implemented a wavefunction localization routine, a time-dependent wavefunction solver and a wavefunction time development scheme.

B.1 Program Structure

The main driver structure of the current version of DRAGON is shown below. A description of the main program features and modifications directly follows. The program line numbers appear on the right of each record (line) within the main program and will be referenced in the subsequent section.

```
MAIN PROGRAM                                    1
implicit real*8 (a-h,o-z)                       2
parameter (nbasis=N)                            3
external totoccfun                              4
```

```
      real*8 x(nbasis),y(nbasis),z(nbasis),val(nbasis)                    5
      real*8 s(nbasis,nbasis),ss(nbasis,nbasis)                           6
      real*8 AA(nbasis),BB(nbasis),CC(nbasis)                             7
      real*8 h(nbasis,nbasis),hr(nbasis,nbasis)                           8
      real*8 am(nbasis,nbasis),qq(nbasis)                                 9
      real*8 q(nbasis),qlast(nbasis)                                      10
      real*8 alfr(nbasis),qqlast(nbasis)                                  11
      real*8 eigenv(nbasis,nbasis),qvec(nbasis)                           12
      real*8 fv1(nbasis),fv2(nbasis) !work arrays                         13
      real*8 cm(nbasis,nbasis),lambda,RMS                                 14
      real*8 cms(nbasis,nbasis)                                           15
      real*8 binmo(nbasis),vaps,vapi,vapstep,vaptop                       16
      real*8 rtable(nbasis,2),r2table(nbasis,2)                           17
      real*8 temp,efermi                                                  18
      integer*4 itable(nbasis,3),nq,it                                    19
      integer*4 symtab(90,4),nleft,nright                                 20
      integer*4 index(nbasis),natoms                                      21
      integer*4 iaccept(nbasis)                                           22
      character*8 type(36)                                                23
      logical opt                                                         24

      call clear(nbasis,h,s,alfr,eigenv,cm)                               25

      open(unit=58,file='CMY')                                            26
      open(unit=3,file='dragon.chk')                                      27
      call getinput(nbasis,norb,nfull,nhalf,x,y,z,itable,                 28
     >                  r2table,symtab,opt,val)                           29

      call printdata(nbasis,norb,x,y,z,itable,r2table,type)               30

      nleft=81                                                            31
      nright=153                                                          32
      vapi=0.0d0                                                          33
      vapstep=0.1d0                                                       34
      vaptop=3.0d0                                                        35
      nvaptop=nint((vaptop-vapi)/vapstep)                                 36

C     execute option to read in s matrix                                  37
      if (opt) then                                                       38
        call reads(nbasis,norb,s)                                         39
      else                                                                40
        call overlap(nbasis,norb,s,itable,r2table,symtab,x,y,z)           41
        call savematrix(nbasis,norb,s)                                    42
      endif                                                               43

      open(unit=19,file='vappop.vec')                                     44
```

```
      open(unit=55,file='FERMI')                                        45

      Do nvap=0,nvaptop,1                                               46
        vaps=(real(nvap)*vapstep)+vapi                                  47

        call linvap(nbasis,x,r2table,rtable,vaps,nleft,nright)          48
        call ABC(nbasis,itable,rtable,AA,BB,CC)                         49

        open(unit=88,file='RMS')                                        50
        open(unit=99,file='SCC')                                        51
        open(unit=66,file='fRMS')                                       52
        open(unit=77,file='OCC')                                        53
        open(unit=57,file='timecorr.mat')                               54

        write(6,*)'At vap = ',vaps                                      55
        write(99,*)'At vap = ',vaps                                     56
        write(55,*)'++++++++++++++++++++++++++++++++++'                 57
        write(55,*)'++++++++++++++++++++++++++++++++++'                 58
        write(55,*)'At vap = ',vaps                                     59

            lambda=-0.05                                                60
            it=1                                                        61
            Do nq=1,1000,1                                              62
              write(6,*)'*******************************'               63
              write(6,*)' At iteration ', nq                            64
              write(55,*)'*******************************'              65
              write(55,*)' At iteration ', nq                           66

              call energy(nbasis,norb,s,h,rtable,nq)                    67
              call renormalize(nbasis,norb,h,s,hr)                      68

              write(6,*)'S matrix:'                                     69
                  do is=1,norb,1                                        70
C                   write(6,1002)(s(is,j),j=1,6) !debug                 71
                    do js=1,norb,1                                      72
                      ss(js,is) = s(js,is) !preserve copy of S matrix   73
                    end do                                              74
                  end do                                                75
 1002   format(6F10.3)  !used only for above debug write                76
               call rs(nbasis,norb,hr,alfr,1,eigenv,fv1,fv2,ierr)       77
      print *,'return code on eigenvalue analysis: ',ierr               78

          call normalize(nbasis,norb,eigenv,cm)                         79
          call output(nbasis,norb,alfr,eigenv,index,itable,type)        80

          call popanal(nbasis,norb,cm,s,index,nfull,nhalf,              81
```

```
     >                  qvec,x,val,alfr,cms)                                82
           call charge(nbasis,itable,qvec,val,qq,natoms,q)                 83
           call scc(nbasis,val,qq,AA,BB,CC,h,qqlast,nq,lambda,             84
     >                  RMS,qqdiffmax,natoms,q,qlast)                       85

                If ((nq.ge.2).and.(RMS.le.0.001))then                       86
                    write(6,*)'RMS = ',RMS, nq, 'Iterations'                87
                    write(6,*)'Maxdiff = ',qqdiffmax                        88
                  Go to 900                                                 89
                End if                                                      90
           End do                                                           91

 900          write(19,*)'At Vap = '                                        92
              write(19,*)vaps                                               93
              write(66,*)nq,' iterations at Vap = ',vaps                    94
              write(66,*)'RMS = ',RMS,' Maxdiff = ',qqdiffmax               95

                 Do n=1,nbasis                                              96
                   write(19,*)qvec(n),x(n),val(n)                           97
                 End do                                                     98

           call dynamicsinput(nbasis,norb,naccept,iaccept,                  99
     >  idyn,s,cms,binmo,tstep,ntstep)                                      100

           if (idyn.ne.0) call timedev(nbasis,norb,naccept,iaccept,         101
     >  alfr,cm,binmo,tstep,ntstep,cms,vaps)                                102

           End do                                                           103

           close(58)                                                        104
           close(55)                                                        105
           close(56)                                                        106
           close(57)                                                        107
           close(77)                                                        108
           close(66)                                                        109
           close(88)                                                        110
           close(99)                                                        111
           close(19)                                                        112
           close(3)                                                         113
           stop                                                             114
           end                                                              115
C       END MAIN PROGRAM
```

B.2 Description

All subroutines that have been added or modified are denoted with a double dagger (‡).

Line 3 – Parameter that specifies the number of basis functions (atomic orbitals) in the molecular system.

Line 25 – Subroutine clear sets all VOIEs, overlap integrals, molecular orbital energies (eigenvalues) and atomic orbital coefficients (eigenvectors) to zero before each run.

Lines 28 and 29 – Subroutine getinput‡ reads the values for center number (atom label), function type (as in orbital type, i.e. 1s, 2s, 2p, 3s, 3p, 3d), atomic number, zeta (effective nuclear charge), VOIE, x-coordinate, y-coordinate, z-coordinate, and valence electrons for every atomic orbital used in the calculation.

Line 30 – Subroutine printdata prints the data that is read by the getinput subroutine to a check file for debugging purposes.

Line 31 – This specifies the atomic orbital (basis function) that is on the low potential side of the applied potential field (V_{ap}). This is not a center number, but the label of the basis function.

Line 32 – This specifies the atomic orbital (basis function) that is on the high potential side of V_{ap}. As in above, this is the basis function label.

Line 33 – This specifies the initial value of V_{ap}.

Line 34 – This specifies the step size to be taken between consecutive cycles of the V_{ap} program loop.

Line 35 – This specifies the final value of V_{ap}.

Line 36 – This calculates the number of steps that will be required for the calculation from the values specified in lines 33 through 35.

Line 39 – Subroutine reads acquires the overlap integrals for the calculation if they have been generated and saved as an external file.

Line 41 – Subroutine overlap calculates the overlap integrals for the atomic basis specified in the input file.

Line 42 – Subroutine savematrix saves the overlap matrix generated above for future use.

Line 46 – Starts the V_{ap} loop.

Line 48 – Subroutine linvap‡ applies the potential in a linear fashion across the molecule as described in chapter 3, section xxx. The values directly affected by this subroutine are the VOIEs. The subroutine prints the original VOIEs next to the new calculated values, redefined as H_{ii} (energy of orbital i) at a given V_{ap}, to the screen for debugging purposes. The subroutine is shown below.

```
Implicit real*8 (a-h,o-z)
real*8 x(nbasis),vaps
real*8 r2table(nbasis,2),rtable(nbasis,2)
real*8 xleft,xright,xmiddle,xlength
integer*4 nbasis,norb,nleft,nright
hperev=3.674930887d-2
vap= vaps*hperev
xleft = x(nleft)
xright = x(nright)
xmiddle = (xleft + xright)/2.0d0
xlength = xright - xleft

write(6,*)'================================='
write(6,*)'In linvap'
```

```
write(6,*)'r2table and rtable are:'
do 150 n=1,nbasis,1
if (x(n).le.xleft) then
rtable(n,2) = r2table(n,2) - vap/2.0d0
end if
if (x(n).ge.xright) then
rtable(n,2) = r2table(n,2) + vap/2.0d0
end if
if ((x(n).gt.xleft).and.(x(n).lt.xright)) then
rtable(n,2) = r2table(n,2) + vap*((x(n)-xmiddle)/xlength)
end if

write(6,*)'In LINVAP'
write(6,*)r2table(n,2),rtable(n,2)   !!!DEBUG!!!
150   continue
write(6,*)'================================='
return
end
```

Line 49 – Subroutine ABC‡ acquires the constants required to calculate the H_{ii} in the self-consistent charge (SCC) portion of the code. The H_{ii} depend quadratically on charge (q) through

$$H_{ii,n}(q_n) = -(A_{i,n}q_n^2 + B_{i,n}q_n + C_{i,n}), \qquad \text{(B1)}$$

where $A_{i,n}$, $B_{i,n}$, and $C_{i,n}$ are specific to orbital type i and atom n. The A and B constants are hard-coded into the subroutine and include values for H, C, N, O, F, Al, S, and Cl. The C constants are the VOIEs that were obtained from the input file. They correspond to the uncharged atom initial guess. It also prints out the values for A, B and C for all the atomic orbitals in the calculation onto the screen for debugging purposes. The subroutine in shown below.

```
Implicit real*8 (a-h,o-z)
Integer*4 itable(nbasis,3)
Real*8 rtable(nbasis,2)
Real*8 AA(nbasis),BB(nbasis),CC(nbasis)
```

```
Real*8 hperK
hperK=4.55788514d-3
write(6,*) 'Coeficients: A, B, C'

 Do n=1,nbasis
   If (itable(n,3).eq.1) then       !H 1s
     AA(n)=109.84*hperK
     BB(n)=219.2*hperK
     CC(n)=rtable(n,2)
   End if

   If (itable(n,3).eq.6) then
     If (itable(n,2).eq.2) then     !C 2s
        AA(n)=27.95*hperK
        BB(n)=141.6*hperK
        CC(n)=rtable(n,2)
     End if
     If (itable(n,2).ne.2) then     !C 2p
        AA(n)=27.95*hperK
        BB(n)=118.2*hperK
        CC(n)=rtable(n,2)
     End if
    End if

   If (itable(n,3).eq.7) then
     If (itable(n,2).eq.2) then      !N 2s
        AA(n)=28.16*hperK
        BB(n)=162.2*hperK
        CC(n)=rtable(n,2)
     End if
     If (itable(n,2).ne.2) then      !N 2p
        AA(n)=28.16*hperK
        BB(n)=133.2*hperK
        CC(n)=rtable(n,2)
     End if
   End if

   If (itable(n,3).eq.8) then
     If (itable(n,2).eq.2) then      !O 2s
        AA(n)=27.95*hperK
        BB(n)=184.6*hperK
        CC(n)=rtable(n,2)
     End if
     If (itable(n,2).ne.2) then      !O 2p
        AA(n)=27.94*hperK
        BB(n)=149.75*hperK
```

```
      CC(n)=rtable(n,2)
   End if
End if

If (itable(n,3).eq.9) then
   If (itable(n,2).eq.2) then      !F 2s
      AA(n)=28.07*hperK
      BB(n)=205.7*hperK
      CC(n)=rtable(n,2)
   End if
   If (itable(n,2).ne.2) then      !F 2p
      AA(n)=27.93*hperK
      BB(n)=165.5*hperK
      CC(n)=rtable(n,2)
   End if
End if

If (itable(n,3).eq.13) then
   If (itable(n,2).eq.6) then      !Al 3s
      AA(n)=13.5*hperK
      BB(n)=89.0*hperK
      CC(n)=rtable(n,2)
   End if
   If (itable(n,2).ne.6) then      !Al 3p
      AA(n)=13.29*hperK
      BB(n)=71.1*hperK
      CC(n)=rtable(n,2)
   End if
End if

If (itable(n,3).eq.16) then
   If (itable(n,2).eq.6) then      !S 3s
      AA(n)=12.23*hperK
      BB(n)=124.0*hperK
      CC(n)=rtable(n,2)
   End if
   If (itable(n,2).ne.6) then      !S 3p
      AA(n)=13.17*hperK
      BB(n)=98.5*hperK
      CC(n)=rtable(n,2)
   End if
End if

If (itable(n,3).eq.17) then
   If (itable(n,2).eq.6) then      !Cl 3s
      AA(n)=13.70*hperK
```

```
        BB(n)=126.7*hperK
        CC(n)=rtable(n,2)
      End if
      If (itable(n,2).ne.6) then      !Cl 3p
        AA(n)=13.49*hperK
        BB(n)=106.3*hperK
        CC(n)=rtable(n,2)
      End if
    End if

  write(6,*)itable(n,2),itable(n,3),AA(n),BB(n),CC(n)


  End do
  return
  end
```

Line 60 – Specifies a convergence parameter for the SCC cycles.

Line 62 – Starts the SCC iterations until convergence is attained.

Line 67 – Subroutine energy calculates the energy matrix from the H_{ii} values. In DRAGON, the off-diagonal elements H_{ij} are calculated by using the Wolfsberg-Helmholtz approximation

$$H_{ij} = \frac{S_{ij}(H_{ii} + H_{jj})1.75}{2}. \qquad \text{(B2)}$$

Line 68 – Subroutine renormalize[‡] performs an orthogonalization on the energy matrix **H**. In the simplest of situations, **S** is a unit matrix and the eigenvectors (molecular orbitals) can be obtained from diagonalizing **H** directly. When **S** is not a unit matrix, which is the case the majority of the time, **H** can be symmetrically orthogonalized with the $\mathbf{S}^{-1/2}$ matrix. $\mathbf{S}^{-1/2}$ is obtained by diagonalizing **S**

$$\mathbf{s} = \mathbf{U}^{t}\mathbf{S}\mathbf{U} \qquad \text{(B3)}$$

with a unitary matrix **U**, taking the inverse square root of the diagonal elements of **s** yielding $\mathbf{s}^{-1/2}$, and then back-transforming with **U** to get $\mathbf{S}^{-1/2}$

$$\mathbf{S} = \mathbf{U}\mathbf{s}^{-1/2}\mathbf{U}^{t}. \quad \text{(B4)}$$

H is transformed to an orthogonalized energy matrix ($\mathbf{H}^{ortho}$) with

$$\mathbf{H}^{ortho} = \mathbf{S}^{-1/2}\mathbf{H}\mathbf{S}^{-1/2}, \quad \text{(B5)}$$

and returned by this subroutine.

Line 77 - Subroutine rs solves the real symmetric eigenvalue problem and returns the eigenvalues (molecular orbital energies) and eigenvectors (molecular orbitals) by diagonalizing $\mathbf{H}^{orth}$. The returned eigenvectors ($\mathbf{C}^{Norm}$) are normalized and have the form

$$\mathbf{C}^{Norm} = \mathbf{S}^{1/2}\mathbf{C}. \quad \text{(B6)}$$

Line 80 – Subroutine output writes the results of subroutine rs to a check file.

Lines 81 and 82 – Subroutine popanal‡ performs a population analysis on the molecular orbitals ($\mathbf{C}^{Norm}$) obtained from rs. Two things must be done by this subroutine before the actual population analysis is applied as described by Appendix A1. First, the molecular orbitals have to be transformed to **C** with the $\mathbf{S}^{-1/2}$ matrix through

$$\mathbf{C} = \mathbf{S}^{-1/2}\mathbf{C}^{Norm} = \mathbf{S}^{-1/2}\mathbf{S}^{1/2}\mathbf{C}. \quad \text{(B7)}$$

Second, the molecular orbital occupancies must be determined at every value of applied potential. It was discussed in chapter 3 that V_{ap} induces fluctuations in the molecular orbital energy levels and this gives rise to convergence issues because of degenerate or close-to-degenerate molecular orbitals within the

Fermi region. This subroutine calculates the electron occupancy (P_i) in each molecular orbital with Fermi-Dirac statistics

$$P_i = \frac{2}{e^{(E_i - E_f)/kT} + 1} \qquad \text{(B8)}$$

where E_f is the Fermi energy, E_i is the molecular orbital energy, k is the Boltzmann constant and T is the Kelvin temperature. The P_i become the occupancy vector ($\bar{v}$) at every value of V_{ap}, and hence have to be recalculated at every iteration in the applied potential cycle. The majority of occupied molecular orbitals will contain exactly 2 electrons ($P_i = 2$), but within the Fermi region, the MOs will have partial occupancies with values anywhere between 0 and 2. The density matrix defined in Appendix A1 can be re-written in terms of the population vector ($\bar{v}$) as

$$D_{ij} = \sum_{n=1}^{N} v_n C_{in} C_{jn}^{*}, \qquad \text{(B9)}$$

where the index n runs through the all of the molecular orbitals (N) in the system. The subroutine then performs the population analysis on the redefined **D** in the way described in appendix A. As a final check, the subroutine takes the sum of the individual atomic orbital populations. This sum should equal the number of electrons in the system. The subroutine is shown below.

```
implicit real*8 (a-h,o-z)
 external totoccfun
 real*8 s(nbasis,nbasis),ss(nbasis,nbasis)
 real*8 x(nbasis),val(nbasis)
 real*8 cm(nbasis,nbasis)  !normalized eigenvectors
 real*8 cms(nbasis,nbasis) !s^(1/2) * normalized eigenvectors
 real*8 pm(nbasis,nbasis)  !population matrix
 real*8 qvec(nbasis)       !gross populations
```

```
      real*8 occ(nbasis)        !MO occupancy vector
      integer*4 index(nbasis)
C     For rs subroutine
      real*8 w(nbasis)          !eigenvalues of s matrix
      real*8 z(nbasis,nbasis)   !eigenvectors of s matrix
      real*8 ww(nbasis,nbasis)  !diagonalized s
      real*8 xx(nbasis,nbasis)  !temporary array
      real*8 zww(nbasis,nbasis) !z * ww
      real*8 fv1(nbasis),fv2(nbasis) !work arrays
C     For dinv subroutine
      parameter (LWORK = 1048)
      real*8 zinv(nbasis,nbasis)     !z^(-1)
      real*8 work(LWORK)
      integer ipvt(nbasis)
C     For occupancy subroutine
      real*8 temp,efermi
      real*8 alfr(nbasis)
      logical fermidirac

C     Make copy of s matrix
      do is=1,norb,1
        do js=1,norb,1
          ss(js,is) = s(js,is)
C           write(6,1003)js,is,ss(js,is)
        end do
      end do

C     Find eigenvalues and eigenvectors of s matrix
      matz = 1 !compute eigenvectors
      call rs(norb,norb,ss,w,matz,z,fv1,fv2,ierr)
      write(3,*)'Return code on s-matrix eigenvalue analysis: ',ierr

C     Form ww = w^(-1/2) from w. (w is the diagonalized s matrix.)
      do i=1,norb,1
        do j=1,norb,1
          if (i.eq.j) then
            ww(i,i) = 1.0d0/(sqrt(w(i)))
          else
            ww(j,i) = 0.0d0
          endif
        enddo
      end do

C     Make copy of z matrix
      do is=1,norb,1
C         write(6,*)'vector ',is
```

```
        do js=1,norb,1
          zinv(js,is) = z(js,is)
C           write(6,1003)js,is,zinv(js,is)
        end do
      end do

C     find zinv = s^(-1), input z returns zinv
      call DGETRF(norb,norb,zinv,norb,ipvt,info)
      write(3,*)'DGETRF INFO code is: ',info
      write(6,*)'DGETRF INFO code is: ',info
      call DGETRI(norb,zinv,norb,ipvt,work,LWORK,info)
      write(3,*)'DGETRI INFO code is: ',info
      write(6,*)'DGETRI INFO code is: ',info

C     Do the inverse similarity transform.
      call dmmult(norb,z,ww,zww)
      call dmmult(norb,zww,zinv,xx)
C     re-normalize cm. cms = s^(-1/2)*cm
      call dmmult(norb,xx,cm,cms)

C     Generate 0 K occupancy vector
      do k=1,nfull,1
        n = index(k)
        occ(n) = 2.0d0
      end do
      do k=nfull+1,nfull+nhalf,1
        n = index(k)
        occ(n) = 1.0d0
      end do
      do k=nfull+nhalf+1,norb,1
        n = index(k)
        occ(n) = 0.0d0
      end do
      write(3,*)'MO    - 0 K Occupancy vector'
      do k=1,norb,1
        write(3,1001)k,occ(k)
      end do


C     Switch off logical fermidirac to skip Fermi-Dirac statistics
      fermidirac = .true.
      temp = 300.0d0            !hard code temperature
        if (fermidirac) then   ! Set occ(*) by Fermi-Dirac statistics
        do i=1,norb,1          !find homo and lumo
          if (occ(i).gt.0) nhomo = i
        end do
```

```
        nlumo = nhomo + 1

C Getting the density of states around the band gap
        ehom = alfr(nhomo)   !HOMO chunk
        ehom1=alfr(nhomo-1)
        ehom2=alfr(nhomo-2)
        ehom3=alfr(nhomo-3)
        ehom4=alfr(nhomo-4)

        elum = alfr(nlumo)   !LUMO chunk
        elum1 = alfr(nlumo+1)
        elum2 = alfr(nlumo+2)
        elum3 = alfr(nlumo+3)
        elum4 = alfr(nlumo+4)

C KWS 10 Sept 2003. Use full spectrum of MO energy levels for
C window within which to locate Fermi level. (Necessary for vap
C =0.)
        ehomo = alfr(1)
        elumo = alfr(nbasis)
        nelect = 2*nfull + nhalf
        write(6,*)'In POPANAL fermi part'
C         write(6,*)nhomo,ehomo,nlumo,elumo
C        Find efermi between ehomo and elumo
        call bisect(totoccfun,occ,alfr,ehomo,elumo,
     >              efermi,temp,nbasis,nelect)

        write(3,*)'The Fermi level is ',efermi
        write(55,*)'The Fermi level is'
        write(55,*) efermi
        write(55,*)'HOMO chunk'
        write(55,*)ehom4,ehom3,ehom2,ehom1,ehom
        write(55,*)'LUMO chunk'
        write(55,*)elum4,elum3,elum2,elum1,elum

        If (efermi.le.ehom) then
          write(55,*)'-------LOW FERMI LEVEL---------'
        End if

        write(3,*)'MO    - Occupancy vector at T = ',temp
C         write(55,*)'MO    - Occupancy vector at T = ',temp

C*************************************************
C            Pop Check
C*************************************************
        esum=0.0d0
```

```
        Do n=1,nbasis,1
          esum=esum+occ(n)
        End do

        write(55,*)'Occ sum is ', esum

C*************************************************
        do k=1,norb,1
          write(3,1001)k,occ(k)
C           write(55,1001)k,occ(k)
        end do
      endif ! End Fermi-Dirac statistics



C Generate P matrix.
C Initialize the matrix.
       do i=1,norb,1
         do j=1,norb,1
           pm(j,i) = 0.0d0
         end do
       end do
C Sum over molecular orbitals (k) to find each element.
       do i=1,norb,1
         do j=1,norb,1
           do k=1,norb,1
C              pm(j,i) = pm(j,i) + occ(k)*cm(j,k)*cm(i,k)
             pm(j,i) = pm(j,i) + occ(k)*cms(j,k)*cms(i,k)
           end do
         end do
       end do
C       do i=1,norb,1
C         do j=1,norb,1
C           write(6,*)i,' ',j,' ',pm(j,i)
C         end do
C       end do
C Populations by diagonal elements of P.S product matrix
       call dmmult(norb,pm,s,xx)
       ptot = 0.0d0
       do i=1,norb,1
C         write(6,*)i,' ',xx(i,i)
          ptot = ptot + xx(i,i)
       end do
       write(6,*)'ptot = ',ptot

C Generate gross population matrix.
```

```
      do i=1,norb,1
        qvec(i) = 0.0d0
      end do
      do i=1,norb,1
        do k=1,norb,1
          qvec(i) = qvec(i) + pm(i,k)*s(k,i)
        end do
      end do

C Print out populations.
      write(3,*)' '
      write(3,*)'Atomic orbital - Population'
      psum = 0.0d0
      do i=1,norb,1
C       write(19,*)qvec(i),x(i),val(i)
        write(3,1001)i,qvec(i)
        psum = psum + qvec(i)
      end do
      write(3,1002)psum

 1001   format(I7,'  ',F10.6)
 1002   format('Total population is:  ',F10.6)
 1003   format(2I7,'  ',F15.9)
      return
      end
```

Line 83 – Subroutine charge‡ adds up all atomic orbital populations on an atom, and finds the charge (Q) on that atom by subtraction the orbital population sum from its nuclear charge (Z). The subroutine is shown below.

```
      Implicit Real*8(a-h,o-z)
      Integer*4 nbasis,itable(nbasis,3),natoms
      Integer*4 orb,ninit,orbs(500),itablew(nbasis,3)
      Real*8 qvec(nbasis),val(nbasis),q(nbasis)
      Real*8 sum,sumf(500),vals,valf(500),qq(nbasis)

      Do n=1,nbasis
        itablew(n,1)=itable(n,1)
      End do

      natoms=1
```

```
C       write(6,*) 'In CHARGE, center number is'
C       Do n=1,nbasis
C         write(6,*)itablew(n,1)
C       End do

        Do n=1,nbasis-1
          If ((itablew(n,1).ne.itablew((n+1),1))) then
            natoms=natoms+1
          End if
        End do

C       write(6,*)'ATOMS',natoms

        ninit=1

        Do i=1,natoms
          orb=0
          sum=0.0
          vals=0.0

          itablew(i,1)=itablew(ninit,1)

          Do n=ninit,nbasis
            If (itablew(n,1).eq.itablew(ninit,1))then
              orb=orb+1
              sum=sum+qvec(n)
              vals=vals+val(n)
            End if
            If (itablew(n,1).ne.itablew(ninit,1))then
C               ninit=n
              Go to 100
            End if

          End do

 100          sumf(i)=sum
             orbs(i)=orb
             valf(i)=vals
             q(i)=valf(i)-sumf(i)

            Do ii=ninit,ninit+orb-1
              qq(ii)=q(i)
C               write(6,*),valf(i),qq(ii)
            End do
```

```
                ninit=n

C               write(6,*)'Atom',i,'with',orbs(i),'orbitals'
C               write(6,*)'With neutral val charge',valf(i)
C               write(6,*)'Has a population',sumf(i)
C               write(6,*)'and a charge of',q(i)
      End do

      open(unit=56,file='Q')
      write(56,*)'Atom and charge'
      Do i=1,natoms
        write(56,*)i,q(i)
      End do

C Assign every atom its charge
C       write(6,*)'In charge:'
      Do n=1,nbasis
C          write(6,*) itable(n,1),qq(n)
      End do

      Return
      End
```

Lines 84 and 85 – Subroutine scc‡ calculates the new values of $\mathbf{H}_{ii}$ by using equation (B1) from the charges acquired from subroutine charge, and the A,B and C constants from subroutine ABC. This subroutine also returns the RMS difference (RMSD) between the atomic charges of two consecutive runs to the main program driver. The RMSD for iteration "i" is defined as

$$\mathrm{RMSD}_i = \sqrt{\frac{\sum_{n=1}^{M}(Q_{n,i} - Q_{n,i-1})^2}{M}}, \qquad \text{(B10)}$$

where n is the atom index, M is the number of atoms, $Q_{n,i}$ is the charge on atom n at iteration i, and $Q_{n,i-1}$ is the charge on atom n from the previous (i-1) iteration. The subroutine is shown below.

```
      Implicit Real*8(a-h,o-z)
      Integer*4 nbasis,orb(500),nq,natoms
      Real*8 val(nbasis),h(nbasis,nbasis),lambda
      Real*8 AA(nbasis),BB(nbasis),CC(nbasis),qq(nbasis)
      Real*8 qqlast(nbasis),qqdiff(nbasis),qdamp(nbasis)
      Real*8 qlast(nbasis),qdiff(nbasis),damp(nbasis)
      Real*8 sum,RMS,RMSold,RMSD,qqdiffmax,q(nbasis)
      Real*8 qsum

C       write(6,*)'Atom and charge'
C       write(6,*)natoms
C       Do i=1,natoms
C         write(6,*)i,q(i)
C       End do

C       evperh=27.212d0


      If (nq.eq.1)then
        Do n=1,nbasis
          qqlast(n)=0.0
          qdamp(n)=qq(n)
        End do
        Do i=1,natoms
          qlast(i)=0.0
          damp(i)=q(i)
          RMSold=0.0
        End do
       Go to 800
       End if


C       write(6,*)'In scc, the values of h come in as'
C       Do n=1,nbasis
C          write(6,*)n, h(n,n)
C       End do

C       write(6,*)'In scc, the qlast,qcurrent,qdiff, and qdamp are:'
      sum=0.0
      Do n=1,nbasis
         qqdiff(n)=qq(n)-qqlast(n)
         qdamp(n)=qqlast(n)-(lambda*(qqdiff(n)))
C          write(6,*)qqlast(n), qq(n),qqdiff(n),qdamp(n)
         sum=sum+((qqdiff(n))*qqdiff(n))
      End do
      qsum=0.0
```

```
      Do i=1,natoms
          qdiff(i)=q(i)-qlast(i)
          damp(i)=qlast(i)-(lambda*(qdiff(i)))
C           write(6,*)qlast(i), q(i),qdiff(i),damp(i)
          qsum=qsum+((qdiff(i))*(qdiff(i)))
      End do

 800      write(6,*)'In scc, after using equation A*q*q + B*q +C'
C       write(6,*)'qdamp, h'
       write(99,*)'++++++++++++++++++++++++++++++++++'
       write(99,*)'At it = ',nq,' and lambda = ',lambda
       write(99,*)'charges , and Q diff are:'
      Do n=1,nbasis
         h(n,n)=-
((AA(n)*qdamp(n)*qdamp(n))+(BB(n)*qdamp(n))+CC(n))
C           write(6,*) qdamp(n),h(n,n)
         write(99,*) qdamp(n),qqdiff(n)
         qqlast(n)=qdamp(n)      !SAVE CURRENT CHARGES
      End do

      Do i=1,natoms
         qlast(i)=damp(i) !SAVE CURRENT CHARGES
      End do

C      Sorting the q differences so meet the second criteria of
C      maximum charge difference

      qqdiffmax=-9000000000.0

      Do i=1,natoms
        If ((abs(qdiff(i))).gt.qqdiffmax) qqdiffmax=abs(qdiff(i))
        write(99,*) qdiff(i)
      End do


      RMS=sqrt(qsum/natoms)
      RMSD=RMSold-RMS
      RMSold=RMS
      write(88,*)'At it = ',nq,' RMS = ',RMS, ' RMSD = ',RMSD
      write(6,*)'QSUM',qsum
      write(6,*)'At it = ',nq,' RMS = ',RMS, ' RMSD = ',RMSD
      write(6,*)'Max Q Diff = ',qqdiffmax
      write(99,*)'At it = ',nq,' RMS = ',RMS, ' RMSD = ',RMSD
      write(99,*)'Max Q Diff = ',qqdiffmax
      return
      End
```

Lines 86 through 90 – This portion of the MAIN program determines if the convergence criteria has been met. If so, the SCC iteration cycle is terminated and the final molecular orbital coefficients (**C)** enter the time-development stage of the program.

Lines 99 and 100 – Subroutine dynamicsinput reads information from an external file (edyn.inp) for the time-development phase. The first record in the external file commands the program to perform the time-dependent propagation. The second record specifies the number of donor and acceptor atomic orbitals. Starting at the third record, the identity of the donor atomic (basis) functions and the weight (a_i, where i is the index of donor functions) placed on each function are listed. For example, consider a carbon atom with a 2s, a 2px, a 2py and a 2pz orbital centered on it, and with basis function labels 1, 2, 3 and 4. To treat this carbon as a donor, one may "localize" an electron on it by distributing the electron into quarters among all the functions centered on the atom. This portion of edyn.inp will read:

1 0.25

2 0.25

3 0.25

4 0.25

As outlined in chapter 3, section (xxx), this subroutine finds the expansion coefficients (b_n) to the localized electron in the molecular orbital basis from the

information in the edyn.inp file. In a basis of N molecular orbitals with N_D donor basis functions, the b_n are specified by

$$b_n = \sum_{i=1}^{N} \sum_{k=1}^{N_D} C_{ni} a_i S_{ik} , \qquad \text{(B11)}$$

To reiterate, **C** is obtained from the SCC procedure, the a_i are the weights assigned to every donor function I in edyn.inp, and **S** was calculated and saved in lines 41 and 42 of the MAIN program.

The next records specify the identity of the acceptor atomic (basis) functions, and the last record gives the interval length between time steps and the number of time steps to be taken.

Lines 101 and 102 – Subroutine timedev time propagates the localized wavefunction (the linear combination of molecular orbitals) obtained by subroutine dynamicsinput. It adds up all the atomic orbital contributions (d_k, where k is the basis function index) at time t by solving

$$d_k = \sum_{k=1}^{N} \sum_{n=1}^{N} b_n C_{kn} e^{\frac{-iE_n t}{\hbar}} , \qquad \text{(B12)}$$

where i is $\sqrt{-1}$, and E_n is the molecular orbital energy.

References

1. Pan YH, Sohlberg K and Ridge DP. Reactions of Co_{1-4}^{+} and $Co_4(CO)_n^{+}$ with Cyclohexane: C-H Activation as a Function of Cluster Size and Ligand Substitution. J. Am. Chem. Soc. 1991; 113: 2406.Pan YH, Sohlberg K and Ridge DP.

Appendix C. Description of the KPAX code

The calculations in Chapter 2 for the charge transfer to the carbonyl acceptor from the methyl donor group, and Chapter 4 for the multi-electron (CI) wavefunction time-development were performed using the KPAX code. This code has had two major versions as outline below.

The first version was developed to perform a population analysis on the ground and/or any excited state from a CI calculation as discussed in 2.2.2.

The second version is an extension of the original which performs a generalized population analysis for any CI state. It can also acquire the population for a linear combination of CI states given their state energies and individual CSF contributions. This is necessary for performing the time development on the CI wavefunction.

There is a complement to the KPAX code called LUNA, which localizes the CI wavefunction by searching for the linear combination of CI states that results in the zwitterionic state that places the most negative charge on the donor atom in the molecule. This appendix provides descriptions of KPAX and LUNA, the FORTRAN programs that perform these procedures, and the files that support the programs.

C.1 KPAX Program Structure

The main driver structure of the current version of KPAX is shown below. A description of the main program features and modifications directly follows. The program line numbers appear on the right of each record (line) within the main program and will be referenced in the subsequent section.

```
C     ***CMAX Piece***                                                    1

      Implicit Real *8 (a-h,o-z)                                          2
      Parameter (NCSF=324, NAMO=36,Nao=43)                                3
      Parameter (NSTATE=10,Natoms=15)                                     4
      Parameter(nstep=300)                                                5
      Real *8 a(5 ,1), CMO(500,500), DM(500,500), SM(500,500)             6
      Real *8 occv(Nao,NCSF),CDM(500,500),tstep,time                      7
      Real *8 cm(NCSF),d(NCSF),CMODPOP(Nao),CSUM                          8
      Real *8 DSM(500,500), POP(NCSF,Nao),WPOP(NCSF,Nao)                  9
      Real *8 SUM, SUMOD,COEF(NSTATE,NCSF)
      Real *8 MODPOP(NSTATE,Nao)                                          10
      Real *8 Z(Natoms),tevcm(NCSF),TIMPOP(NCSF,Nao)                      11
      Real *8 TMODPOP(Nao),t(nstep),CHECKPOP(NCSF,Nao)                    12
      Integer *4 Ngroup, Nrem, Nao, Ngocc, Neocc, NFZC                    13
      Integer *4 ICSF(NSTATE,NCSF),LAB(Nao),ntstep,nbasis                 14
      Integer *4 nstep,it                                                 15
      Complex*16 czero,uni,zt                                             16
      Character *(1) Eig, OrbitalNumber, Lin, Symmetry                    17
      Character *(1) DMatrix,EVALS,STATENUM                               18
      Character *(1) CSFLIN, DASH,ID                                      19
      Character *(1) ORB(Nao)                                             20
      Open (file="MOn=2-pl3.log",unit=10)                                 21
      Read (10,*) NA                                                      22
      Read (10,*) Eig                                                     23
      Read (10,*) Lin                                                     24
      tstep=1.0d0                                                         25
      nbasis=Nao                                                          26

C ****For the First Set of 5 MOs****                                      27

      Ngroup=(Nao/5)                                                      28
```

```
      Nrem=MOD(Nao,5)                                                  29
      Print *, Ngroup, Nrem, Nao                                       30

C     ***This is for the groups with 5 Eigenvectors***                 31

      Do K=1,Ngroup                                                    32


        Read (10,*) OrbitalNumber                                      33
        Read (10,*) EVALS                                              34
        Read (10,*) Symmetry                                           35

        Do L=1,Nao                                                     36
          Read (10,*) (a(M,1),M=1,5)                                   37
C         Print *, (a(M,1),M=1,5)                                      38
            Do I=1,5                                                   39
              M=((K-1)*5)+I                                            40
                CMO(M,L)=a(I,1)                                        41
C             Print *, CMO(M,L)                                        42
              End do                                                   43
        End Do                                                         44

C         Print *, '_____'                                             45

      End Do                                                           46

C     ***Now for the remainder group***                                47

      If (Nrem.NE.0) Then                                              48

      Read (10,*) OrbitalNumber                                        49
      Read (10,*) EVALS                                                50
      Read (10,*) Symmetry                                             51

      Do L=1,Nao                                                       52
        Read (10,*) (a(M,1),M=1,Nrem)                                  53
C         Print *, (a(M,1),M=1,Nrem)                                   54
          Do I=1,Nrem                                                  55
            M=((Ngroup)*5)+I                                           56
            CMO(M,L)=a(I,1)                                            57
          End do                                                       58
      End Do                                                           59

      End If                                                           60

      Do N=1,Nao                                                       61
```

```
C       Print *, (CMO(M,N),M=1,Nao) !DEBUG                              62
C       Print *, '_____'                                                63
        End Do                                                          64

       Close (10)                                                       65

C  ***SMAX Piece***                                                     66

      Open (file="Sn=2-pl3.log",unit=30)                                67
      Read (30,*) OrbitalNumber                                         68

C                ****For the First Set of 5 MOs****                    69

C      ***This is for the groups with 5 Columns***                      70

      Do K=1,Ngroup                                                     71

         J=Nao-((K-1)*5)                                                72
         Do L=1,J                                                       73
         If (L.LT.5.OR.L.EQ.5) Then                                     74
         Read (30,*) (a(M,1),M=1,L)                                     75

               Do I=1,L                                                 76
                 M=((K-1)*5)+I                                          77
                 N=((K-1)*5)+L                                          78
                 SM(M,N)=a(I,1)                                         79
               End Do                                                   80
         End If                                                         81


         If (L.GT.5) Then                                               82
         Read (30,*) (a(M,1),M=1,5)                                     83

               Do I=1,5                                                 84
                 M=((K-1)*5)+I                                          85
                 N=((K-1)*5)+L                                          86
                 SM(M,N)=a(I,1)                                         87
               End Do                                                   88
         End If                                                         89

         End Do                                                         90

        Read (30,*) OrbitalNumber                                       91

      End Do                                                            92
```

```
C       ***Now for the remainder group***                                93

        If (Nrem.NE.0) Then                                              94
           J=Nrem                                                        95
           Do L=1,J                                                      96
              If (L.LT.5.OR.L.EQ.5) Then                                 97
               Read (30,*) (a(M,1),M=1,L)                                98

               Do I=1,L                                                  99
                 M=(Ngroup*5)+I                                          100
                 N=(Ngroup*5)+L                                          101
                 SM(M,N)=a(I,1)                                          102
               End do                                                    103
              End If                                                     104
         End Do                                                          105
        End If                                                           106

       Close (30)                                                        107

       call basisgen(Natoms) !Identify the atoms by expanding the basis. 108


C *****Calculation of the Density Matrix (CDM)***                        109
C *****Also of the Mulliken Atomic Overlap Population-DS Matrix***       110

C       I.  First Read in the occupancy information (CSFs) used to calculate 111
C       the CI states.                                                   112

       Open (file="n=2-spaced", unit=40)                                 113
       Open (file="Density.chk",unit=50)                                 114
       Open (file="POPMat.chk",unit=60)                                  115
       Open(file="Mullpop.chk",unit=70)                                  116
       Read (40,*) NFZC                                                  117

       Do M=1,NCSF                                                       118

          Do J=1,NFZC                                                    119
            occv(J,M)=2.0d0  !Setting the occ for frozen core            120
          End do                                                         121

          Read(40,*)(occv(N,M),N=NFZC+1,Nao)                             122

        End do                                                           123
```

```
 Close (40)                                                          124

Do L=1,NCSF !*******START CSF loop here***************              125

  write (70,*)'*******CSF= ',L,' *****************'                 126

    Do N=1,Nao                                                       127
      Do M=1,Nao                                                     128

        SUM=0.0                                                      129

        Do K=1,Nao                                                   130
            SUM=SUM+((occv(K,L))*(CMO(K,M))*(CMO(K,N)))              131
        End Do                                                       132

        CDM(M,N)=SUM                                                 133
        DSM(M,N)=(CDM(M,N))*(SM(N,M))                                134

      End Do                                                         135

 End Do                                                              136

     Do K=1,Nao                                                      137
       Do N=1,Nao                                                    138
         write(50,*) CDM(K,N)                                        139
         write(60,*) DSM(K,N)                                        140
       End do                                                        141

       write(60,*)'----------------'                                 142
       write(50,*)'----------------'                                 143
     End do                                                          144

C ***Calculating the Mulliken Population in each AO for each CSF***  145

    Do M=1,Nao                                                       146
      SUM=0.0                                                        147
      Do N=1,Nao                                                     148
         SUM=SUM+DSM(N,M)                                            149
      End Do                                                         150

      SUMOD=0.0                                                      151

       If (M.GT.1) Then                                              152
        Do K=1,M-1                                                   153
          SUMOD=SUMOD+DSM(M,K)                                       154
        End Do                                                       155
```

```
        End If                                                          156

       POP(L,M)=SUM+SUMOD    !POP should never change                  157
       write (70,*) POP(L,M) !AO Population for every CSF              158
     End Do                                                             159
     End do                                                             160

C     ********Read in contributions to every CSF for the CI states****  161

     Open(file="STtestn=2-pl3.log",unit=80)                             162
     Open(file="coef.chk",unit=90)                                      163

     Do N=1,NSTATE                                                      164

       Read(80,*)STATENUM                                               165
       Read(80,*)CSFLIN                                                 166
       Read(80,*)DASH                                                   167

       Do M=1,NCSF                                                      168
         Read(80,*)ICSF(N,M),COEF(N,M)                                  169
         write (6,*)ICSF(N,M),COEF(N,M)                                 170
       End do                                                           171

     End do                                                             172
     Close(80)                                                          173

     Do N=1,NSTATE                                                      174

        Do M=1,NCSF                                                     175
          write(90,*) ICSF(N,M),'    ',COEF(N,M)                        176
        End do
                                                                        177
     End do                                                             178

     Open(file="wpop.check",unit=95)                                    179
     Open(file="StatePop.chk",unit=97)                                  178

     Do N=1,NSTATE                                                      179
       write (95,*)'*****FOR STATE ', N, ' *******'                     180
       Do M=1,NCSF                                                      181
         write(95,*)'_____CSF ', M,' _____________'                     182
         Do L=1,Nao                                                     183
           WPOP(M,L)=POP(M,L)*((COEF(N,M))**2)                          184
           write(95,*) WPOP(M,L), POP(M,L), COEF(N,M)                   185
         End do                                                         186
       End do                                                           187
```

```
C *****Loop to add up the individual atomic orbitals contributions from each  188
C                          CSF. *****                                         189

          write(97,*)'For state ',N                                           190

          write(97,*)'sum of CSF contributions to POP vector'                 191

          SUMCHECK=0.0d0                                                      192

          Do L=1,Nao                                                          193

            STSUM=0.0d0                                                       194

            Do M=1,NCSF                                                       195
              STSUM=STSUM+WPOP(M,L)                                           196
            End do                                                            197

            MODPOP(N,L)=STSUM                                                 198

            write(6,*) STSUM                                                  199
            write(97,*)STSUM, MODPOP(N,L)                                     200

            SUMCHECK=SUMCHECK+STSUM                                           201

          End do                                                              202

          write(97,*)'Population check -',SUMCHECK,' Electrons'               203

        End do                                                                204

        Close(95)                                                             205
        Close(97)                                                             206


         czero = (0.0d0,0.0d0)                                                207
         zt = czero                  !Initialize time                         208

         Do it=1,nstep                                                        209

         write(6,*)zt, '****'                                                 210

        call timedev(nbasis,norb,tstep,ntstep,NSTATE,NCSF,COEF,               211
     >              tevcm,POP,TIMPOP,TMODPOP,zt)                              212
```

```
      call popgen(Natoms,Nao,NSTATE,TIMPOP,TMODPOP,zt,                213
     >            CMODPOP)                                             214

C       write(6,1001)t,dsum                                            215
        zt = zt + dcmplx(tstep)                                        216

      end do          !time loop                                       217

      Stop                                                             218
      End                                                              219
```

C.2 Description

Lines 3 and 4 – Parameters that specify the number of Configuration state functions or CSFs (NCSF), the number of CSF active molecular orbitals or the valence orbitals (NAMO), the number of basis functions (Nao), the number of CI states (NSTATE), and the number of atoms (Natoms). These parameters must be changed for every molecular system.

Lines 27 through 64 – This portion of KPAX reads the molecular orbitals

$$\phi_i = \sum_{j=1}^{Nao} c_{ji}\chi_j \qquad \text{(C1)}$$

from a GAMESS electronic structure output file.

Lines 71 through 106 – This portion of KPAX reads the overlap integrals

$$S_{ij} = \int \chi_i \chi_j d\tau \qquad \text{(C2)}$$

from a GAMESS electronic structure output file.

Line 108 – Subroutine <u>basisgen</u> expands atomic xyz data from a GAMESS input file into the correct order of atomic orbitals. This is to identify

which atomic orbitals belong to a particular atom in the molecule. The subroutine is shown below.

```
Implicit Real*8 (a-h,o-z)
Character *(1)DASH
Integer *4 Natoms
Integer*4 CN(Natoms)
Real *8 Z(Natoms),x(Natoms)

Open(file="ATOMIDn=2-pl3.log",unit=77)
Open(file="basisgen.chk",unit=76)

Read(77,*)DASH
Read(77,*)DASH
Read(77,*)DASH

Do k=1,Natoms
Read(77,*)CN(k),Z(k),x(k)
write(6,*)CN(k),Z(k),x(k)
End do

Close(77)

ih=1
io=1
Do i=1,Natoms
        If (Z(i).eq.1.0) then
        ih=ih+1
        End if
        If (Z(i).ne.1.0) then
        io=io+1
        End if
End do

nbasis=(ih-1)+((io-1)*5)
write(76,*)'NBASIS :'
write(76,*) nbasis

ib=1
Do i=1,Natoms

        If(Z(i).eq.1.0) then
        write(76,*)CN(i),Z(i),x(i),1.0
        ib=ib+1
        End if
```

```
      If (Z(i).eq.6.0)then
      write(76,*)CN(i),Z(i),x(i),6.0
      ib=ib+1

      Do m=1,4
      write(76,*)CN(i),Z(i),x(i),0.0
      ib=ib+1
      End do
      End if

C       *****For Oxygen containing species*******
      If (Z(i).eq.8.0)then
      write(76,*)CN(i),Z(i),x(i),8.0
      ib=ib+1

      Do m=1,4
      write(76,*)CN(i),Z(i),x(i),0.0
      ib=ib+1
      End do
      End if
C       ****************************************

C       *****For Nitrogen containing species*******
      If (Z(i).eq.7.0)then
      write(76,*)CN(i),Z(i),x(i),7.0
      ib=ib+1

      Do m=1,4
      write(76,*)CN(i),Z(i),x(i),0.0
      ib=ib+1
      End do
      End if
C       ****************************************

C       *****For Fluorine containing species*******
      If (Z(i).eq.9.0)then
      write(76,*)CN(i),Z(i),x(i),9.0
      ib=ib+1

      Do m=1,4    !F 2p
      write(76,*)CN(i),Z(i),x(i),0.0
      ib=ib+1
      End do
      End if
C       ****************************************
```

```
End do

Close(76)
Return
End
```

Line 117 – Parameter specifying the number of frozen core orbitals (NFZC), which is read form an external file.

Lines 118 through 123 – This portion of the code sets the occupancy vector ($\vec{v}$) for every CSF. The occupancies for the core molecular orbitals are set as $v_{n=1...NFZC} = 2$. The occupancies for the remaining orbitals, the CI active orbitals, $v_{n=NFZC+1...Nao}$ are read from a GAMESS CI output file as the CSF occupancies. There will be one $\vec{v}$ for every CSF, and they will not change from CI state to CI state.

Lines 127 through 136 – This portion calculates the density matrix **D** for every CSF

$$D^{L}_{mn} = \sum_{k=1}^{N} v^{L}_{k} C_{km} C^{*}_{kn}, \qquad \text{(C3)}$$

where L is the CSF index and N=Nao. It is important to note that **C** does not change from CSF to CSF; the $\vec{v}$ do. The population matrix is also calculated by multiplying $\mathbf{D}^{L}$ by the elements of the overlap matrix **S**,

$$\underline{DS}^{L}_{mn} = (\sum_{k=1}^{N} v^{L}_{k} C_{km} C^{*}_{kn}) S_{mn}. \qquad \text{(C4)}$$

Lines 146 though 160 – This portion calculates the population (ρ_m) for every CSF

$$\rho_m^L = \sum_m^N \sum_n^N \underline{DS}_{mn}^L = \sum_m^N \sum_n^N (\sum_{k=1}^N v_k^L C_{km} C_{kn}^*) S_{mn} , \qquad (C5)$$

where L is the CSF index.

Lines 179 through 187 – This calculates the population for every CI state J given the linear combinations of CSFs (eigenvectors) with expansion coefficients "f" as

$$\rho_m^{JL} = \sum_L^M \sum_m^N f_{JL} f_{JL} \rho_m^L , \qquad (C6)$$

where J is the CI state index, L is the CSF index, M=NCSF and f_{JL} is the contribution from CSF L to CI state J. The contributions "f" are read from a GAMESS output file.

Lines 211 and 212 – Assuming that the localized wavefunction is already specified (the linear combination of CI states with expansion coefficients b_n is known), the subroutine <u>timedev</u> propagates the wavefunction. It adds up the contributions to each CSF (d^{JL})

$$d^{JL} = \sum_{L=1}^M \sum_{J=1}^K b_J f_{JL} e^{\frac{-iE_J t}{\hbar}} , \qquad (C7)$$

where i is $\sqrt{-1}$, E_J is the CI state energy, and K=NSTATE. This is found for every time in the time iteration cycle.

Lines 213 and 214 – Subroutine <u>popgen</u>, discussed in more detail in Appendix A2, calculates the population P(t) on atomic orbital "A" from the d^{JL} acquired above and the population for every CSF (ρ_A^L)

$$P(t)_A = \sum_L^M \sum_A^M d^{JL} d^{JL^*} \rho_A^L \,. \qquad \text{(C8)}$$

C.3 Specifying the localized wavefuntion

Before the time development portion of the code is performed, the linear combination of CI states must be chosen. Here, the combination that yields the largest charge separation between donor and acceptor atoms is desired. If the charge on the donor is Q_D and the charge on the acceptor is Q_A,

$$\Delta Q = Q_D - Q_A \qquad \text{(C9)}$$

should be minimized. The procedure to find the b_J is as follows:

1. Run KPAX without time development. Files containing the atomic charges for every CI state will be generated.
2. Extract the charges for the donor and acceptor atoms for every CI state. These are denoted as acceptor charge vector QV_A and donor charge vector QV_D, both of dimension NSTATE.
3. Subtracting the charge vectors above and normalizing the resultant vector ($\Delta QV = N*QV_D - N*QV_A$) becomes the initial guess for the CI state expansion coefficients ($b_{n,guess}$) since it contains information about which states contribute to large charge differences.
4. The FORTRAN code LUNA takes the $b_{n,guess}$ and performs a population analysis by calculating

$$P(t)_A = \sum_L^M \sum_A^N d^{JL} d^{JL^*} \rho_A^L$$

at t=0.

5. ΔQV is recalculated, and step 4 is repeated. This procedure is iterated until equation C9 is minimized, and the appropriate b_n enter the time development phase of KPAX.

C.4 KPAX and LUNA file system

Below is Table C1 showing the files important to the FORTRAN programs KPAX and LUNA.

File Name	unit	Read	Write	Description	How is it Generated?	LUNA Read	LUNA Write
MO*file*.log	10	x		Molecular orbitals or Eigenvectors. The fist record contains the number of atomic orbitals (NA,Nao, or nbasis).	MOEDIT on gamess log file		
S*file*.log	30	x		Overlap Matrix	SEDIT on gamess log file (QPL=3)		
file-spaced	40	x		The CSFs with spacing between the characters	SPACER perl script		
STtest*file*.log	80	x		Reads the individual CSF contributions to every CI state	STEDIT on gamess log file		
ATOMID*file*.log	77	x		Conatins the number(label) and Z forevery atom in the moelcule	ATOMID on gamess log file	**x**	
BINSTATES	65	x		Non-eigenvector to be propagated	LUNA		**x**
STATE-ENERGY	66	x		Collection of CI state energies	by hand from gamess log file	**x**	
Density.chk	50		x	Density Matrix for every CSF. This stays the same in every state.	Written by KPAX		
POPMat.chk	60		x	Population matrix (DS) for every CSF. This stays the same in every state.	Written by KPAX		
Mullpop.chk	70		x	Population Vector for every CSF. This stays the same in every state.	Written by KPAX	**x**	
coef.chk	90		x	Collects individual CSF contributions for every state, COEF(N,M), where N =NSTATE, and M=NCSF	Written by KPAX	**x**	
wpop.check	95		x	This is the population matrix for every CI state.	Written by KPAX		
StatePop.chk	97		x	Population vector for every CI state.	Written by KPAX		
StatePop.chk	87	x		Population vector for every CI state. Called on by pogen subroutine.	"		
basisgen.chk	76		x	Expands the xyz file into the full basis including valence information	Written by KPAX		**x**
basisgen.chk	88	x		Expands the xyz file into the full basis including valence information. Called on by popgen subroutine	"	**x**	
state_q.txt	86		x	Atomic charges per CI state	Written by KPAX		
TIME_q.txt	89		x	Atomic charges at every time. This is a contraction of CI states	Written by KPAX		**x** **t =0.0**
STATE-CON	67		x	Sum of all state contributions to every CSF	Written by KPAX		
TIMEV-POP	68		x	Population Matrix, TIMPOP(M,L), at time *t*.	Written by KPAX		
TIMEV-MULL -POP	69		x	Population Vector at time *t*.	Written by KPAX		

Appendix D. Hartree-Fock calculation of the H_3^- complex

As chemists, the image we carry in our minds of electrons occupying a localized region of space termed “orbital” is very intuitive [1, 2]. From this idea we can infer the three dimensional shape of molecules, determine magnetic behavior and make statements about the strength of bonds, among many other predictions [1]. While this model has been invaluable in forming the basis of our chemical intuition, it must not be forgotten that an orbital, as we know it, is nothing more than a mathematical function attempting to describe the behavior of an electron in a molecule. This model is better known as Hartree-Fock theory (HF), and although it is an approximation it serves as a starting point to the more sophisticated *ab initio* calculations today [2], i.e. Møller-Plesset Perturbation Theory, Configuration Interaction (CI) [3]. Other methods are motivated by Hartee-Fock theory and describe electronic structure in an analogous fashion. For example, in Density Functional Theory (DFT) the description is virtually identical to the HF description except for the inclusion of terms that depend on electron density [1]. The purpose of this appendix is to outline a HF calculation, and thereby acquaint the reader with this fundamental quantum chemical method.

In order to understand the way a HF calculation is conducted, let’s first think about the most complete description of an N-electron, and M-nuclei system, by listing the operators that address all possible events taking place in the molecule at any point in time.

1) The electrons are moving so they will have kinetic energy. The corresponding operator is

$$\hat{T}_e = -\frac{1}{2}\sum_i \nabla_i^2 , \qquad \text{(D1)}$$

where i is the index running over N electrons ∇^2 is the kinetic energy operator in an appropriate coordinate system.

2) The nuclei are also moving, very slowly, but there is still a kinetic energy contribution from them. The corresponding operator is

$$\hat{T}_n = -\frac{1}{2}\sum_\alpha \frac{1}{m_\alpha}\nabla_\alpha^2 , \qquad \text{(D2)}$$

where α is the index running over all M nuclei, and m_α is the mass of nucleus α.

3) The electrons and nuclei are attracted to each other through coulomb interactions represented by a potential energy term. The corresponding operator is

$$\hat{V}_{ne} = -\sum_\alpha \sum_i \frac{Z_\alpha}{r_{\alpha i}}, \qquad \text{(D3)}$$

where $r_{\alpha i}$ is the distance between nucleus α and electron i, and Z_α is the nuclear charge of nucleus α.

4) The electrons will interact with each other through repulsive coulomb potential energy terms. The corresponding operator is

$$\hat{V}_e = \sum_j \sum_{i>j} \frac{1}{r_{ij}}, \qquad \text{(D4)}$$

where r_{ij} is the distance between electron i and j.

5) Finally, the nuclei will repel each other through coulomb potential energy terms as well. The corresponding operator is

$$\hat{V}_n = \sum_{\alpha} \sum_{\beta>\alpha} \frac{Z_\alpha Z_\beta}{r_{\alpha\beta}}, \qquad \text{(D5)}$$

where $r_{\alpha\beta}$ is the distance between nucleus α and β, and Z_α and Z_β are the corresponding nuclear charges.

Overall, the molecular Hamiltonian can be written as the sum of terms (D1) through (D5), leading to the simplest and completely accurate description of any molecular system

$$\hat{H} = \hat{T}_e + \hat{T}_n + \hat{V}_{ne} + \hat{V}_e + \hat{V}_n. \qquad \text{(D6)}$$

The implicit problems in describing these terms is quantifying the electron-electron interactions and the relationship between nuclear and electronic motion. As of right now the molecular Hamiltonian is in terms of nuclear and electronic coordinates, and this situation is at the root of the first simplification: the Born-Oppenheimer approximation. Because nuclei are so much heavier than electrons, the nuclei are regarded as static while the electrons are zipping by them, making the internal motions in the molecule separable. This simplifies things by reducing (D5) to a constant term that depends on the nuclear coordinates only. In addition, the term (D2) goes to zero because the nuclei have no kinetic energy under this assumption. The molecular Hamiltonian can be rewritten in terms of the electronic coordinates only as,

$$\hat{H} = \hat{T}_e + \hat{V}_{ne} + \hat{V}_e + V_n. \qquad \text{(D7)}$$

Next, we make the independent electron approximation

$$\Psi(r_1, r_2 ... r_N) = \phi_i(r_1)\phi_j(r_2)...\phi_k(r_N), \quad \text{(D8)}$$

where the overall wavefunction (Ψ) is written as a product of one-electron wavefunctions (ϕ), and r is the collection of coordinates for electron N. This description of Ψ is also known as the Hartree product and it has a couple of shortcomings. First, it assumes that other electrons affect an electron's position only in an average way. This means that an electron "feels" an electron right next to it as much as it "feels" an electron on the other side of the molecule.

Second, the Hartree product violates the Pauli exclusion principle, which states that electrons must be identical and indistinguishable, instead of placing electrons in specific ϕ orbitals. For example, in a two-electron system, one can write the Hartree product as,

$$\Psi(r_1, r_2) = \phi_i(r_1)\phi_j(r_2), \quad \text{(D9)}$$

but in order to not violate the Pauli exclusion principle, the Hartree product should also be written as,

$$\Psi(r_2, r_1) = \phi_i(r_2)\phi_j(r_1). \quad \text{(D10)}$$

To account for all possible electron-orbital combinations, a Slater determinant is written as a linear combination of the above possible configurations

$$\Psi(r_1, r_2) = N[\phi_i(r_1)\phi_j(r_2) - \phi_i(r_2)\phi_j(r_1)], \quad \text{(D11)}$$

where N is a normalization factor. Rewriting the wavefunction as a Slater determinant still leaves the problem of the averaged out effect electrons have on each other, and as you will see, it is the fundamental approximation in Hartree-Fock theory.

From a mathematical standpoint, an infinite number of functions would give the HF limit energy, but in reality this would require an infinite amount of time. This is why the primary objective of Hartree-Fock theory is to find the set of orbitals that best approximates the ground state of an N-electron system, i.e. find the collection of functions that gives the lowest calculated energy. This is the Basis set approximation. Two questions immediately arise: First, what kind of functions would be the best ones to use? Second, how many of them should be used? We can expand any of the ϕ molecular orbitals in a basis of atomic orbitals χ as

$$\phi_i = \sum_{\alpha} c_{\alpha i} \chi_{\alpha} , \qquad \text{(D12)}$$

where α is the number of atomic orbitals, and $c_{\alpha i}$ is the contribution of χ_{α} to the molecular orbital. The economical answer to the questions posed above is to use a smaller number of functions that closely resemble the overall system, but that are easy to manipulate mathematically. While there are functions that adequately describe electronic behavior, Gaussian functions are favored because they are easier to work with. Their properties allow more of them to be used and simplify the mathematics, as opposed to using better functions (like Slater-type functions) that are more cumbersome to employ. The most attractive feature of Gaussian functions is that they have spherical symmetry, and when taking the product of two of them, you end up with a new Gaussian function with a new center. The new center and area of the product of Gaussians have simple

definitions and the integrals involving them for Hartree-Fock calculations have already been solved and for this reason they are used in this exercise.

The problem now is to find the $c_{\alpha i}$ that minimize equation (D12), and for that we need a matrix representation of the molecular Hamiltonian. As derived by Roothaan and Hall [3], the variational problem can be written as

$$F_\alpha \sum_i^N c_{i\alpha}\chi_i = E\sum_\alpha^N c_{i\alpha}\chi_i \,, \tag{D13}$$

where F is the Fock operator, C is the coefficient matrix and S is the overlap matrix. The Fock operator has the form

$$F_\alpha = h_\alpha^{core} + \sum_\alpha^N (J_\alpha - K_\alpha), \tag{D14}$$

where N is the number of atomic orbitals. The first term of (D14) is the sum of the kinetic energy and the nucleus-electron coulombic attraction for electron α; equations (D1) and (D3) respectively. The second part of (D14) describes the electron-electron terms arising from coulombic repulsions (J_α) and exchange (K_α).

Multiplying both sides of (D13) by ϕ_β, and writing it in matrix notation yields

$$\mathbf{FC} = \mathbf{SCE}, \tag{D15}$$

where

$$F_{\beta\alpha} = \left\langle \chi_\beta \middle| F \middle| \chi_\alpha \right\rangle, \tag{D16}$$

and

$$S_{\beta\alpha} = \left\langle \chi_\beta \middle| \chi_\alpha \right\rangle. \tag{D17}$$

It will be useful to write (D16) in terms of the density matrix **D** as

$$F_{\beta\alpha} = h_{\beta\alpha}^{core} + \sum_{ij}^{N} D_{ij}\left(\left\langle \chi_\beta \chi_\alpha \middle| \chi_j \chi_i \right\rangle - \left(\frac{1}{2}\right) \left\langle \chi_\beta \chi_i \middle| \chi_i \chi_\alpha \right\rangle \right), \tag{D18}$$

where the **D** is defined over the occupied molecular orbitals as

$$D_{ij} = \sum_{k}^{N/2} c_{ik} * c_{jk} . \tag{D19}$$

Expression (D18) is typically written more compactly as

$$F_{\beta\alpha} = h_{\beta\alpha}^{core} + \sum_{ij}^{N} D_{ij} G_{\beta\alpha ij} . \tag{D20}$$

where $G_{\beta\alpha ij}$ is the two electron portion of equation D18. Expression (D15) implies that the molecular orbitals can be acquired by solving the eigenvalue problem, but the operator itself depends on the wavefunction, that is, the operator depends on the coefficients it is supposed to solve for. The solution to (D15) must be found iteratively. Conventionally, in a Hartree-Fock calculation the density matrix is used to converge the calculation, giving rise to the name Self-Consistent Field (SCF).

The Hartree-Fock procedure is outlined below for the H_3^- species. The molecule is modeled as an equilateral triangle with side dimension = 1.824 Bohr. The basis is composed of three identical Gaussian functions (χ) of the form

$$\chi_A = \left(\frac{2\alpha}{\pi}\right)^{3/4} e^{-\alpha(r-R_A)^2} , \tag{D21}$$

where the Gaussian exponent α = 0.4166214 and R_A is the coordinate of atom A. Figure D.1 shows the molecule and dimensions of the system used in this study. For more information on the integrals discussed below, refer to Reference [2].

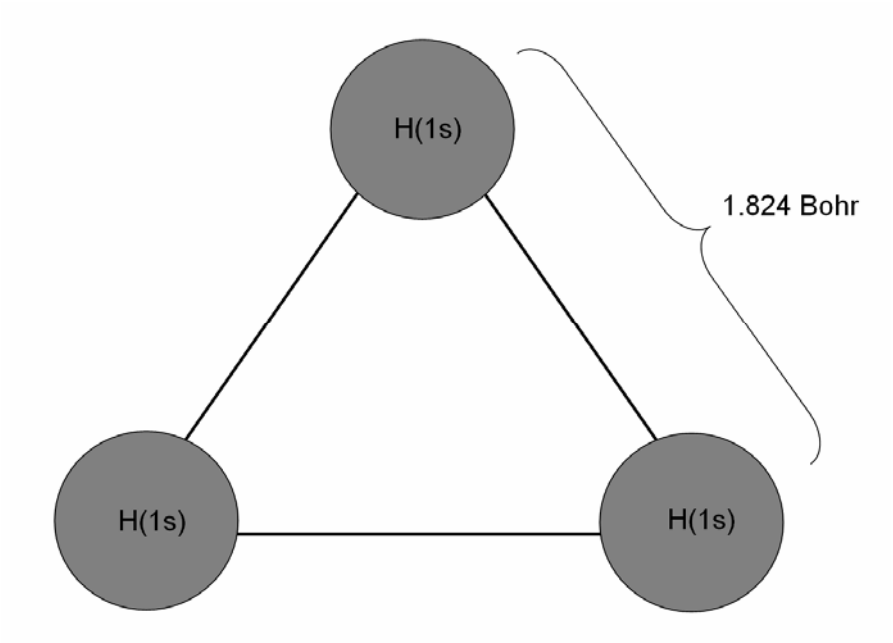

Figure D. 1. The molecule used in the Hartree-Fock (HF) study.

1. The overlap matrix will be necessary for several steps in the Hartree-Fock calculation. Conveniently, the overlap (product) of two Gaussian orbitals is already known as

$$\chi_A \chi_B = K \chi_P . \tag{D22}$$

where K is a proportionality constant of the form

$$K = e^{-\frac{\alpha^2}{\alpha+\alpha}|R_A - R_B|^2}. \quad \text{(D23)}$$

The new Gaussian function χ_P is centered on coordinate R_P

$$R_P = \frac{\alpha(R_A + R_B)}{2\alpha}, \quad \text{(D24)}$$

and has an exponent ρ

$$\rho = 2\alpha. \quad \text{(D25)}$$

Now the overlap matrix **S** can be built by taking the 9 possible overlaps

$$S := \begin{bmatrix} 1 & 0.5000009716 & 0.5000009716 \\ 0.5000009716 & 1 & 0.5000009716 \\ 0.5000009716 & 0.5000009716 & 1 \end{bmatrix} \quad \text{(D26)}$$

2. The Kinetic energy integrals specified by (D2) are also known. In atomic units, they have the form

$$\langle \chi_A | -\frac{1}{2}\nabla^2 | \chi_B \rangle = \frac{\alpha^2}{2\alpha}\left(3 - \frac{2\alpha^2}{2\alpha}|R_A - R_B|^2\right)\left(\frac{\pi}{2\alpha}\right)^{3/2} e^{-\frac{\alpha^2}{2\alpha}|R_A - R_B|^2}, \quad \text{(D27)}$$

and building the kinetic energy matrix **T** yield

$$T := \begin{bmatrix} 0.6249186003 & 0.1680731760 & 0.1680731760 \\ 0.1680731760 & 0.6249186003 & 0.1680731760 \\ 0.1680731760 & 0.1680731760 & 0.6249186003 \end{bmatrix}. \quad \text{(D28)}$$

3. The potential energy due to the coulombic attraction between electrons and nuclei “C” as specified by (D3) have been evaluated. There will be 3 matrices. Conceptually they correspond to I - the interactions between electron on atom A and all nuclei (V_A), II - the interactions between electron on atom B

and all nuclei (V_B), III – and the interactions between the combined electron density of electrons on atom A and B to all the nuclei (V_C). The integral describing the attraction of electron on atom B for nucleus A is

$$\left\langle \chi_A \left| -\frac{Z_A}{r_{AB}} \right| \chi_B \right\rangle = -\frac{\pi}{2\alpha}\left(\frac{2\alpha}{\pi}\right)^{6/4}\left(\frac{\pi}{\tau}\right)^{1/2} \mathrm{erf}(\tau^{1/2}), \tag{D29}$$

where τ is defined as

$$\tau = 2\alpha(R_B - R_A)^2. \tag{D30}$$

The three resultant matrices are

$$VA := \begin{bmatrix} -1.029997459 & -0.4171631139 & -0.4171631139 \\ -0.4171631139 & -0.5380407760 & -0.3033953493 \\ -0.4171631139 & -0.3033953493 & -0.5380407760 \end{bmatrix}, \tag{D31}$$

$$VB := \begin{bmatrix} -0.5380407760 & -0.4171631139 & -0.3033953493 \\ -0.4171631139 & -1.029997459 & -0.4171631139 \\ -0.3033953493 & -0.4171631139 & -0.5380407760 \end{bmatrix}, \text{ and} \tag{D32}$$

$$VC := \begin{bmatrix} -0.5380407760 & -0.3033953493 & -0.4171631139 \\ -0.3033953493 & -0.5380407760 & -0.4171631139 \\ -0.4171631139 & -0.4171631139 & -1.029997459 \end{bmatrix}. \tag{D33}$$

4. The initial guess is the core Hamiltonian matrix ($\mathbf{H}_{core}$), which is built by adding T, VA, VB, and VC. The resultant matrix is

$$Hcore := \begin{bmatrix} -1.481160411 & -0.9696484010 & -0.9696484010 \\ -0.9696484010 & -1.481160411 & -0.9696484010 \\ -0.9696484010 & -0.9696484010 & -1.481160411 \end{bmatrix}. \tag{D34}$$

5. The two electron integrals have to be computed next, and they have also been solved. There will be 81 integrals with 6 unique values. For example, integral (AA|BB) is the repulsion felt by electrons on separate atoms, and it has the form

$$(AA|BB) = \frac{\pi^{5/2}}{4\alpha^2(4\alpha)^{1/2}}\left(\frac{2\alpha}{\pi}\right)^{12/4}\left(\frac{\pi}{\lambda^{1/2}}\right)\mathrm{erf}(\lambda^{1/2}). \qquad \text{(D35)}$$

The number of integrals, their identity and corresponding values are:

3 x (AA|AA) = 0.728318,

6 x (AA|BB) = 0.495632,

24 x (AB|AA) = 0.326126,

12 x (AB|AB) = 0.182080,

24 x (AB|AC) = 0.163064, and

12 x (AA|BC) = 0.269251.

6. For the SCF portion of the calculation, the initial guess must be orthogonalized as discussed in previous sections of this thesis. Here, the canonical orthogonalization is used, where the transformation matrix $\mathbf{X}=\mathbf{U}\mathbf{s}^{-1/2}$. The $\mathbf{s}^{-1/2}$ is found diagonalizing **S** with a unitary matrix **U**, and taking the inverse square root of the diagonal elements. The procedure is as follows. Using the fact that there must be a matrix **U** that diagonalizes **S** so that $\mathbf{U}^t\mathbf{S}\mathbf{U}=\mathbf{s}$, where **s** is the eigenvalue matrix, transforming matrix **U** is found to be

$$U := \begin{bmatrix} \frac{1}{3}\sqrt{3} & \frac{1}{3}\sqrt{3} & \frac{1}{3}\sqrt{3} \\ \frac{1}{3}\sqrt{3} & \frac{1}{2}-\frac{1}{6}\sqrt{3} & -\frac{1}{2}-\frac{1}{6}\sqrt{3} \\ \frac{1}{3}\sqrt{3} & -\frac{1}{2}-\frac{1}{6}\sqrt{3} & \frac{1}{2}-\frac{1}{6}\sqrt{3} \end{bmatrix}. \qquad \text{(D36)}$$

The $\mathbf{s}^{-1/2}$ is

$$sis := \begin{bmatrix} 0.7071067814 & 0. & 0. \\ 0. & 1.414213562 & 0. \\ 0. & 0. & 1.414213562 \end{bmatrix}, \tag{D37}$$

yielding transformation matrix **X**

$$X = \begin{bmatrix} 0.23570\sqrt{3} & 0.47140\sqrt{3} & 0.47140\sqrt{3} \\ 0.23570\sqrt{3} & 0.70710 - 0.23570\sqrt{3} & -0.70710 - 0.23570\sqrt{3} \\ 0.23570\sqrt{3} & -0.70710 - 0.23570\sqrt{3} & 0.70710 - 0.23570\sqrt{3} \end{bmatrix} \tag{D38}$$

The core Hamiltonian matrix is the initial guess for the Fock matrix (**F**≈$\mathbf{H}_{core}$). The matrix **X** found above used to perform a unitary transformation on **F**

$$\mathbf{F'} = \mathbf{X}^t\mathbf{F}\mathbf{X}, \tag{D39}$$

in order to obtain **F'**

$$Fp0 := \begin{bmatrix} -1.7103 & 0.0001 & 0.0001 \\ 0.00002 & -1.0232 & 0.00005 \\ 0.00002 & 0.00005 & -1.0232 \end{bmatrix}. \tag{D40}$$

7. Diagonalizing **F'** results in a unitary **C** matrix (**C'**)

$$\mathbf{F'C'} = \mathbf{C'E} \tag{D41}$$

with eigenvectors **C'**

$$Cp0 := \begin{bmatrix} 1.00000 & 0.00021 & -0.22851 \\ 0.00003 & 0.70711 & -0.70711 \\ 0.00003 & 0.70711 & 0.70711 \end{bmatrix}, \tag{D42}$$

with a corresponding eigenvalue matrix **E**

$$E0 := \begin{bmatrix} -1.71030 & 0. & 0. \\ 0. & -1.02315 & 0. \\ 0. & 0. & -1.02315 \end{bmatrix}. \quad \text{(D43)}$$

To get back to the real coefficients, **C'** must be transformed with **X**

$$\mathbf{C} = \mathbf{XC'}, \quad \text{(D44)}$$

in order to obtain **C**

$$C0 := \begin{bmatrix} 0.40825 & 1.15470 & 0. \\ 0.40825 & -0.57735 & 1.00000 \\ 0.40825 & -0.57735 & -1.00000 \end{bmatrix}. \quad \text{(D45)}$$

8. The first density matrix **D** can be built now. In this system, there are 4 electrons which occupy 2 molecular orbitals; therefore **D** only includes the first two eigenvectors of **C**

$$D_{ij} = \sum_{k=1}^{2} C_{ik} * C_{jk} \ , \quad \text{(D46)}$$

where **D**

$$DO := \begin{bmatrix} 3.00000 & -1.00000 & -1.00000 \\ -1.00000 & 1.00000 & 1.00000 \\ -1.00000 & 1.00000 & 1.00000 \end{bmatrix}. \quad \text{(D47)}$$

9. Now that the **D** is known, the first complete Fock matrix can be assembled. The two electron portion (**G**) as specified by (D20), can be calculated as

$$TEI0 := \begin{bmatrix} 0.36416 & 0.16306 & 0.16306 & 0.16306 & 0.40459 & 0.18772 & 0.16306 & 0.18772 & 0.40459 \\ 0.16306 & 0.091040 & 0.081530 & -0.06574 & 0.16306 & 0.02844 & 0.02844 & 0.081530 & 0.18772 \\ 0.16306 & 0.081530 & 0.091040 & 0.02844 & 0.18772 & 0.081530 & -0.06574 & 0.02844 & 0.16306 \\ 0.16306 & -0.06574 & 0.02844 & 0.091040 & 0.16306 & 0.081530 & 0.081530 & 0.02844 & 0.18772 \\ 0.40459 & 0.16306 & 0.18772 & 0.16306 & 0.36416 & 0.16306 & 0.18772 & 0.16306 & 0.40459 \\ 0.18772 & 0.02844 & 0.081530 & 0.081530 & 0.16306 & 0.091040 & 0.02844 & -0.06574 & 0.16306 \\ 0.16306 & 0.02844 & -0.06574 & 0.081530 & 0.18772 & 0.02844 & 0.091040 & 0.081530 & 0.16306 \\ 0.18772 & 0.081530 & 0.02844 & 0.02844 & 0.16306 & -0.06574 & 0.081530 & 0.091040 & 0.16306 \\ 0.40459 & 0.18772 & 0.16306 & 0.18772 & 0.40459 & 0.16306 & 0.16306 & 0.16306 & 0.36416 \end{bmatrix}. \quad \text{(D48)}$$

Multiplying **G** by **D** and adding this to $\mathbf{H}^{core}$ yields the Fock Matrix **F** of the next iteration cycle

$$Fp := \begin{bmatrix} 0.14374 & -0.15494 & -0.15494 \\ -0.15494 & 0.12604 & -0.27495 \\ -0.15494 & -0.27495 & 0.12604 \end{bmatrix}. \quad \text{(D49)}$$

10. Steps 6 through 9 are repeated until **D** has converged to within some criteria. This calculation converges in two iterations. The final molecular orbitals (**C**) are

$$C1 := \begin{bmatrix} 0.28984 & 1.18996 & 0. \\ 0.46434 & -0.53329 & -1.00000 \\ 0.46434 & -0.53329 & 1.00000 \end{bmatrix}, \quad \text{(D50)}$$

with corresponding molecular orbital energies (**E)**

$$E1 := \begin{bmatrix} -0.13554 & 0. & 0. \\ 0. & 0.51212 & 0. \\ 0. & 0. & 0.80198 \end{bmatrix}. \quad \text{(D51)}$$

References

1. Jensen F. Introduction to Computational Chemistry. Wiley, Chichester, England, 1999.

2. Szabo A and Ostlund NS. Modern Quantum Chemistry. Introduction to Advanced Electronic Structure Theory. Dover, Mineola, N.Y., 1996.

3. Foresman JB and Frisch A. Exploring Chemistry with Electronic Structure Methods, Gaussian, Inc., Pittsburgh, PA, 1996.

Appendix E. List of Abbreviations

AO – Atomic Orbital

CI – Configuration Interaction

CSF – Configuration State Function

CTS – Charge Transfer State

DFT – Density Functional Theory

DOS – Density Of States

E_a – Adiabatic attachment Energy

EHT – Extended Hückel Theory

E_n – Vertical detachment Energy

E_v – Vertical attachment Energy

HF – Hartree-Fock Theory

HOMO – Highest Occupied Molecular Orbital

LUMO – Lowest Unoccupied Molecular Orbital

MO – Molecular Orbital

NDR – Negative Differential Resistance

SAM – Self-Assembled Monolayer

SCC – Self Consistent Charge

TDSE – Time-dependent Schrödinger Equation

TISE – Time-independent Schrödinger Equation

Vita

Natalie Ruth Carroll

Education
Drexel University - Ph.D. candidate in Chemistry. *Expected graduation 8/2004.*
University of North Carolina at Charlotte (UNCC) - B.S. Chemistry/Biochemistry, Cum Laude.

Honors and Awards
2004 – Outstanding Graduate Student Award – College of Media Arts and Design at Drexel University
2004 – Teaching Assistant of the Year Award at Drexel University
2004 – Honorable Mention at the Drexel University-wide Research Day
2004 – Rohm and Haas Company Award for overall best poster at the American Chemical Society (ACS) Graduate Student poster session (Philadelphia Chapter).
2003 – NSF-IGERT Program in Nanoscale Science and Engineering fellowship recipient.
2003 – Honorable Mention at the Drexel University-wide Research Day
2003 – Dupont Award at the American Chemical Society (ACS) Graduate Student poster session (Philadelphia Chapter).
2001 – 2nd Prize at the College of Arts and Science's annual research day at Drexel University
2000 – Teaching Assistant of the Year Award at Drexel University

Publications and Presentations

- Zheng, Xiange; Vedova-Brook, Natalie; Sohlberg, Karl. **Application of a Lumped-Inertia Technique to Vibrational Analysis of the Torsional-Twisting Modes of Low Molecular Weight Polyphenylenes and Polyethynylphenylenes.** *Journal of Physical Chemistry A* **108** (2004) 2499.
- Carroll, Natalie. **Hyperchem Workshop**. *Presented as the first seminar in the "trainee workshop series" for the NSF-IGERT program.*
- Carroll, Natalie. **The IGERT experience – Our perspective.** *Presented at* the Drexel/Upenn IGERT Retreat 2004
- Carroll, Natalie; Sohlberg, Karl. **Application of time-dependent quantum mechanics to electron transport through molecular junctions.** *Presented at* the ACS Graduate Student poster session 2004, the Drexel/Upenn IGERT Retreat 2004, the Drexel University College of Arts and Science Research Day 2004, *and* the 6th Annual Research Day at Drexel University 2004 .
- Vedova-Brook, Natalie; Matsunaga, Nikita, Sohlberg; Karl. **Correlating substituent parameter values to electron transport properties of molecules.** *Chemical Physics* **299** (2004) 89.
- Carroll, Natalie; Sohlberg, Karl. **Theoretical investigations into the time dependence of electron transport in beta-carotene.** *Presented at* the 5th Annual Research Day at Drexel University 2003.
- Carroll, Natalie; Matsunaga, Nikita; Sohlberg, Karl. **Correlation of substituent parameter values to electronic properties of molecules.** *Materials Research Society (MRS) Symposium Proceedings* (2002), 734.
- Carroll, Natalie; Matsunaga, Nikita; Sohlberg, Karl. **Correlating substituent parameters to properties desirable for the fabrication of molecular electronic devices.** *Presented at* MRS 2002 Fall meeting *and at* the ACS Graduate Student poster session 2003.
- Carroll, Natalie; Sohlberg, Karl. **Conical Intersections – Opportunity to do the electronically forbidden.** *Presented at* the Drexel University College of Arts and Science Research Day 2002.